Unraveling the puzzles of the QRS axis

Desentrañando el rompecabezas del eje QRS

Desvendando o quebra-cabeças do eixo QRS

Case from Madhav Bhargava
Safdarjung Hospital
New Delhi, India

New electrocardiographic interpretation

Case report

A 16-year-old boy presented with progressive shortness of breath on exertion (class II NYHA) for 1 year. He said that there was no fever, chest pain, cough, palpitations, syncope, or any physical trauma. He had no significant medical history. He also has no significant family medical/surgical history. Inspection of the chest showed marked chest wall deformity (pectus carinatum) and thin patient, ectomorph biotype.

Other particularities on physical examination were unremarkable.

The chest X-ray showed the classical particular deformity of pectus carinatum (PA and lateral views).

His echocardiogram was normal.

An electrocardiogram was performed.

Questions:

Which is the diagnosis? Where is the QRS axis in the frontal and horizontal planes?

ECG

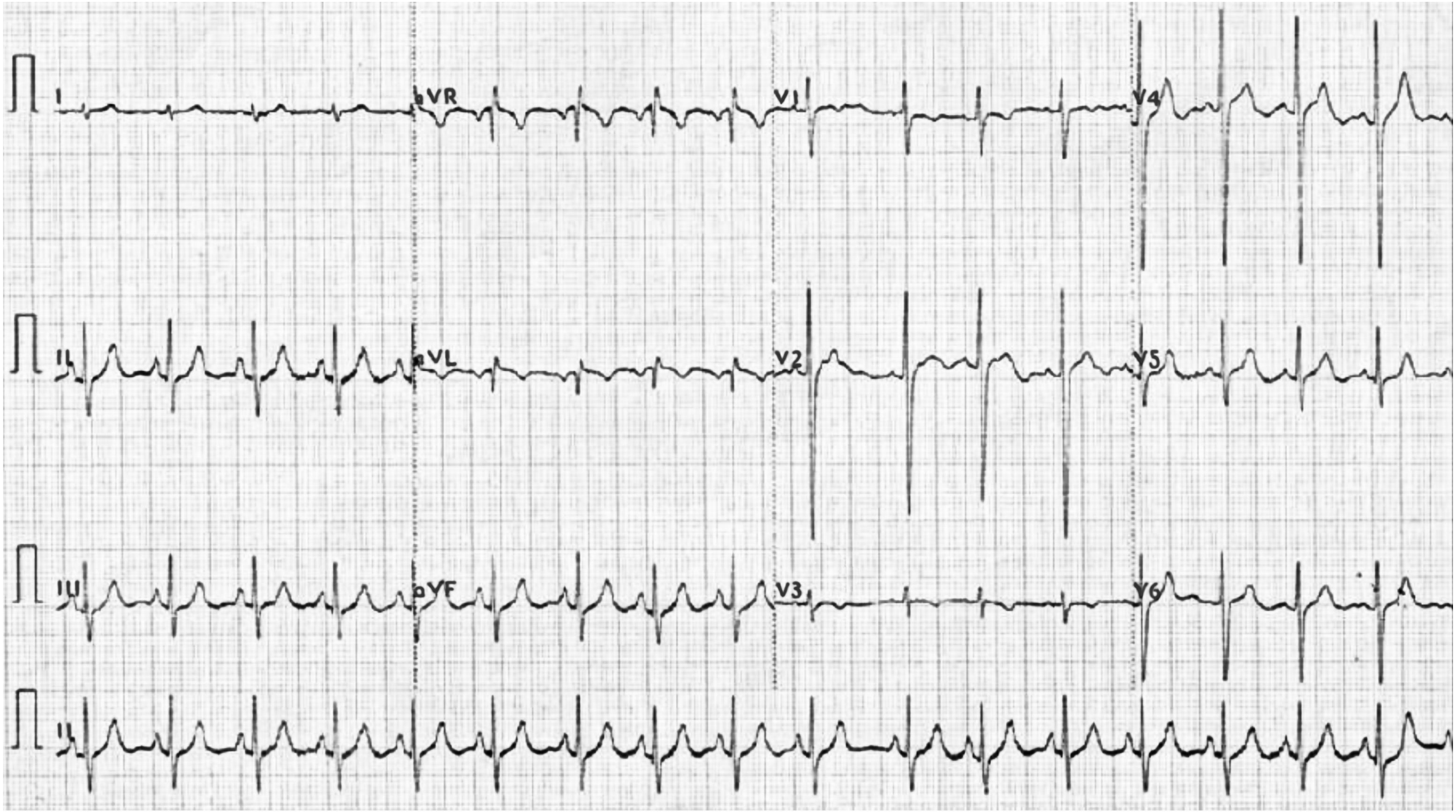

Opinión de los colegas

Opinião dos colegas

Colleagues' opinion

Spanish

Queridos amigos quisiera analizar el electrocardiograma presentado por nuestro admirado y eximio maestro. En este trazado existen 2 fenómenos electrofisiológicos

1. **El corazón está en posición vertical con ondas R I < III, y onda P negativa con q en aVL**
2. **El segundo fenómeno es el síndrome onda SI,SII,SIII que siempre va acompañado con R' en aVR , (y a veces con R‘ en V1) con ondas S precordiales desde V1 a V6 y sin onda Q en V5, V6 (en adultos) El maestro Mauricio Rosenbaum decía: el patrón SI,SII,SII tiene eje indeterminado.**

Un fraternal abrazo

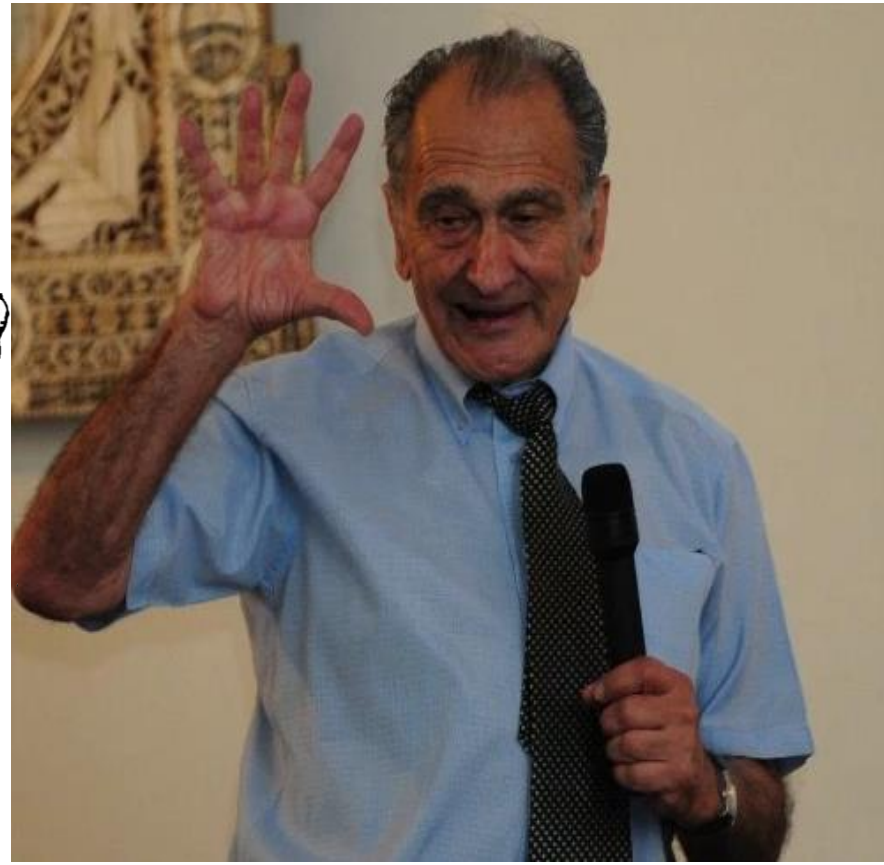

Dear friends, I would like to analyze the electrocardiogram presented by our admired and excellent teacher.

In this ECG there are two electrophysiological phenomena:

1) **The heart is vertically positioned with RI < III, and negative P wave with q in aVL lead like "Don Quijote".**
2) **The second phenomenon is the SI-SII-SIII pattern that is always accompanied by R' in aVR, (and sometimes with R' in V_1) with precordial persistent S waves from V1 to V6 and without Q wave in V5, V6 (in adults) Our master Mauricio Rosenbaum said: "the pattern SI, SII, SII has frequently an indeterminate axis".**
3) **A brotherly embrace**

Samuel Sclarovsky MD Emeritus Professor Tel Aviv University Israel (He is argentinian by birth)

Samuel Schakowsky ´s pearls

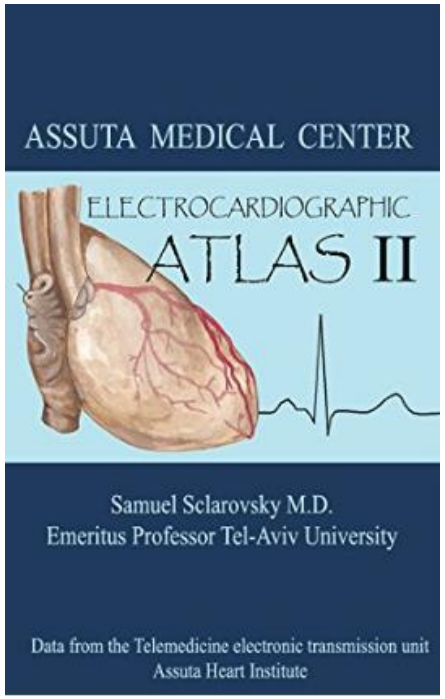

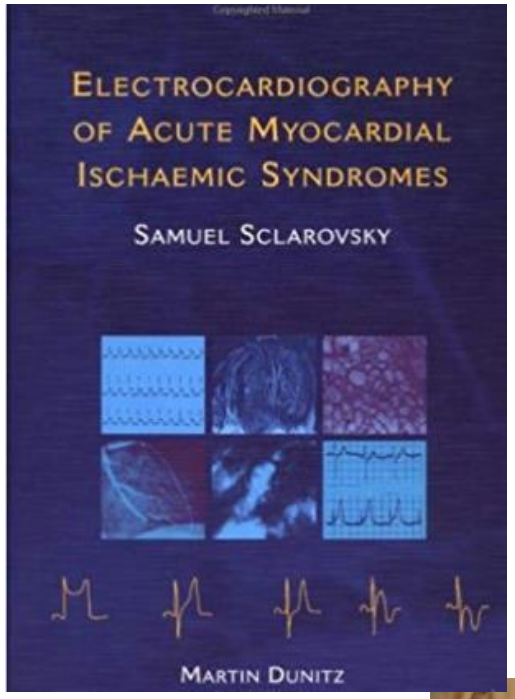

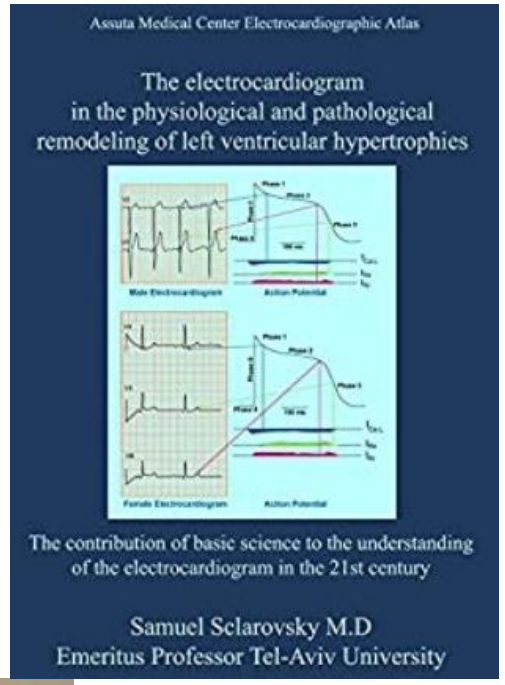

Spanish Edition

Spanish

...y decíamos que tenia un corazón con la punta para atrás. Contrario al punta adelante con q1,q2 y q3 con zona de transición a la derecha solo qR de V3 a V6 sin S.

English

... and we said that he had a heart with the tip directed to the back. Contrary, to the heart with the forward tip which has the q1, q2 and q3 pattern, and with the precordial transition zone dislocated to the right with qR from V3 to V6 and without S wave.

Gerardo Naum MD Buenos Aires/ Argentina. Member of Rosenbaum School

Clinical significant observation related precordial transition Zone from Andrés Ricardo Pérez-Riera: The transition zone is defined as the precordial lead where QRS pattern had changed from an rS to an Rs configuration, or the lead where an isoelectric RS pattern is registered. A delayed transition is defined as the transition occurring at V_5 or beyond. In a diverse community-based population free of cardiovascular disease and compared with normal rotation, clockwise rotation was associated with increased risk of all-cause and cardiovascular disease mortality while counterclockwise rotation was associated with lower risk of all-cause mortality and non-significant association with cardiovascular disease mortality. These findings call for attention to these often neglected ECG markers, and probably call for revising the current definition of normal rotation.**(1)**

1. Bradford N, Shah AJ, Usoro A, Haisty WK Jr, Soliman EZ. Abnormal electrocardiographic QRS transition zone and risk of mortality in individuals free of cardiovascular disease. Europace. 2015 Jan;17(1):131-6. doi: 10.1093/europace/euu149

PA chest X-Ray

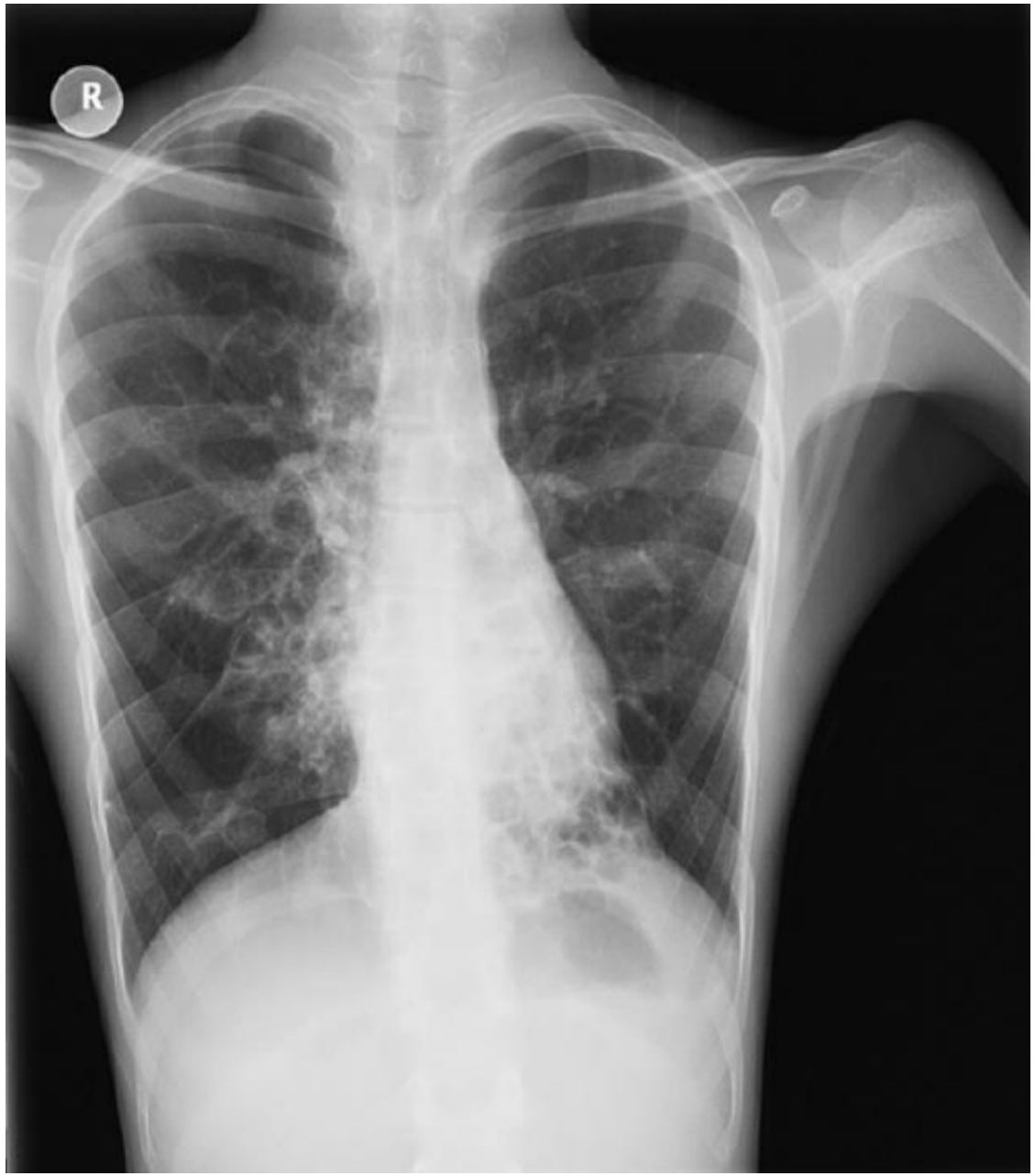

Lateral chest X-Ray

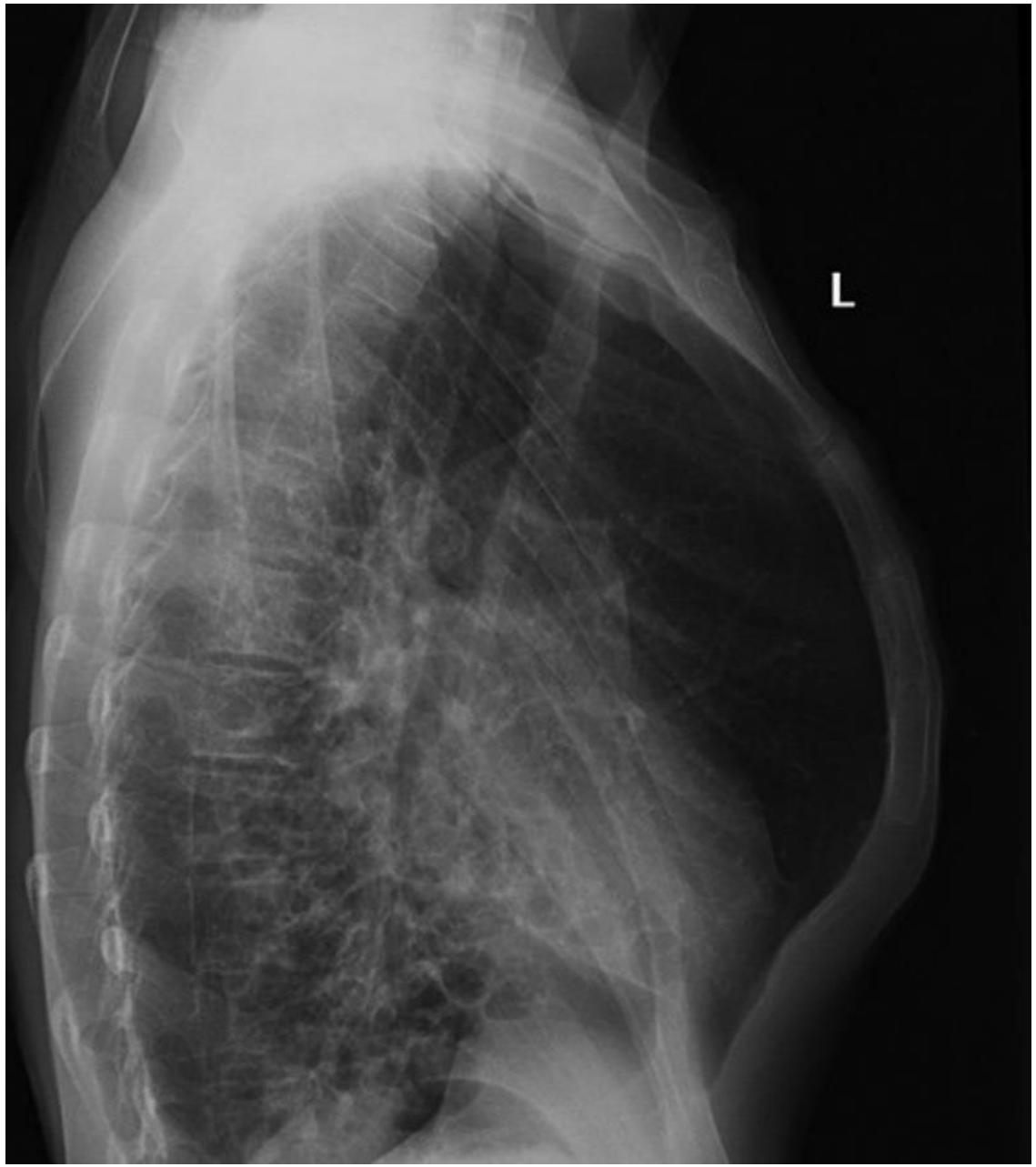

Unraveling the puzzles of the QRS axis

Final comments by Andrés Ricardo Pérez-Riera, MD PhD
Laboratório de Metodologia de Pesquisa e Escrita Científica,
Faculdade de Medicina do ABC, Santo André, SP, Brasil

Figure 1

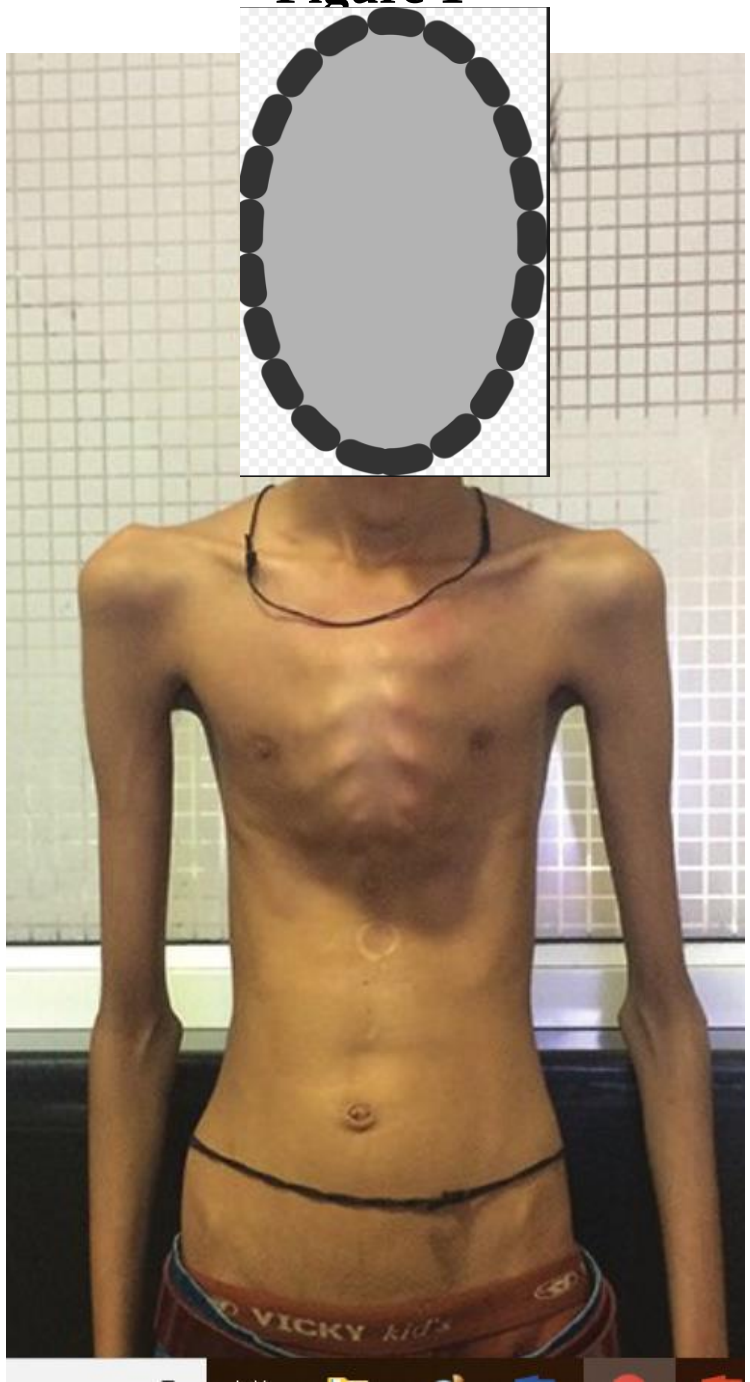

Figure 2

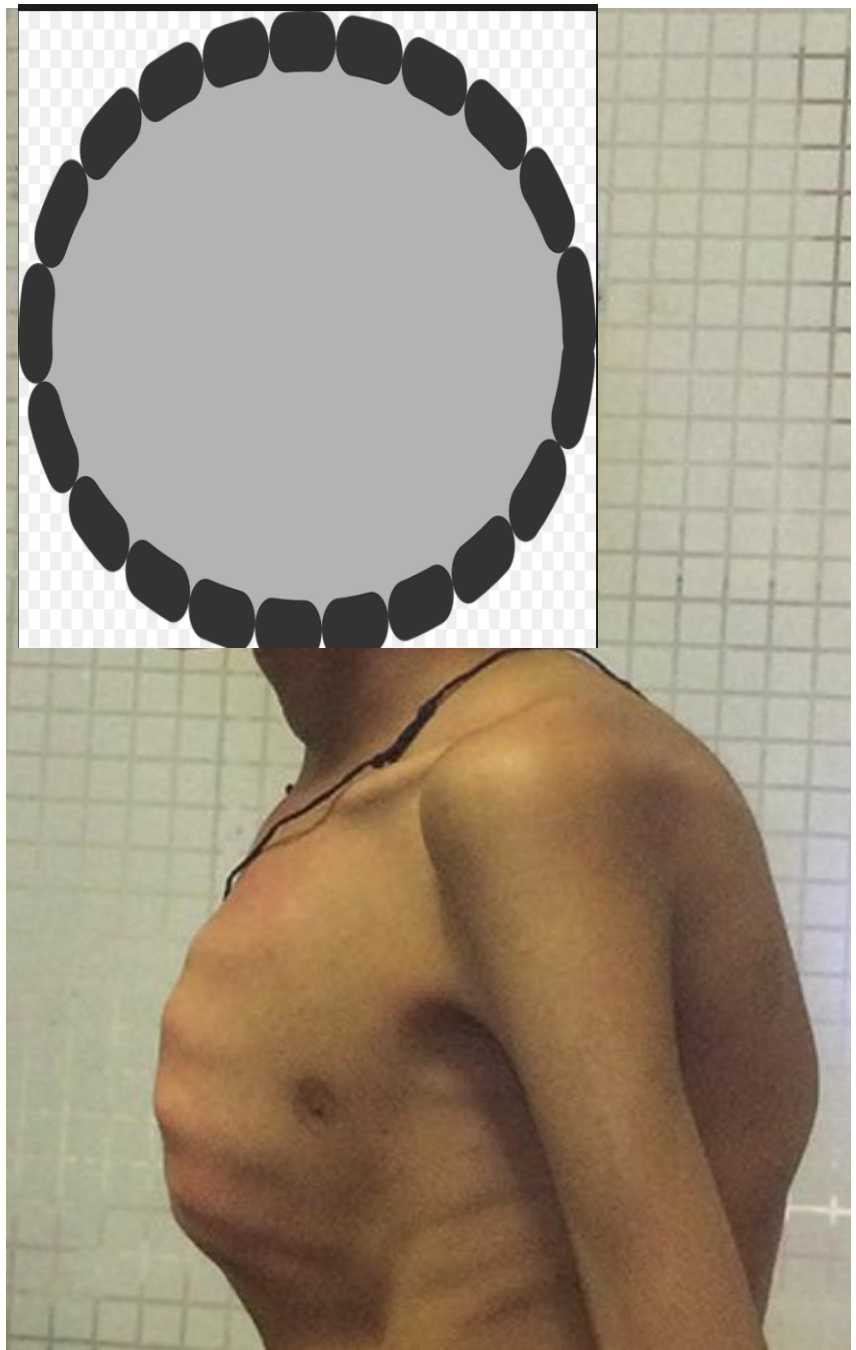

Figure 3

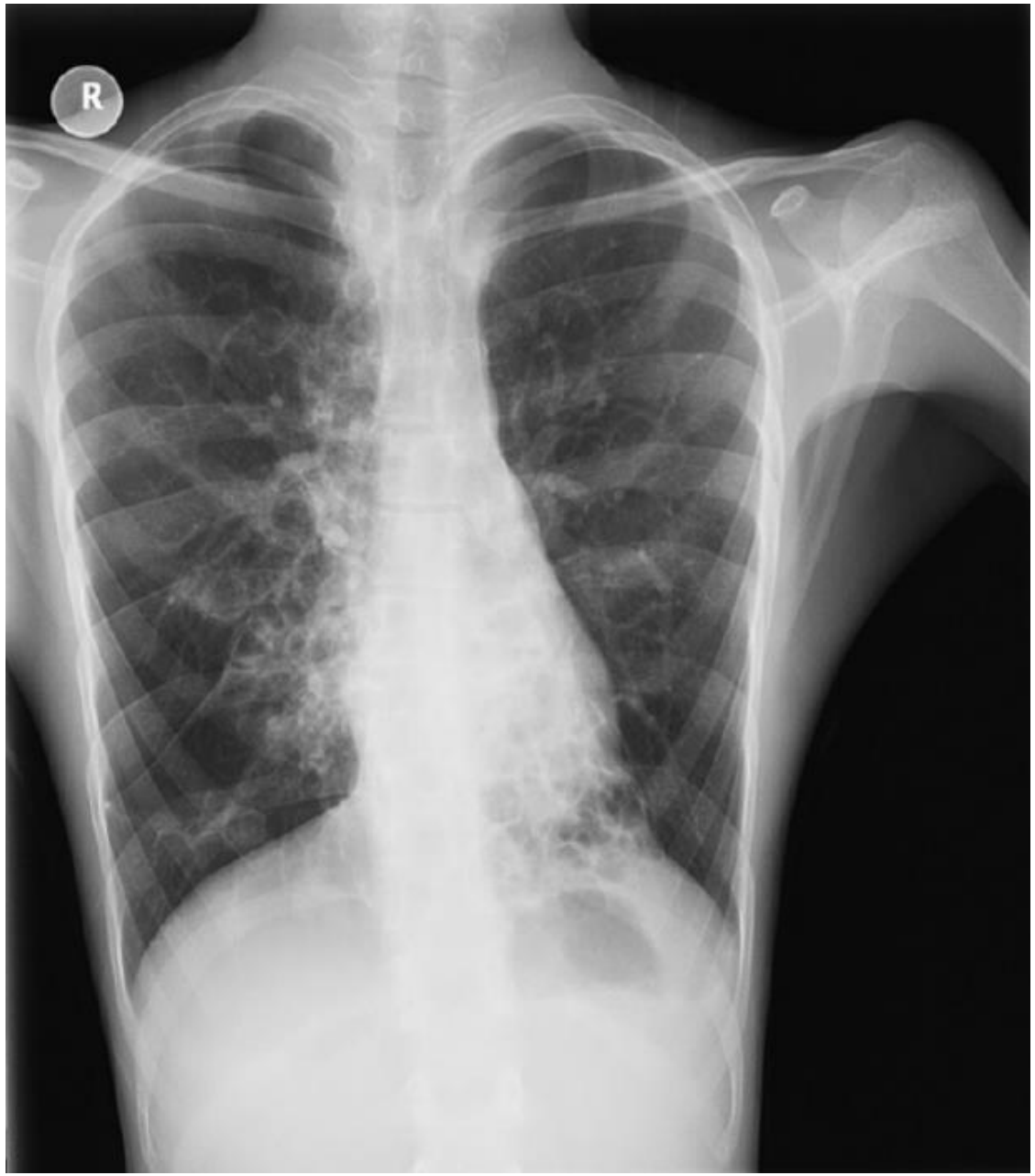

Figure 4

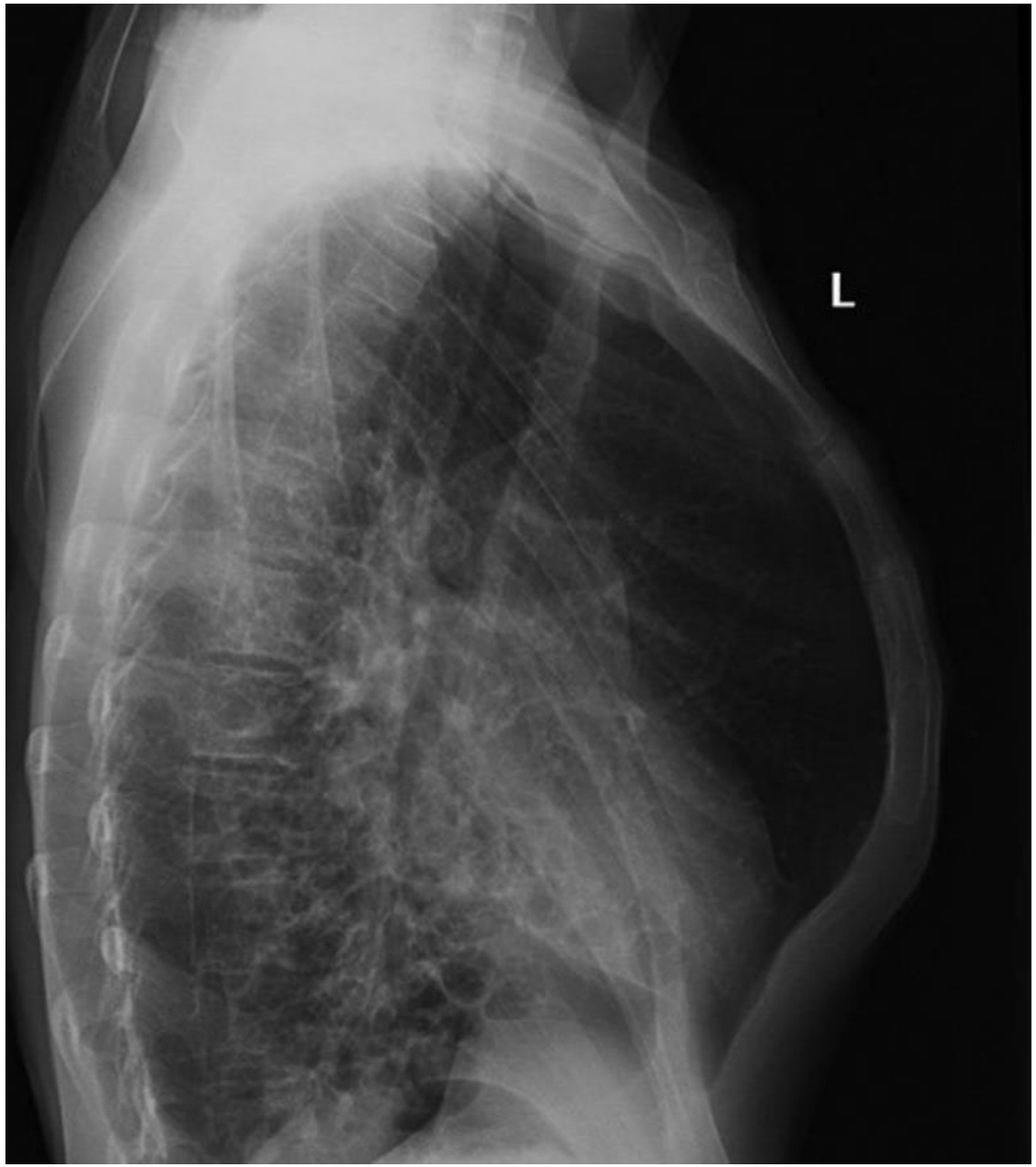

Figure 5 Pigeon chest ECG

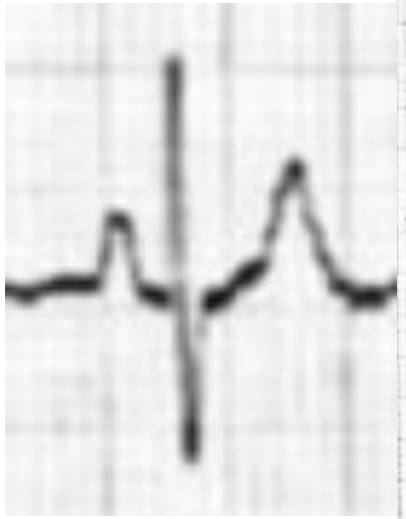

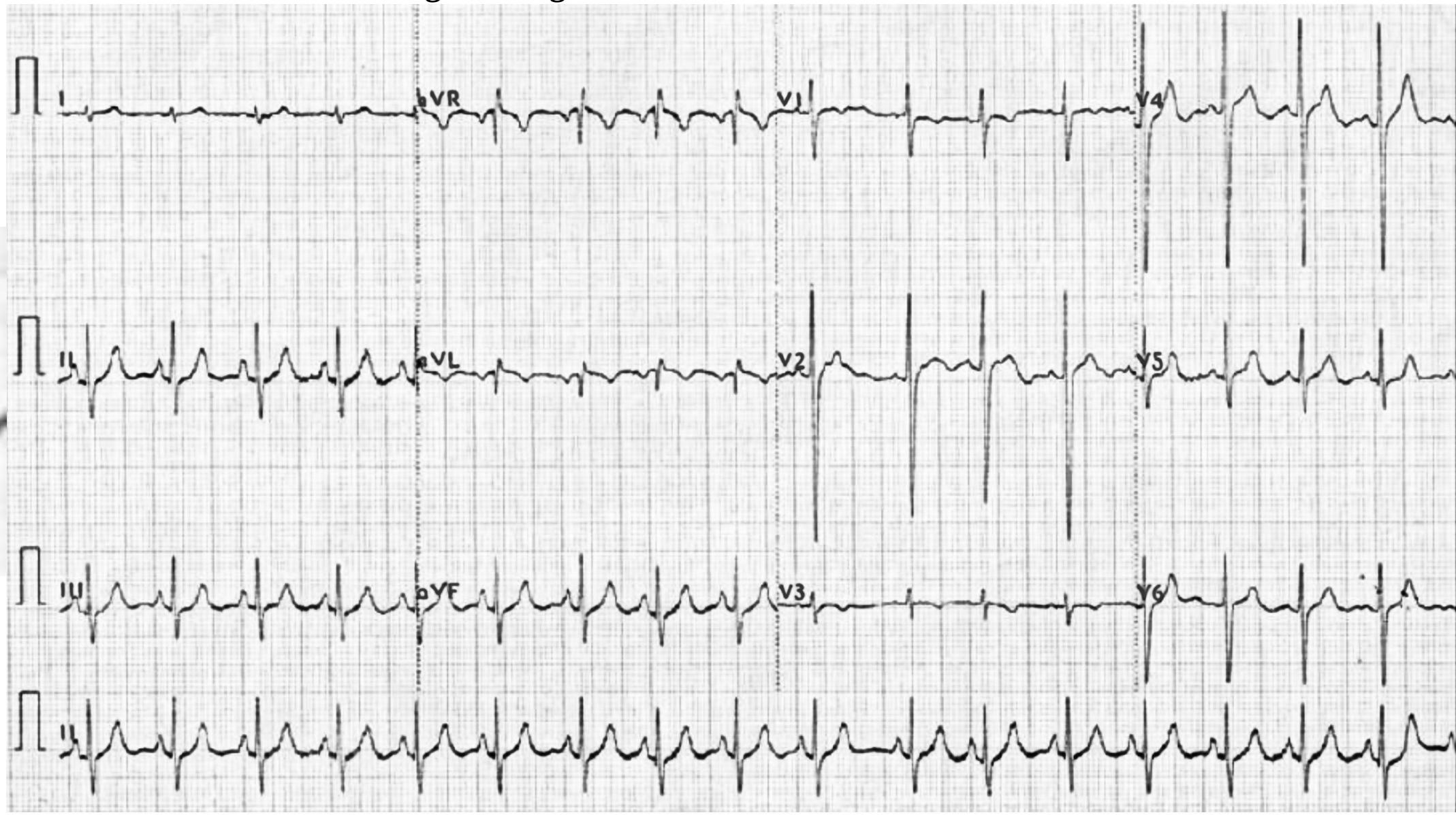

This ECG belongs to a teenager with severe pigeon chest. Note right atrial enlargement, equiphasic QRS complexes in all leads (frontal and precordial leads), QRS perpendicular to the frontal plane: indeterminate axis. Presence Katz-Walchtel's phenomenon of Katz-Walchtel sign **(Katz 1937):** Wide isodiphasic QRS complexes in the intermediary precordial leads. It indicates possible biventricular hypertrophy/enlargement (BVE).

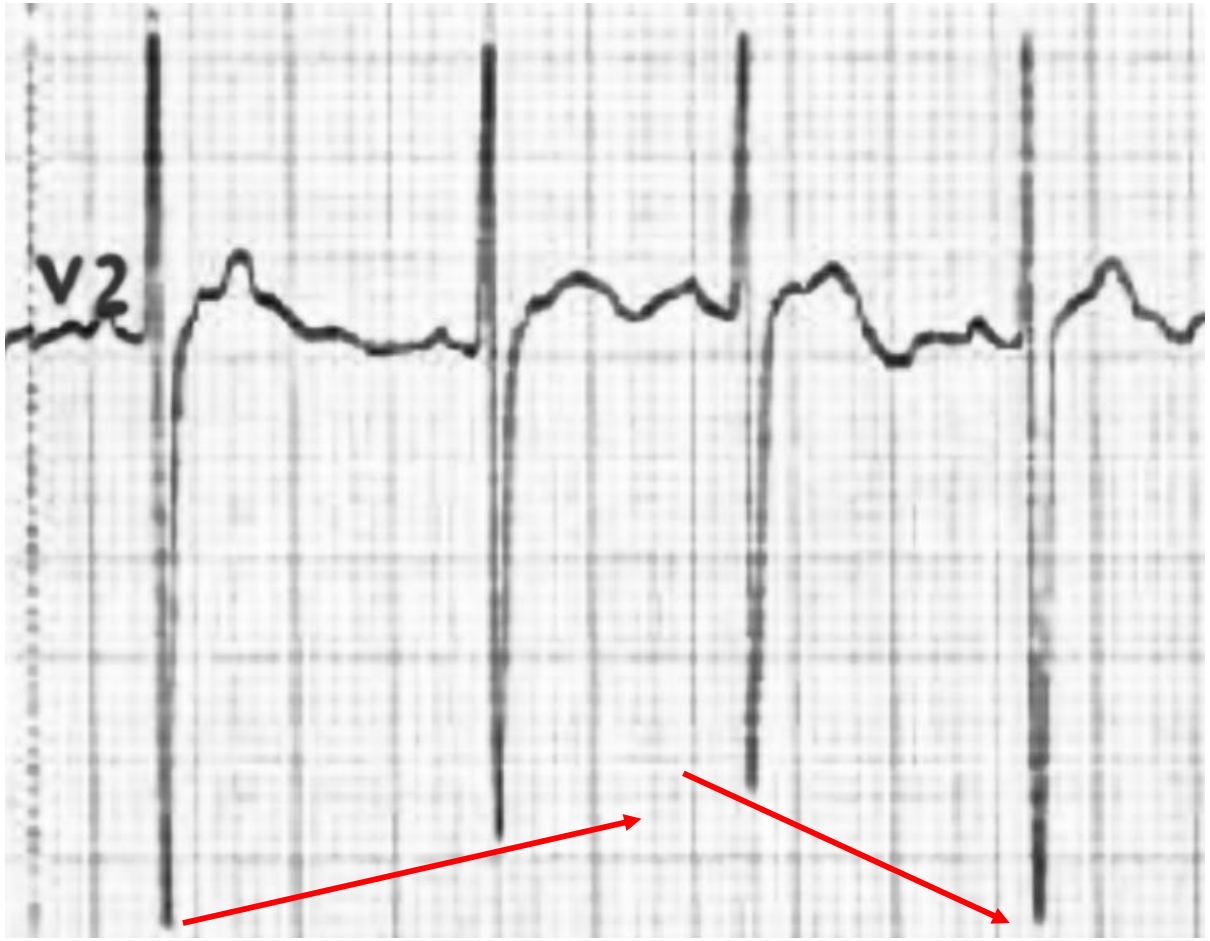

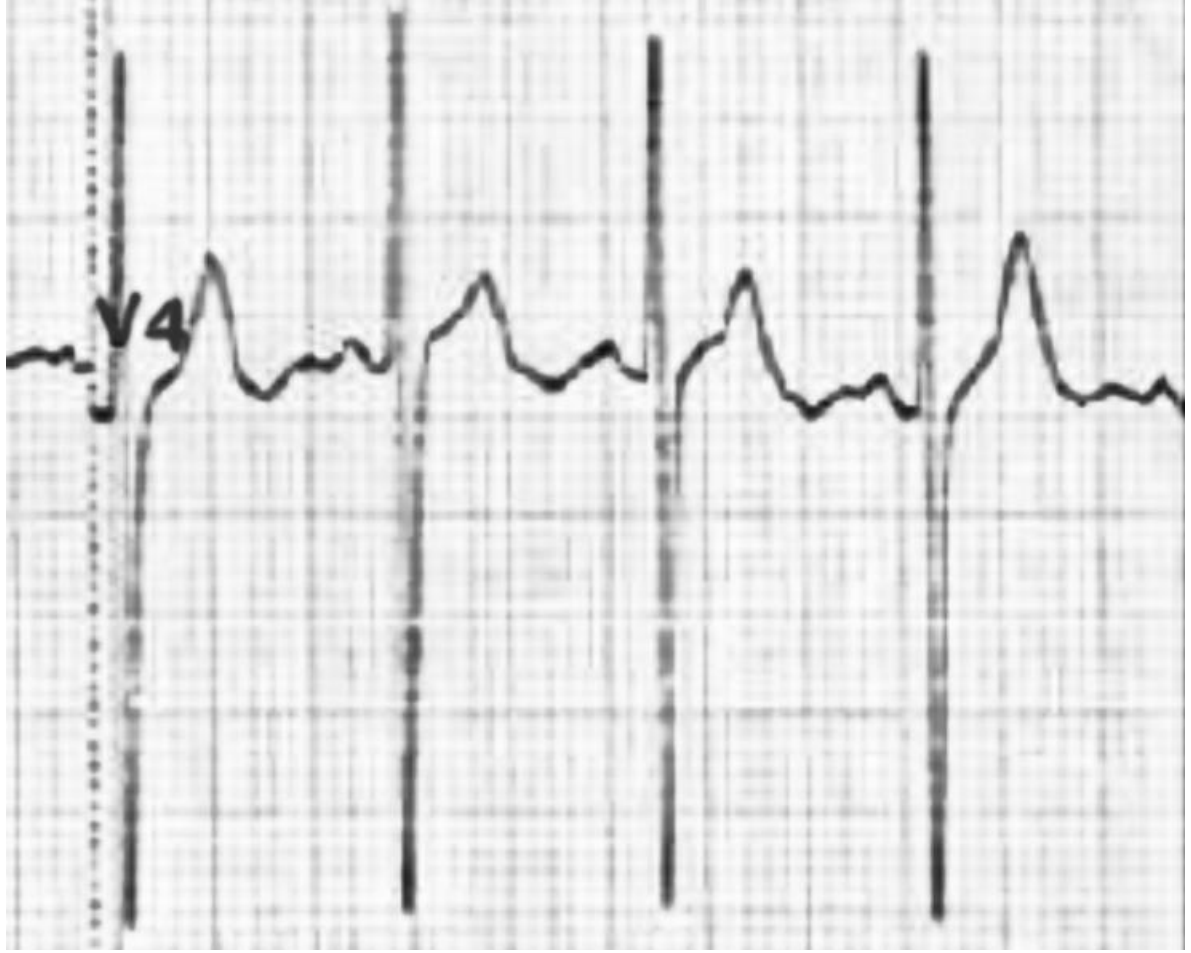

Sign or phenomenon of Katz-Walchtel (Katz 1937) Wide isodiphasic QRS complexes in the intermediary precordial leads. It indicates biventricular hypertrophy. QRS voltage amplitude variations are consequence of respiratory movements.

Modulation of QRS amplitude

Several anatomical and physiological factors determine the amplitudes of the Q, R, and S waves in the ECG of a normal person. These factors include the physical mass of the heart (particularly the left ventricle), the path the electrical current takes as it spreads from the AV node through the conduction system of the ventricles, the position of the recording and ground electrodes on the skin surface, and the position of the heart with respect to the positive (+) and the negative (-) electrodes. To simplify this discussion: The dominant positive R wave is discussed; the Q wave and S wave are not discussed. In the bipolar limb leads (Lead I, Lead II, and Lead III), the Q wave and the S wave are usually negative and low-amplitude compared to the dominant positive R wave. Lead II (right arm (-), left leg (+), right leg (gnd)) is used for explanatory purpose;

During the cardiac cycle, electrical current flows from the SA node through the atria to the AV node, and then from the AV node through the AV bundle, bundle branches, fascicles, and Purkinje fibers to ventricular muscle. The preponderant direction and magnitude of current flow varies from moment to moment, and at any given moment can be expressed as a ***vector***. All of the individual momentary vectors measured during the spread of current through the ventricular conduction system during one cardiac cycle can be summed and expressed as a single resultant vector. The direction of the resultant vector with respect to a horizontal line (±180° / 0°) running through the base of the heart is known as the ***mean QRS axis***, or the mean electrical axis of the ventricles. The magnitude of the resultant vector, measured in millivolts, is known as the ***mean QRS potentia*l**, or the mean ventricular potential. In the frontal plane, the mean QRS axis is typically between 0° and +90°, usually around +50°. The anatomical axis of the adult heart is around +55°, meaning the apex of the heart points to the lower left rib cage. The electrical axis of Lead II is +60°, therefore both the anatomical axis of the heart and the mean electrical axis of the ventricles are usually close to the electrical axis of Lead II. In electrocardiography, electrical current flowing toward a positive electrode results in a positive (upright) waveform display. Electrical current flowing away from the positive electrode results in a negative (downward) waveform display. In Lead II, the R wave is therefore positive. If a positive electrode is placed on the right 4th intercostal space and a negative electrode is placed on the left mid-clavicular line, a lead arrangement designated MCL1, the R wave becomes inverted (negative) because the current is now flowing away from the positive electrode. The amplitude and direction of the R wave depends on the “electrical picture” the recording electrodes “see” as current spreads through the ventricular conduction system. The closer the mean QRS axis is to the electrical axis of Lead II, the larger the amplitude of the R wave. This means that if the anatomical axis of the heart, in other words the position of the heart in the chest, were to shift toward or away from the electrical axis of Lead II, the amplitude of the R wave would increase or decrease.The size, shape, and position of the heart may vary from individual to individual, and also from time to time in the same individual. The variations are related to body type (tall and slender vs. short and stocky), age, posture (prone, supine, sitting or standing), and respiration (quiet respiration vs. deep inspiration and expiration). The position and movements of the diaphragm determine the position of the heart because the pericardium is firmly attached to the central tendon of the diaphragm. With deep inspiration, the diaphragm contracts and becomes flatter and less dome-shaped. As it does, the heart descends, moves backward, and rotates to the right so that it becomes narrower and more vertical. The apex beat is lower and more medial. During deep expiration, the diaphragm relaxes, elevates, and becomes more dome-shaped, and movements of the heart are the converse of those that occur during deep inspiration. The degree of the directional movements of the heart during quiet breathing is similar but reduced compared to deep breathing and, in some persons, may be hardly noticeable.Thus, diaphragmatic breathing cyclically affects the position of the heart with respect to the position of the electrodes on the skin, causing the “electrical picture” the recording electrodes “see” to change, and along with it, the amplitude of the R wave

The hexaxial reference system. Note that the position of each limb lead is calculated according to its position relative to lead I, which is at 0°.

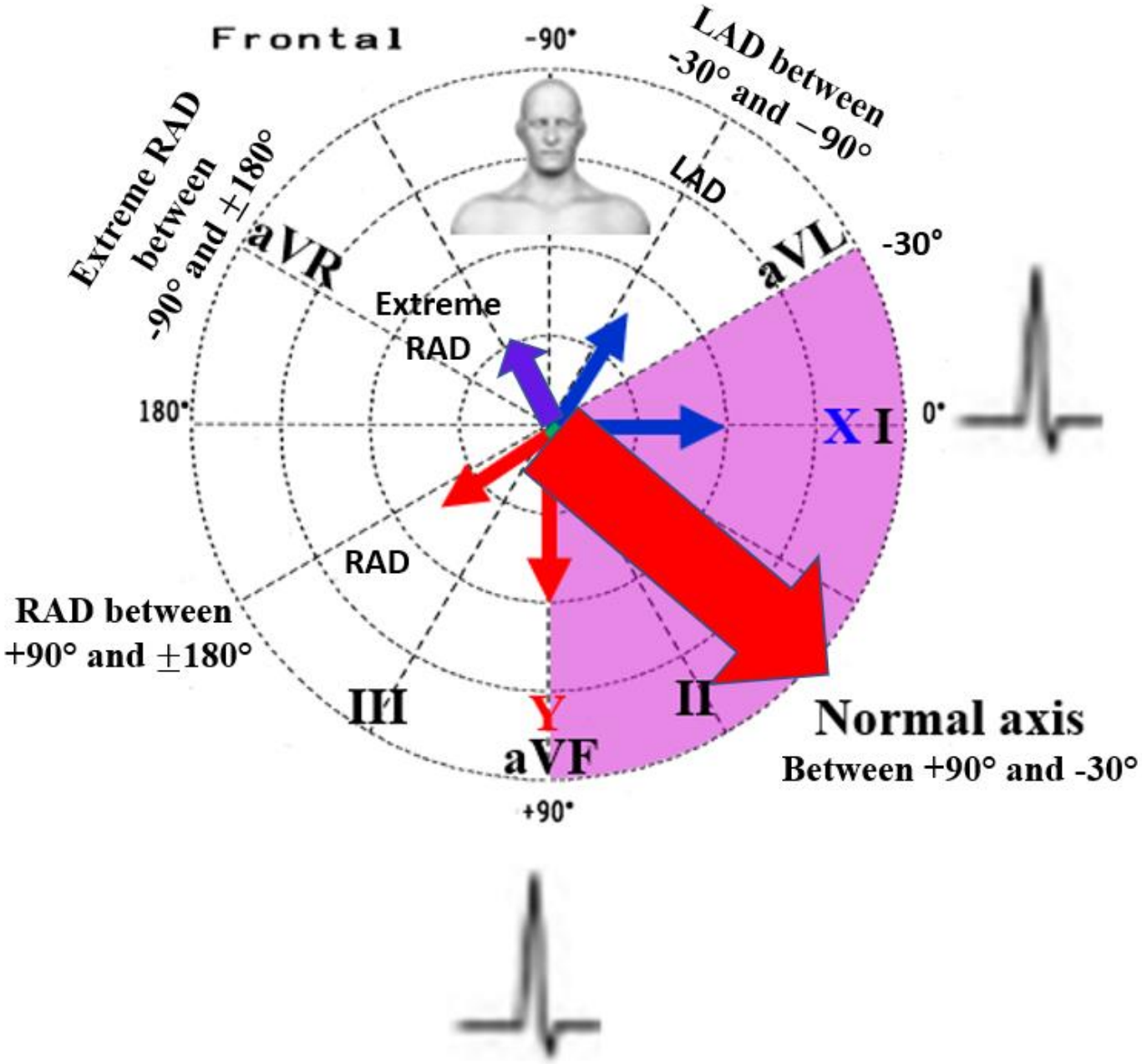

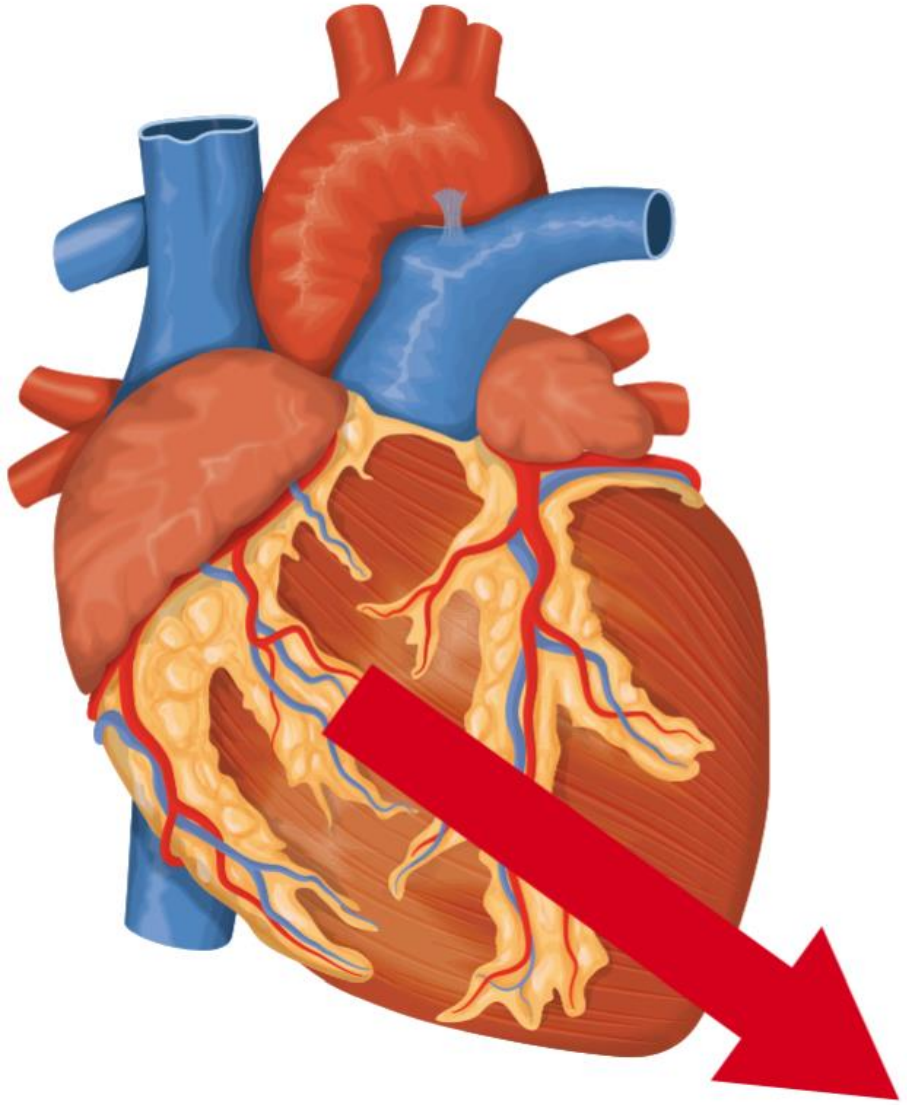

The normal QRS axis in adults is downward and towards the left

ECG/VCG correlation in the right sagittal plane

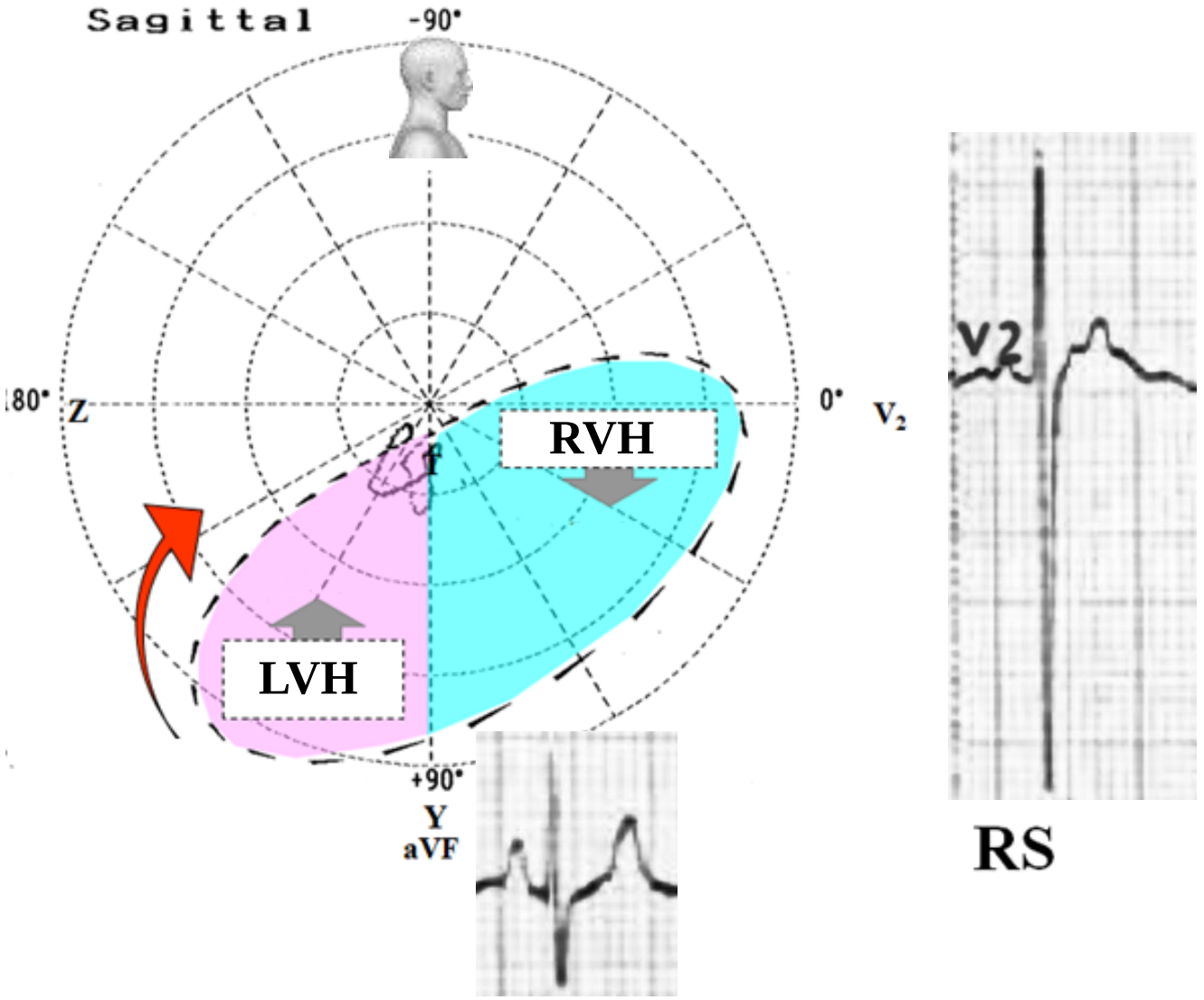

Isodiphasic R=S pattern with great voltage: Katz-Walchtel phenomenon: biventricular or combined ventricular hypertrophy/enlargement. Increase in both anterior (RVH) and posterior (LVH) QRS forces.

Electrical Axis Classification

There are five main electrical axis classifications:

1. Normal Axis
2. Left Axis Deviation (LAD)
3. Right Axis Deviation (RAD)
4. Extreme Axis Deviation, and
5. **Indeterminate Axis: the present case**

There is some disagreement on the exact degrees that define each type, but there are some general cutoffs that can be used for the QRS axis.
The QRS axis moves leftward throughout childhood and adolescence and into adulthood. At birth, the normal QRS axis lies between +30 degrees and +190 degrees. Between the ages of 8 to 16 years, the axis moves leftward with normal lying between 0°to +120° . The normal adult QRS axis is between -30° and +90°, which is directed downward and to the left. This adult range is sometimes extended from -30° to +100°. The following axis classifications described are based on adults. If the QRS axis falls between -30° and -90°, it is considered *LAD*. In this case, the QRS vector is directed upward and to the left. If the QRS axis falls between +90° and 180°, or beyond +100° if the adult range is used, then *RAD* is present. The QRS vector would be directed downward and to the right. If the QRS axis happens to fall between -90° and ±180°, this would be referred to as *extreme axis deviation*, whereby the ventricular vector is directed upward and to the right. Lastly, if the QRS complex is isoelectric or equiphasic in all leads with no dominant QRS deflection, it is considered *indeterminate axis*.

Approach to Determining Axis

There are multiple methods to determine the electrical axis. The following are a few of these simple and adequate approaches to assess the ventricular (QRS) axis. Hence, the focus will be on the QRS complexes in specific leads.
The main QRS complexes to evaluate are those in leads I, II, and aVF. The positive ends of these three leads fall within the normal axis region. The positive ends of leads I, II, and aVF are 0 degrees, + 60°, and +90°, respectively. Therefore, if all three of these leads have positive QRS complexes, the axis is normal.

Method 1. One simple way to learn how to determine electrical axis is to inspect limb leads I and aVF. This is referred to as the quadrant approach or two-lead method. Each of the four quadrants represents 90°, and an axis type. In other words, 0°, to + 90°, is normal axis, + 90°, to 180°, is RAD, 0° to -90° is LAD, and -90° to ±180° is extreme axis. Therefore, if leads I and aVF are both positive, then the axis falls within the normal axis range. If lead I is positive and lead aVF is negative, then there is LAD. If lead I is negative and lead aVF is positive, then there is RAD. And, if both leads I and aVF are negative, then the axis falls within the extreme axis range. This quadrant approach is summarized in Figure3.

One issue with this method is that it only gives a close approximation to the true axis. In addition, it narrows the normal axis range. This can result in an inaccurate interpretation of the true electrical axis. For instance, if using this approach with a positive lead I and negative lead aVF, the axis would be interpreted as LAD. However, if the true axis were -20°, which lies in the LAD quadrant using this method, it would still be within the normal axis range. Nevertheless, this method is easy to learn and sufficient in most cases. One way to resolve these issues is by locating the most isoelectric limb lead and knowing that the true axis lies nearly perpendicular to it. Using this can help narrow the axis down to within 10° of the normal axis.

Method 2. A more accurate approach that the simple quadrant approach takes into account leads I and aVF, as well as lead II. This is referred to as the three-lead method. If the net QRS deflection is positive in both leads I and II, the QRS axis is normal. If the net QRS deflection is positive in lead I, but negative lead II, then there is LAD. Notice that in both cases lead aVF was not needed. In other words, if lead I is positive, look next to lead II. Now, if lead I is negative, look next to lead aVF. If lead aVF is positive, then the axis is rightward; however, if lead aVF is also negative, then there is the extreme axis.

Method 3. Another simple way to estimate the ventricular (QRS) axis is to locate the most isoelectric limb lead along the frontal plane. The isoelectric (equiphasic) lead represents the lead with a net amplitude of zero and smallest overall amplitude. The QRS axis is approximately perpendicular (90 degrees) from the positive pole of that lead.

In order to determine which direction to move 90 degrees from that positive pole, look at the net deflection in another lead. For example, if the isoelectric limb lead is lead II, which has a positive end directed at +60 degrees, then the electrical axis is directed approximately 90 degrees from +60 degrees in either direction. Therefore, the axis can lie at around +150° (RAD) or -30° (borderline LAD). If lead I, with a positive pole at 0°, has a net positive QRS deflection, then the axis will be closer to -30° (LAD); and, if lead I has a net negative QRS deflection, then the axis will be closer to +150° degrees (RAD). Finally, it's important to note that these three methods determine the electrical axis in the frontal plane. There is also a horizontal plane with a horizontal axis. The axis along this plane can be determined by viewing the heart under the diaphragm. The axis can be considered to have a clockwise or counter-clockwise rotation depending on when the transition from mostly negative QRS complexes to mostly positive QRS complexes occurs along the precordial leads (V1-V6). Ideally, this would be the isoelectric precordial lead. Normally, this transition

occurs between leads V3 and V4. If it occurs earlier, it is considered to a counterclockwise rotation and an early transition. This would indicate that the left ventricular forces are directed more anteriorly. On the other hand, if it occurs later in which there is poor R wave progression, then it is considered a clockwise rotation and a late transition. This would indicate that the left ventricular forces are directed more posteriorly.

Key Points

I. QRS axis represents the net direction of depolarization within the ventricles, and is measured using the limb leads. A normal axis lies between -30° and -90°; anything outside of this range is referred to as axis deviation.

II. Axis deviation may be a normal variant, but is often the result of structural or electrical heart disease. Incorrect limb lead placement and dextrocardia also affects axis, and should be suspected when other unusual features such as P-wave inversion and a positive QRS in aVR are seen.

III. Axis is calculated by most ECG machines, This is usually highly accurate, but c should be able to verify axis manually, in case of machine error. Several method can be used, including the quadrant approach and identification of the isoelectric lead.

IV. If all other causes fo axis deviation have been excluded,, a diagnosis of fascicular block may be made, This has important prognostic implications, especially in the patients with co-existing rign bundle bfranch block and first degree AV block. In these individuals, careful evaluation must be made for higher degrees of AV block. If they are found, a pacemaker should be implanted.

	Lead I	Lead II	aVF
Normal axis 0° to 90°	+	+ or -	+
Left-axis deviation 0° to -30° physiological *Left-axis deviation 0° to -30° pathological -30° to -90°*	+	-	-
Right-axis deviation between + 90°to ± 180°	-		+
Extreme-axis right deviation between -90° to ± 180° (Northwest axis "no man's land") or "right shoulder axis" aVR RVOT		+ or -	+-
Indeterminate axis (perpendicular to the frontal plane)	Isoelectric	Isoelectric	Isoelectric

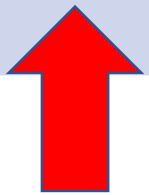

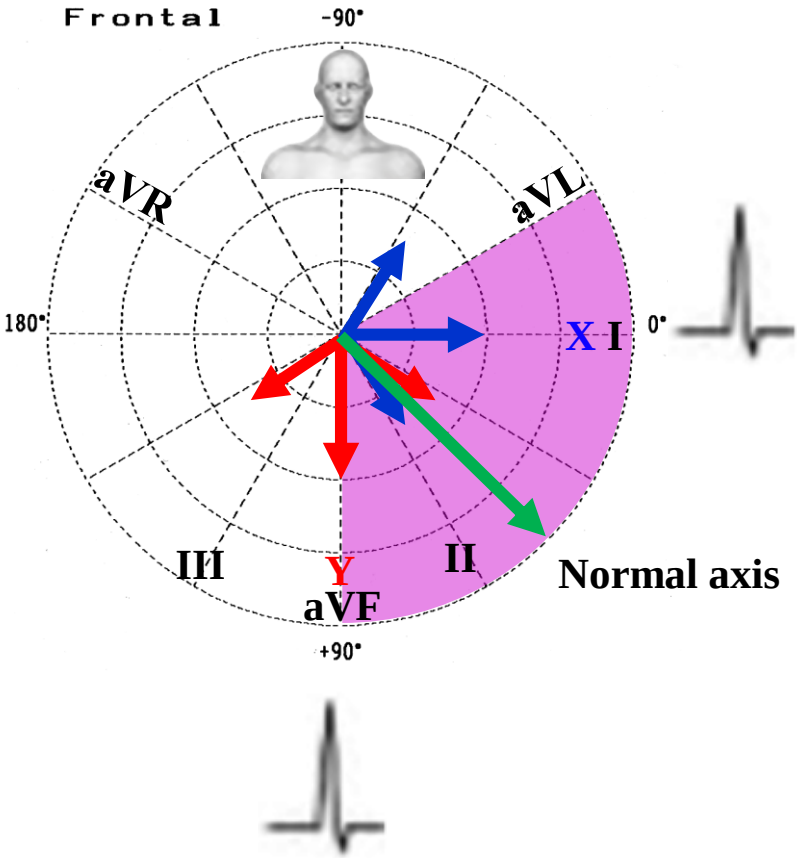

Normal axis

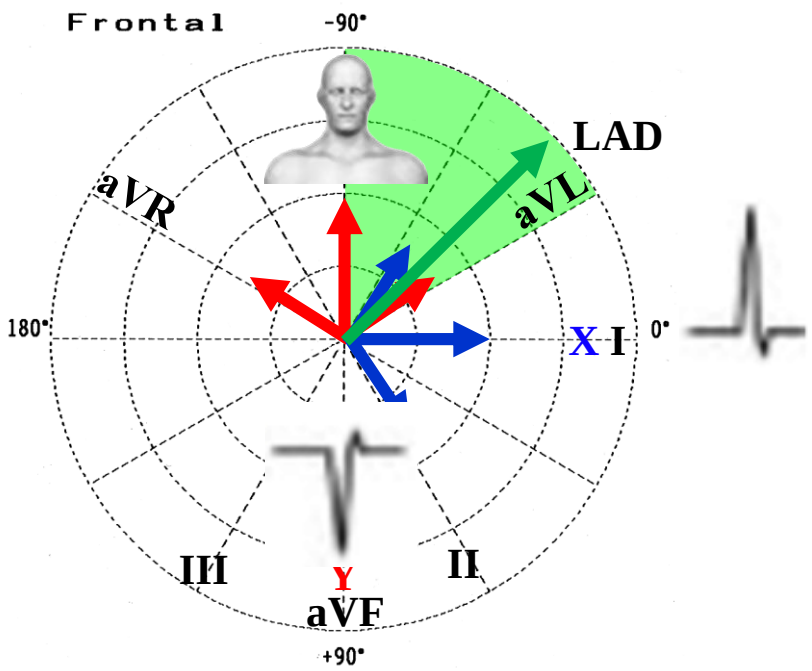

LAD. In early life, the leftward shift of the frontal plane QRS axis is determined chiefly, if not solely, by the relative weights of the ventricles. Once adult ventricular weight ratios are reached, there is a long period of axis stability, then a gradual leftward drift of the QRS, governed principally by LAFB. Consequently, the normal QRS axis is age-dependent, and left axis deviation must be considered accordingly (**Perloff 1979**) LVH, LBBB, Inferior MI, ventricular pacing /ectopy WWW-S, primum ASD – rSR' pattern, LAFB. Horizontally orientated heart. short, squat patient

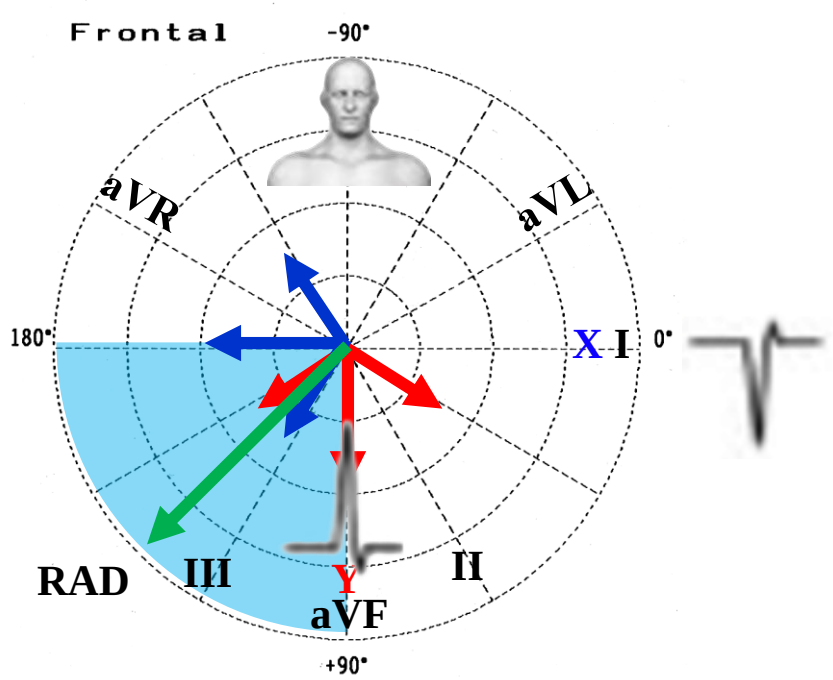

Right-axis deviation (RAD) QRS axis between + 90° to ± 180° Causes: Right ventricular hypertrophy /enlargement type A and B, acute right ventricular strain, e.g. due to pulmonary embolism, chronic lung disease, e.g. COPD Lateral STEMI, hyperkalaemia, sodium-channel blockade, e.g. TCA poisoning Wolff-Parkinson-White syndrome, dextrocardia, secundum ASD – rSR' pattern, Normal pediatric ECG

Left posterior fascicular block (diagnosis of exclusion), vertically orientated heart – tall, thin patient and TCA poisoning

Left -axis deviation (LAD) is defined as QRS axis between - 30° to -90° in adults Causes of LAD include:

1. Normal variation

a. Pregnancy: Slight degrees of LAD have been attributed to a horizontal heart position resulting from the mechanical effects of abdominal distension, such as the physiological event of pregnancy.(**Schwartz 1979**)

b. Healthy children. LAD defined as a mean frontal QRS complex axis between -30° and -90° has a rate of 0.4% and 1.4% **(Calcaterra 1989) (Gup 1965)**

2. Centripetal obesity defined as increased waist-to-hip and waist-to-thigh ratios, waist circumference and sagittal abdominal diameter, which is accompanied by an increased risk of cardiovascular disease. Visceral and central abdominal fat and waist circumference show a strong association with type 2 diabetes

3. Left Anterior Fascicular Block: Frontal plane with QRS axis between −45° and −90°.(**Surawicz 2009**). Because the QRS axis may be ≤45° in cases of incomplete LAFB, the degree of left axis deviation required for the accurate diagnosis of complete LAFB is ≥45°.(**Rosenbaum 1968; Rosenbaum 1970; Elizari 2007**). **Frontal plane criteria:** Extreme shift of SÂQRS in the left superior quadrant (beyond 30° up to - 90°). Some authors accept between - 45° and – 90° (**Elizari 2012**); rS in II, III and aVF. If SÂQRS was in -30° II would be R = S; r III > r II (it indicates CCW rotation in the FP). The voltage of the r waves is 3 to 5 mm in average; SIII > SII: this criterion differentiates it from RECD of the right branch and SI-SII-SIII syndrome, where SII > SIII; qR pattern in I and aVL; Frequent notch of the descending limb of R wave in I and aVL (this sign would be present in 80% of the cases); R-peak time in aVL ≥ 45 ms; aVR always begins with q or Q wave: qR, QR or Qr. QS is rare; Possible notch in R wave of aVR; QRS duration <120 ms. **Horizontal plane criteria (Elizari 2007):** This plane is very little affected when compared to the frontal plane; Possible dislocation to the left of the transition area: normally it is in V3 and V4. In LAFB it may

3. be in V5 and V6; Voltage decrease of R wave and concomitant increase in S wave depth in V5 and V6, as a consequence of the superior dislocation of the forces; Possible pattern of pseudo anterior infarction with appearance of q wave in the right precordial leads, as a consequence of the initial forces heading below and back. In case of doubt, recording one intercostal space below removes the q wave from pseudo infarction (**McHenry 1971**). The congenital entities that may show the pattern of LAFB are: Endocardial cushion defects: LAFB + RBBB + BVH (**Brandenburg 1956**), Complete A-V canals of Down's Syndrome/Primum atrial septal defect(AVSD) (**Caro 2015**).

Normal intraventricular conduction system

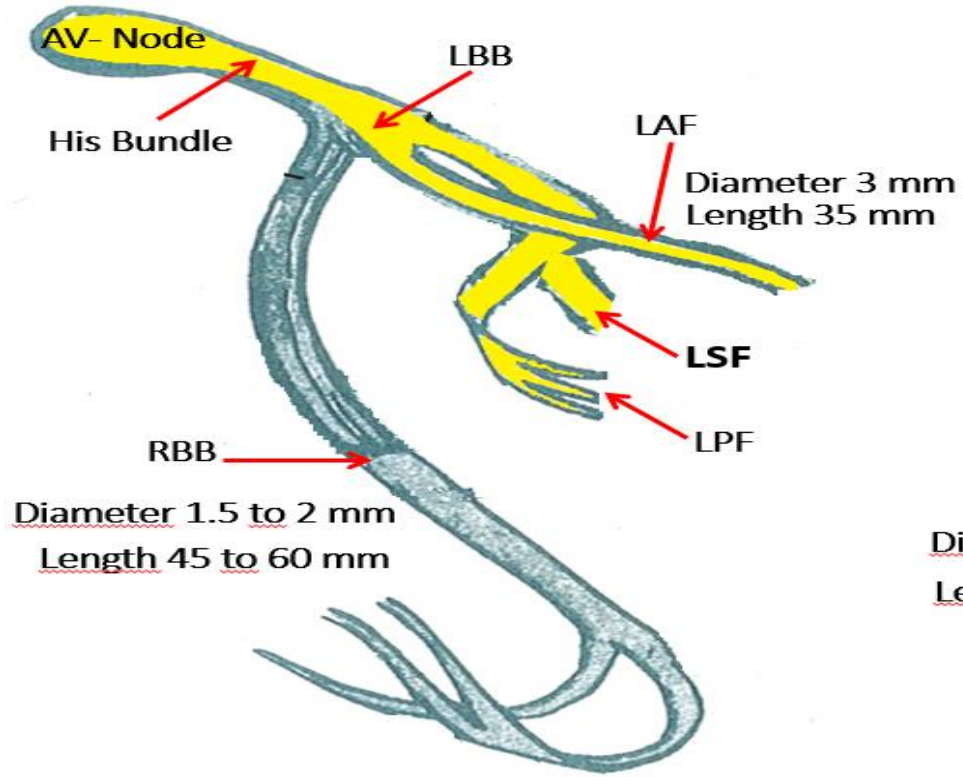

Anatomical alterations of the intraventricular His system in endocardial cushion defects (Caro 2014)

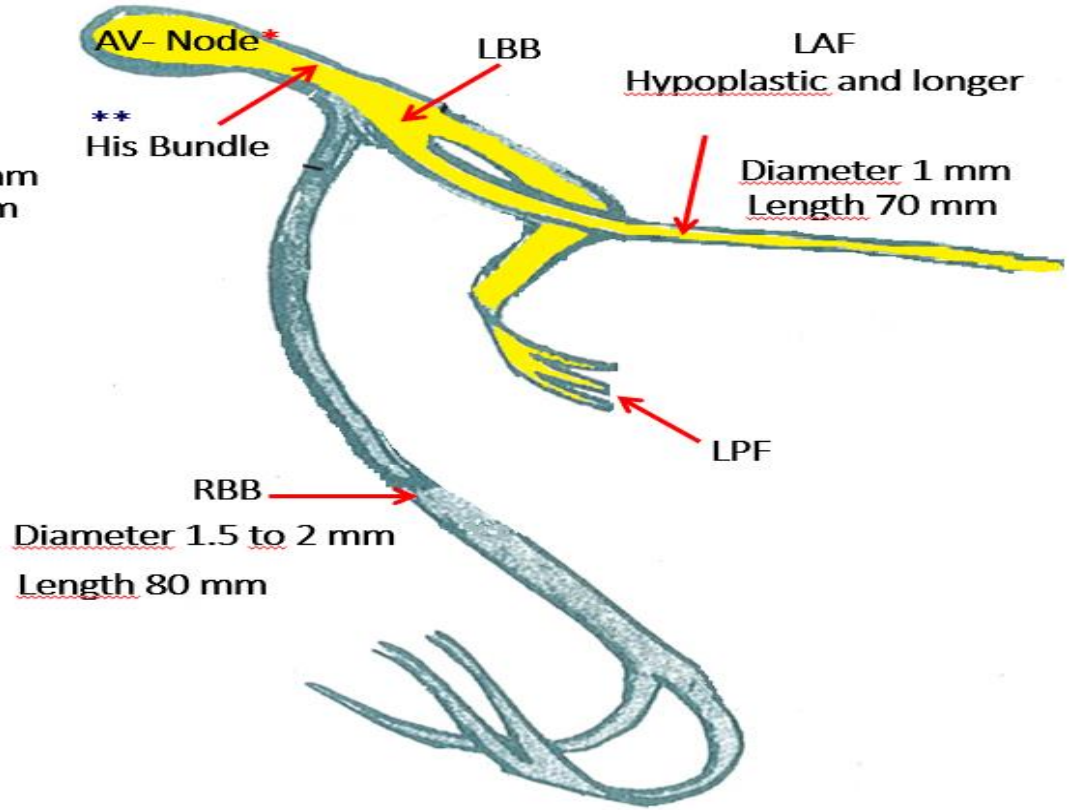

***AV Node in dorsal position related to the normal one; ****shorter His bundle and shifted backward LBB = Left Bundle Branch; RBB = Right Bundle Branch; LAF = Left Anterior Fascicle; LPF = Left Posterior Fascicle; LSF: Left Septal Fascicle**

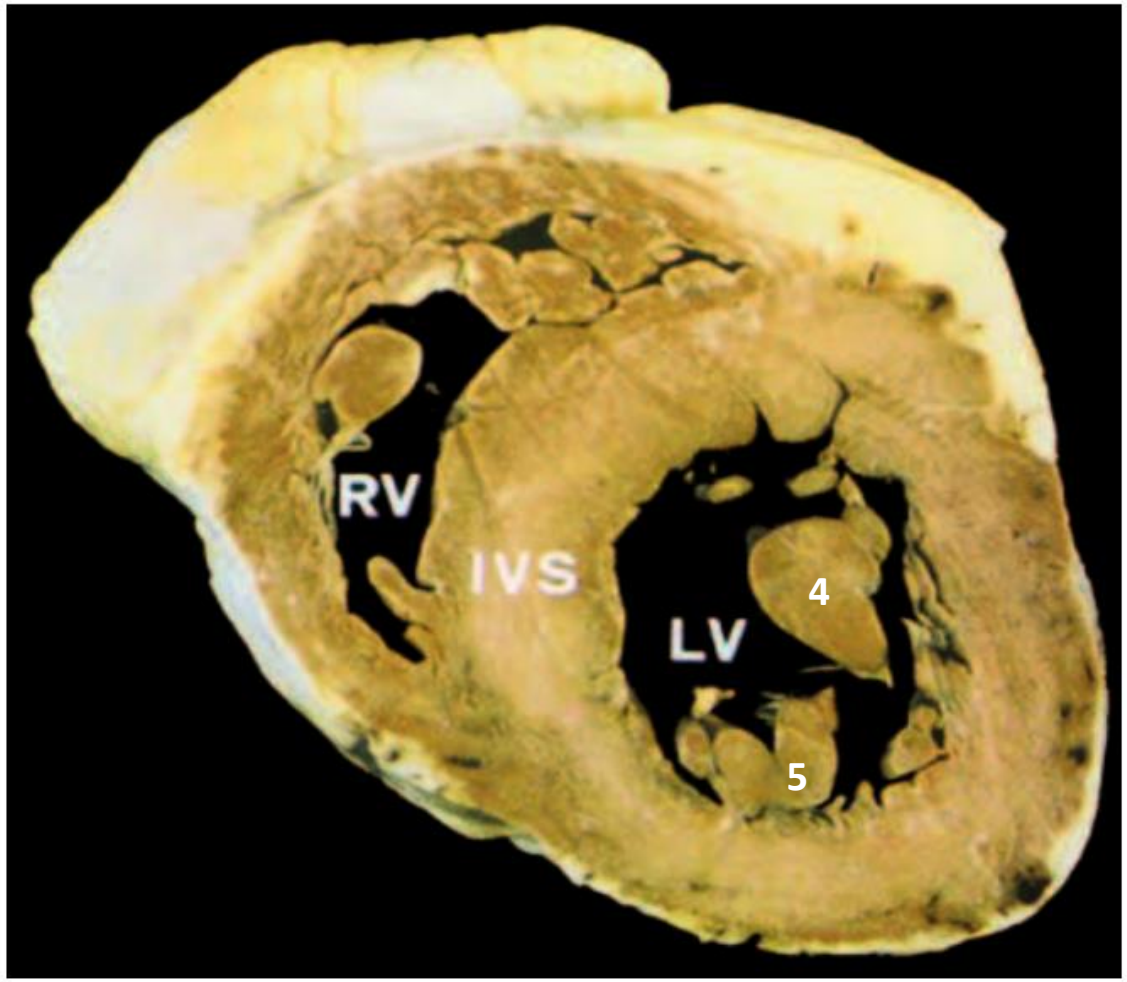

Normal position of Papillary Muscles

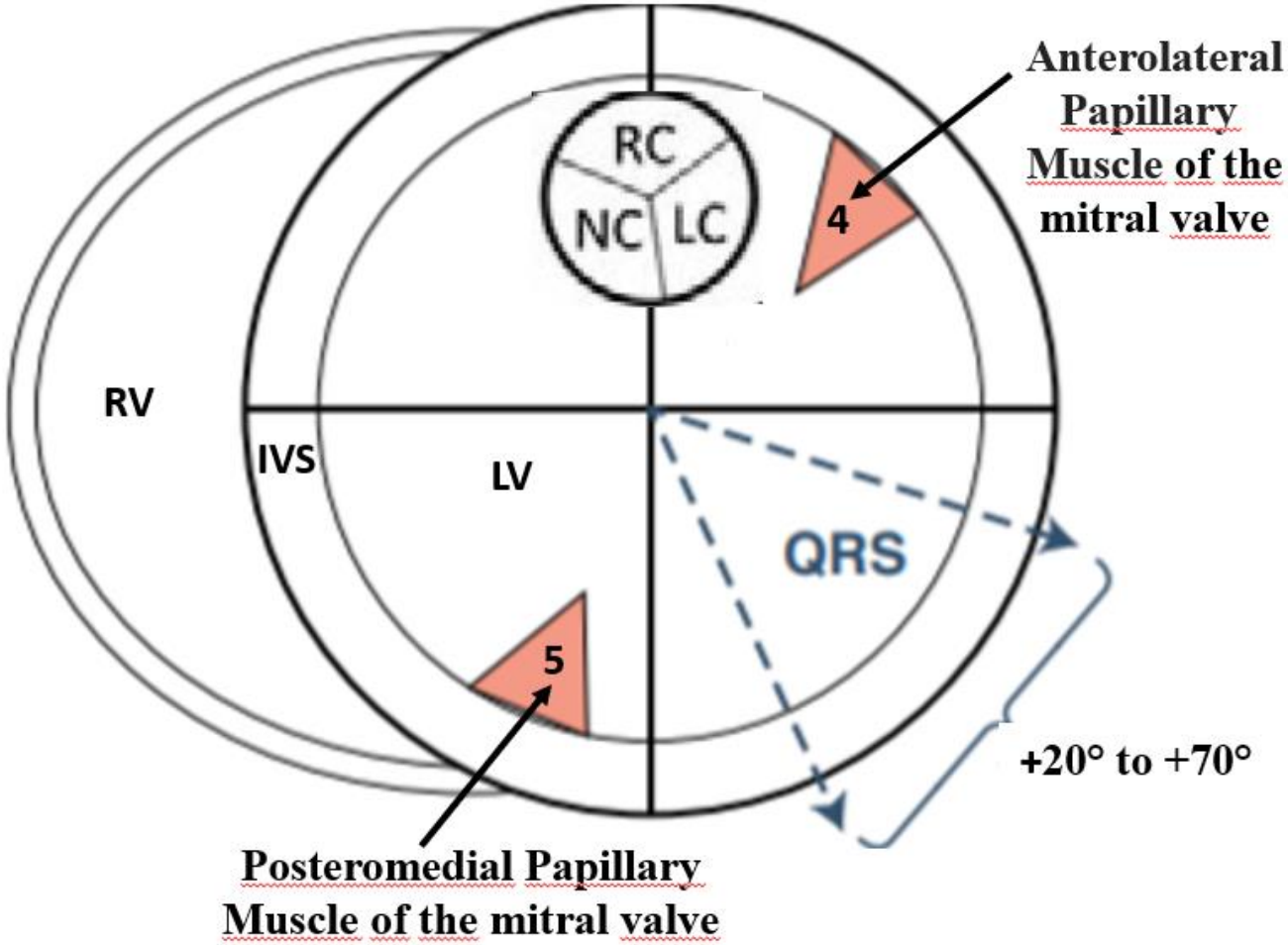

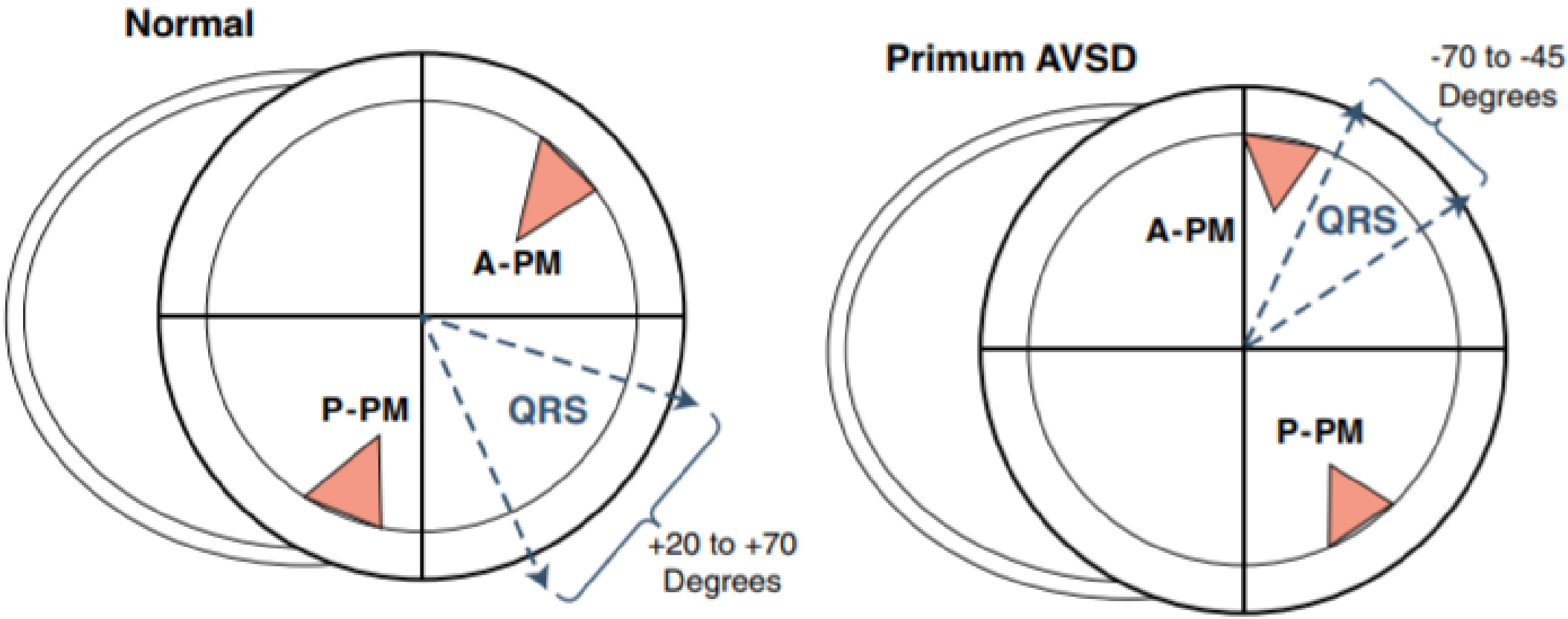

This figure emphasizes the presence of electroanatomic relationships and the difference in those relationships between normal subjects and primum AVSD patients. The frontal ECG plane, represented as a horizontal and vertical line, is superimposed on the short-axis view of the heart. The PMs are shown as triangles. The area between the 2 arrows represents the mean 1 SD of the QRS axis direction. In normal subjects, the P-PM is positioned closer to the septum than the A-PM. In contrast, in primum AVSD patients, imbalance of the PMs is present, with P-PM further from the septum than A-PM. Associated with this, the QRS axis is deviated inferiorly in normal subjects and leftward in primum AVSD patients. This electroanatomic relationship can be explained as follows. Because LBB block fascicles cover the septal area between PMs, PMs reflect borders of the LBB block fascicles. The area not covered by the LBB block fascicles is depolarized slowly, cell by cell, and causes deviation of the average QRS axis to that direction. This area can be appreciated to be inferior in normal subjects and more superior in primum AVSD patients. Deviation of the QRS axis therefore can be appreciated to be inferior in normal subjects and leftward in primum AVSD patients. LBB left bundle branch.

Ostium Atrium Ventricularis Comunis (OAVC) total form

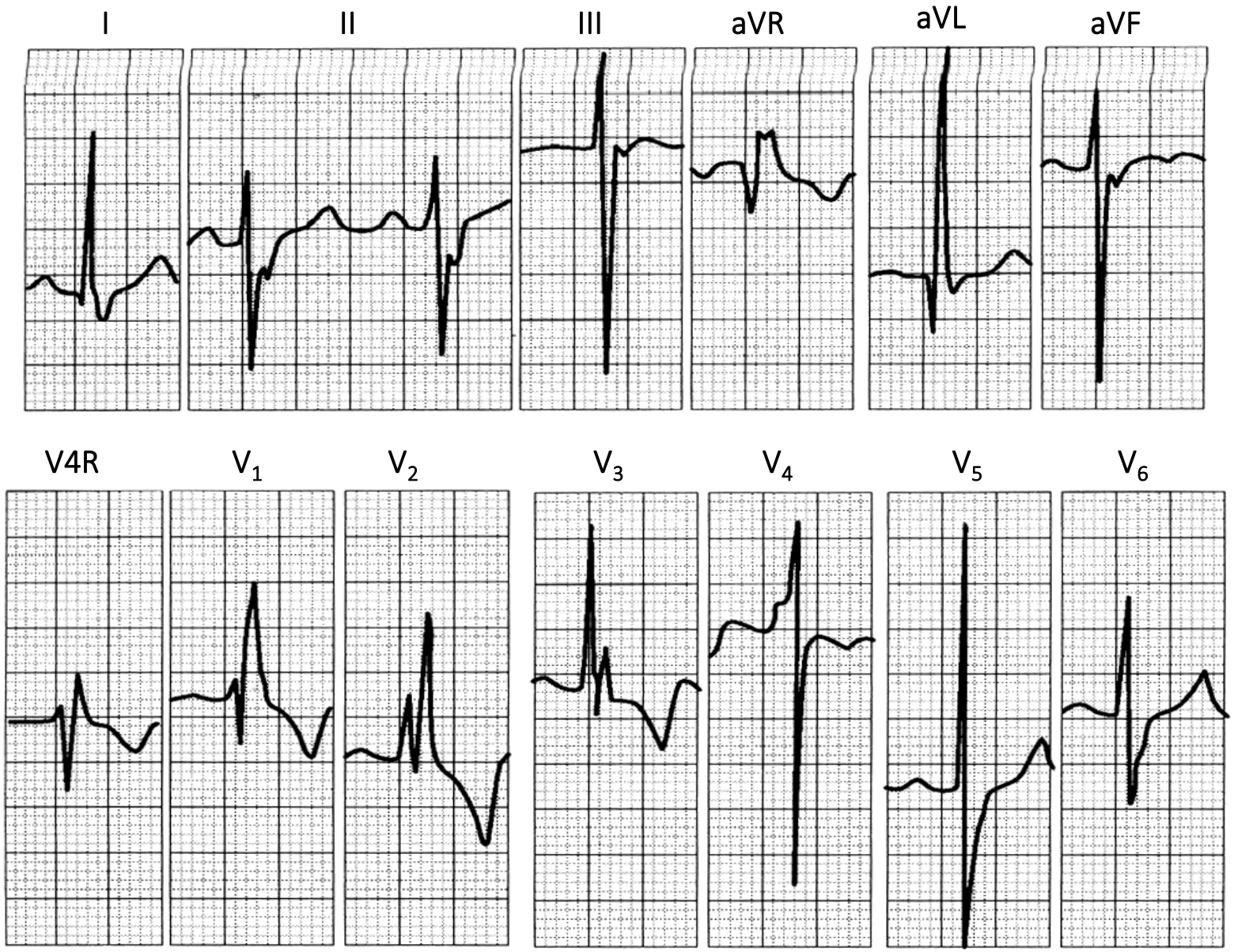

Typical ECG of endocardial cushion defects: 1st degree AV block, biventricular enlargement. Right bundle branch block and left anterior fasicular block. 1st degree AV block + BVE + CRBBB + LAFB

ECG/VCG correlation: LAFB in the FP and Grishman-type CRBBB in the HP

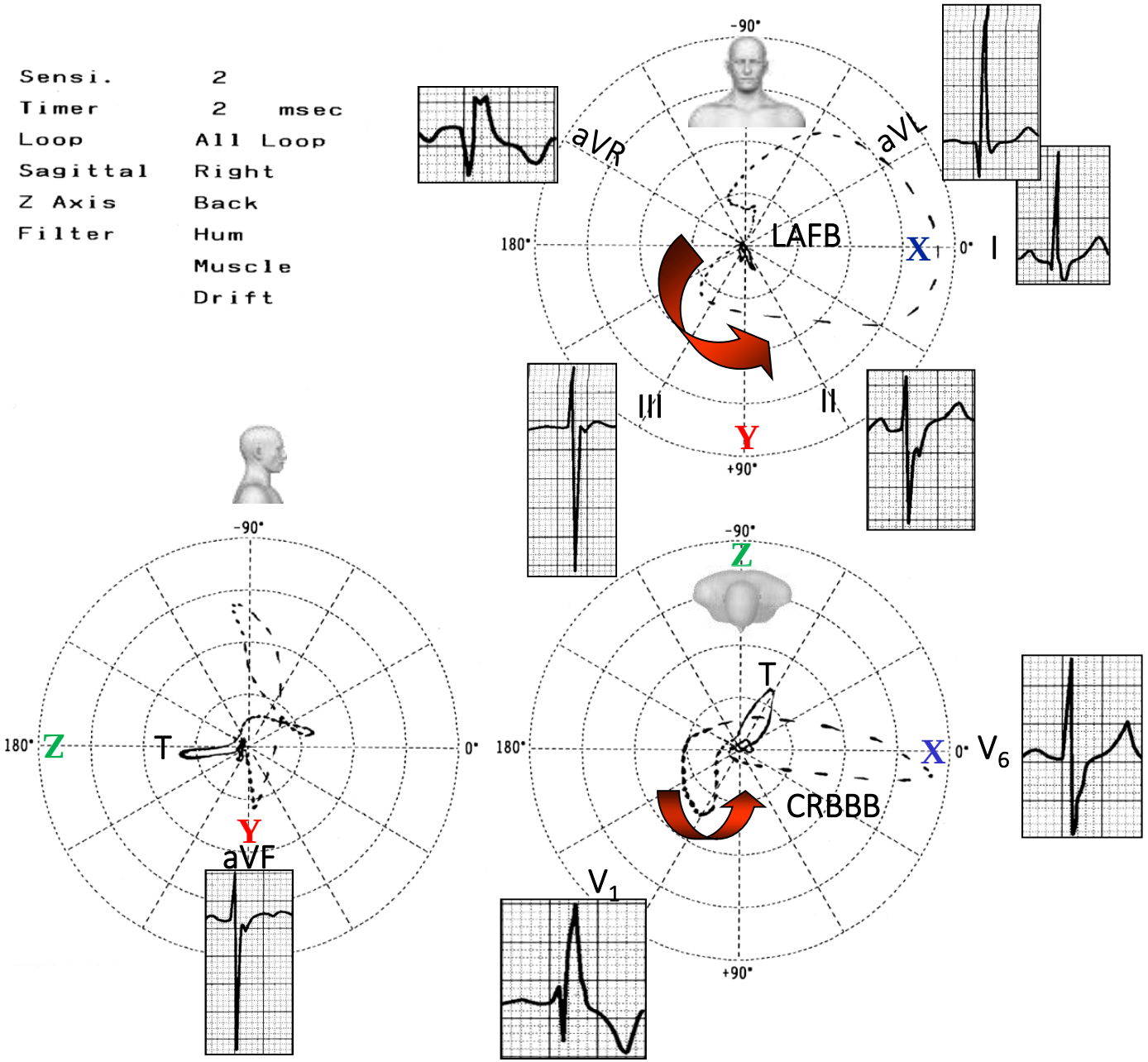

Atrioventricular canal defect. (AVCD)/endocardial cushion defect, the highest reported prevalence 82.9% have an imbalance in the positions of the left ventricular papillary muscles compared with healthy subjects, and that this anatomic imbalance correlates with LAD. The imbalance of papillary muscles correlated with LAD (**Hakacova N, 2009**); Ventricular septal defect (VSD) ranges from 6.2 to 20.3% depending on the location of defect . In patients with clinical findings of VSD, the existence of abnormal LAD especially if it is associated with mild RVH, should raise the possibility of perimembranous VSD with VSA formation. (**Tutar 2001**);Tricuspid atresia: the prevalence of LAD is as high as 81%, RAE or BAH + LVH + LAFB + cyanosis (**Reddy 2003**); Hypertrophic cardiomyopathy: 30% of the cases (**Pérez-Riera 2013**). Large Q and S waves in lead III distinguished athletes from patients with HCM, independent of axis and well-known ECG markers associated with HCM. The correlation between IVS thickness in patients with HCM and III_{Q+S} suggests a partial explanation for this association; Persistence of arterial canal (PAC) of rubella syndrome (**Mirowski 1962**); Univentricular heart with infundibulum to the right (**Davachi 1969**); Anomalous origin of the left coronary artery of the pulmonary artery truncus or Bland-White-Garland syndrome (**Lipoff 1988**); Transposition of the great arteries, congenitally corrected (**Daliento 1986**) Transposition of the great arteries (**Rautenburg 1983**.); Double outlet RV with subaortic VSD without PS (**Krongrad 1972**); VSD: 15% - mainly to basal posterior location;(**Feldt 1970**), Post-operative of total correction of tetralogy of Fallot with septal approach pathway (in this case, associated to CRBBB: Bifascicular Block) (**Pietrzak 2012**). It was observed in 12.3% of the cases (**Basagoitia 1991**).

4. **Left Bundle Branch Block (LBBB)** and LAD patients may have poor response to resynchronization therapy (CRT). LBBB and LAD patients show a specific pattern of mechanical asynchrony. Patients with HF, presenting LBBB and LAD, show a specific pattern of ventricular asynchrony, with latest activation at anterior wall. This finding could affect target vessel selection during CRT procedures in these patients(**Sciarra 2018**). According to electrical axis of QRS complex in the Frontal Plane LBBB

   a. With QRS axis not deviated: between -29° and +60° (≈ 65% to 70% of cases)

   b. With QRS axis with extreme deviation to the left: beyond –30⁰: between -30° and -90° (**Parharidis 1997**) (≈25% of cases). The presence of LAD had a 41.9% sensitivity and a 91.6% specificity for the presence of organic heart disease. Aortic valve disease in LBBB pts seems to be frequently accompanied by left axis deviation. In LBBB patients, those without left axis deviation seem to benefit more from cardiac resynchronization therapy with defibrillator (CRT-D) than those with left axis deviation**(** **Brenyo 2013**).

   c. With QRS axis deviated to the right: between +60° and +90° (≈ 3.5 a 5% of case

   d. With QRS axis with extreme deviation to the right: beyond +90° (< than 1% of cases). It is named "paradoxical type of Lepeschkin" (**Lepeschkin 1951**). The majority of subjects had dilated cardiomyopathy with biventricular enlargement (**Childers 2000**). The uncommon combination of LBBB and right axis deviation is a marker of severe myocardial disease, specially primary congestive cardiomyopathy. The mechanism of production of this ECG pattern appears to be diffuse conduction system involvement in advanced myocardial disease (**Nikolic 1985**). Causes that determine paradoxical complete LBBB:

      I. Complete LBBB associated to right ventricular hypertrophy/enlargement or severe cardiomyopathy with biventricular enlargement. or diffuse advanced myocardial disease.(3) >98% of cases. Ominous prognosis;

II. Fascicular Complete LBBB (LAFB + LPFB) with a higher degree of block in the posteroinferior fascicle. In presence of AF LBBB with intermittent right axis deviation is explained by an additional LPFB accompanying predivisional LBBB (**Patenè 2008; 2012**)

III. LBBB in Wegener granulomatosis (**Khurana 2000**)

IV. Complete LBBB associated to lateral myocardial infarction

V. Complete LBBB with accidental exchange of limb electrodes

VI. Complete LBBB associated with true dextrocardia (**Salazar 1978**)

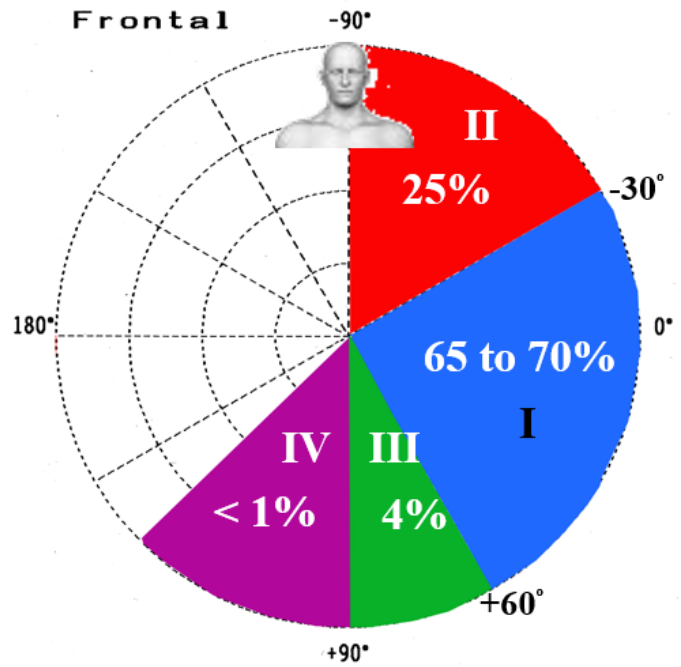

With QRS axis not deviated: between -30° and +60° (≈ 65% to 70% of cases)

With QRS axis with extreme deviation to the left: beyond –30⁰ (≈25% of cases)

With QRS axis deviated to the right: between +60° and +90° (≈ 3.5 a 5% of cases)

With QRS axis with extreme deviation to the right: beyond +90° (< than 1% of cases). It is named "paradoxical type of Lepeschkin“ (**Lepeschkin 1951**). Causes that determine paradoxical complete LBBB.

Perrotta et investigate the prognostic impact of QRS axis deviation (AD) in HF patients with LBBB undergoing CRT. The authors retrospectively evaluated 707 HF patients with LBBB who underwent CRT at five centers. Baseline QRS axis was defined as normal (NA: -30° to 90°), right axis deviation (RAD: 90° to 180°) and left axis deviation (LAD: <-30°). The primary endpoint was a composite of all cause death/HF hospitalization. The risk of endpoint by AD was evaluated with both Kaplan-Meier and Cox proportional hazard analysis. Among 707 patients 46% had NA, 359 (51%) LAD, and 25 (3.5%) RAD. Baseline clinical characteristics were similar between the three groups. Over a mean follow-up of 32 ± 25 months, 141 deaths occurred (21%) and 36% (n = 255) met with the composite endpoint. A significantly higher proportion of RAD patients (52%) reached the endpoint (LAD 40%, NA 30%). KM analysis showed that RAD and LAD patients had worse event free survival and in multivariate analysis both LAD and RAD were independently associated with worse clinical outcome. Right or left axis deviation in the presence of LBBB in HF patients undergoing CRT are independent predictors of poor prognosis (**PerrottaL 2016).**

5. **Hypertrophic cardiomyopathy:** Large Q and S waves in lead III distinguished athletes from patients with HCM, independent of axis and well-known ECG markers associated with HCM. The correlation between IVS thickness in patients with HCM and III_{Q+S} suggests a partial explanation for this association. Large Q and S waves in lead III are observed in patients with HCM, and IIIQ+S (the sum of the Q and S waves in lead III) exhibits correlation with septal wall thickness on echocardiography. Addition of IIIQ+S>1.0 mV to the International Criteria improves sensitivity of HCM detection without sacrificing specificity (**Froelicher V,**)

6. **Inferior wall myocardial infarction:** LAFB development during AIMI can be an indicator of LAD lesions, multivessel coronary artery disease, and impaired left ventricular systolic function. (**Ozdemir 2001**). Additionally, proximal dominant RCA with inferior infarction is extensive, and it compromises the whole inferior wall, thus explaining the absence of r or R wave in II, III and VF and superior QRS axis

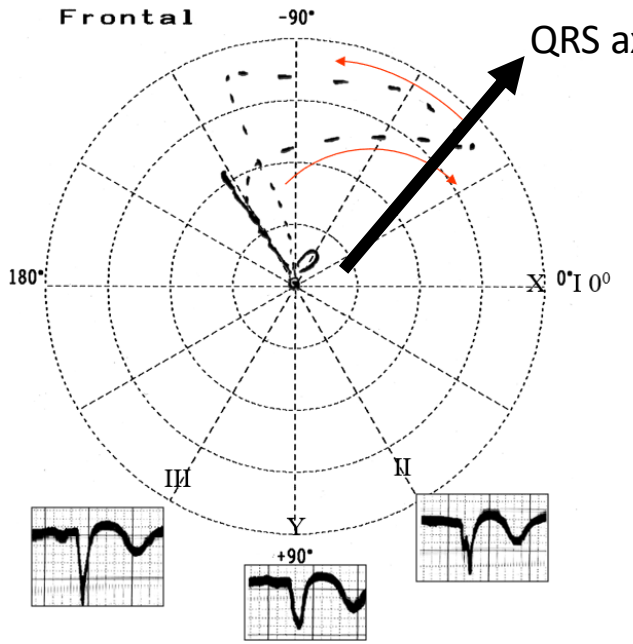

QRS axis with LAD

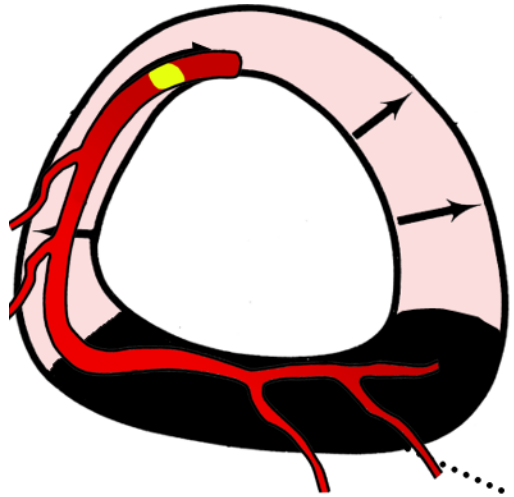

7. **A large lateral wall STEMI:** QS in I and aVL and extensive lateral MI with involvement of basal areas may cause an opposite electric vector, which may explain the presence of a positive main wave direction of QRS in lead aVR
8. **Acute anterior MI and anterior ischemia, eventually develop transient right axis deviation with a LPFB pattern during the acute phase of MI or ischemia.** higher incidence of significant RCA obstruction and collateral circulation between the left coronary system and the posterior descending artery (**Sclarovsky1986**)
9. **Hyperkaliemia** (**Ewy 1971**)(**Galloway 2019**)
10. **Sodium-channel blockade, e.g. TCA poisoning:** Drug toxicity tricyclic antidepressants (TCA) poisoning has been reported to cause a right-axis deviation of 130 ° to 270 ° in the terminal 40-ms frontal plane QRS axis (T40-m saxis) of the ECG.(**Gheshlaghi 2013**.)
11. **Ventricular preexcitation syndromes** (e.g., Wolff-Parkinson-White syndrome) with an accessory pathway from the left atrium to the left ventricle, will result in the left ventricle finishing depolarization earlier than the right
12. **Congenital heart disease example Secundum ASD, pulmonary stenosis, pulmonary hypertension (Einsenmenger)**
13. **Left pneumothorax** (**Liu 2017**)
14. **Mechanical shift, such as with inspiration or emphysema**
15. **Giant abdominal tumor** Similarly, morbidly obese patients or patients with ascites or an abdominal tumor may have a left axis deviation because of the heart's position in the chest. A right axis deviation is apparent when lead I is negative and lead aVF is upright.
18. **Ascites**
19. **Mechanical shifts, such as expiration, high diaphragm (pregnancy, ascites, abdominal tumor)**
20. **Pacemaker rhythm**

21. **Limb-lead reversal (left- and right-arm electrodes)** Lead reversals are very common in clinical practice, comprising 0.4% to 4.0% of all performed ECGs.(**Rudiger 2007**)

22. **Dextrocardia**

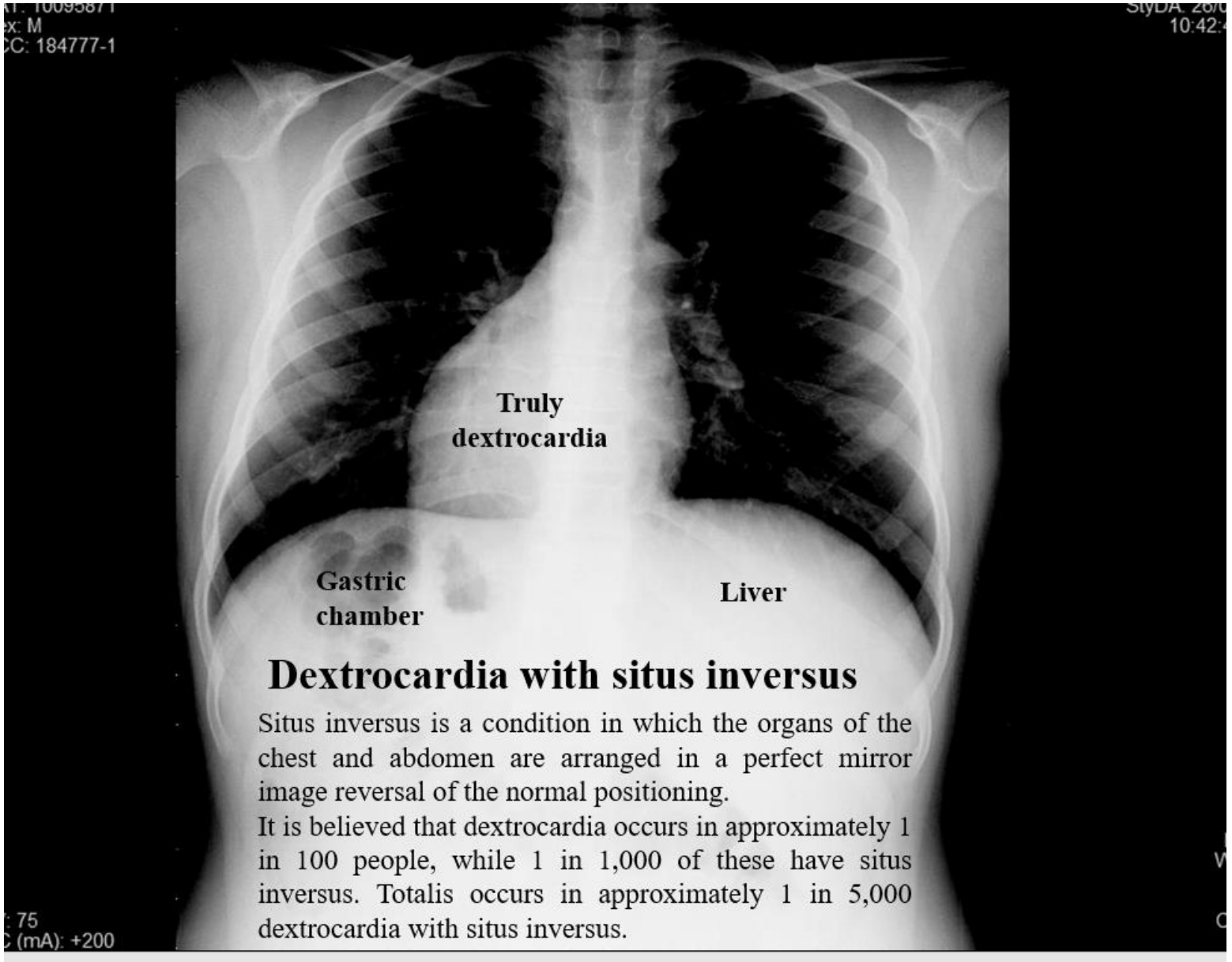

Name: SMSS**; Sex:** F; **Age:** 21 y/o; **Ethnic group:** Caucasian; **Weight:** 56 kg**; Height:** 1.59 m**;**
Date: 04/19/2004; **Medication in use:** nothing stated.

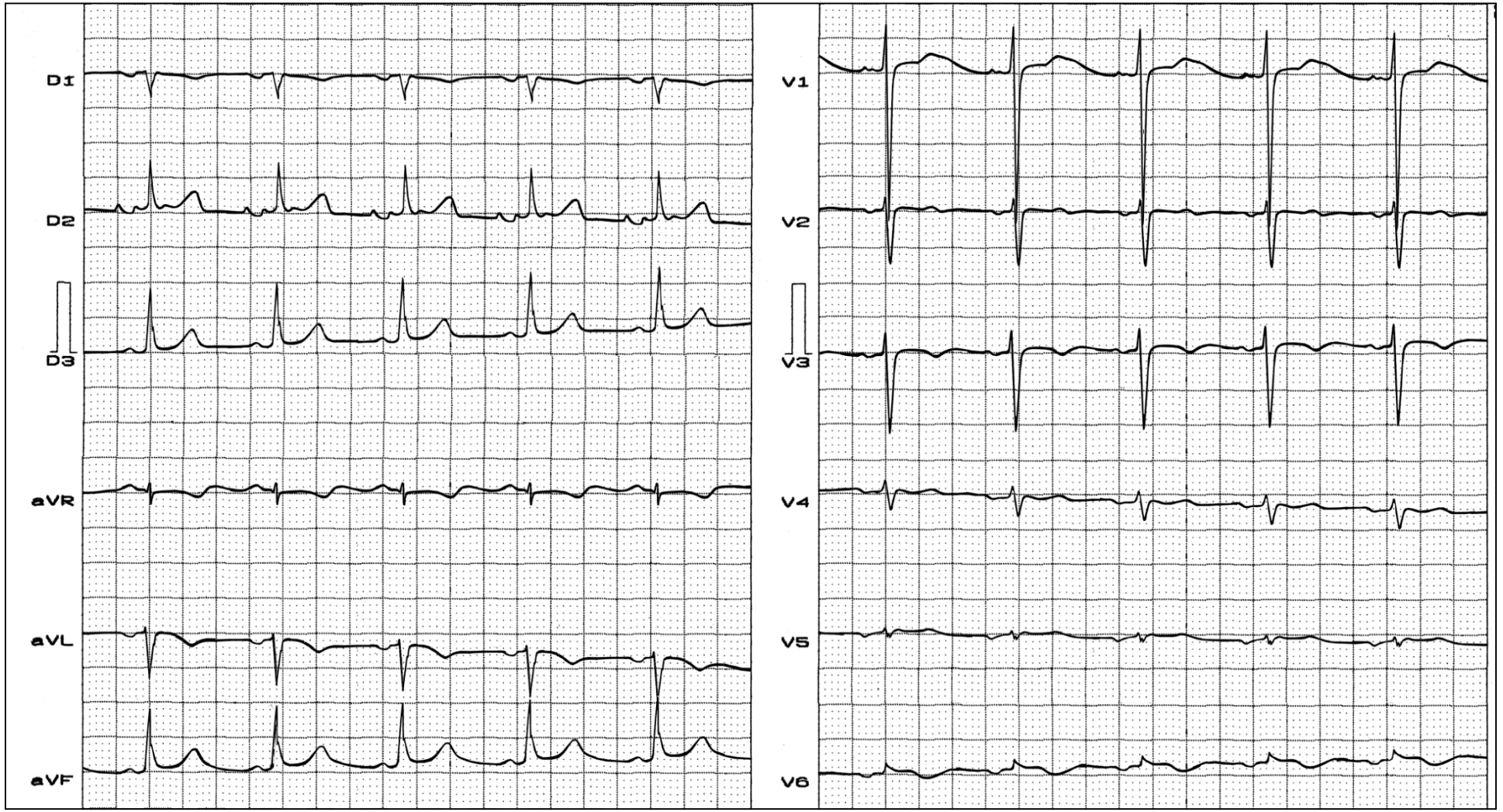

Clinical diagnosis: simple true dextrocardia: mirror image. Total atrio-visceral situs inversus with no heart disease.

ECG diagnosis: SÂP to the right and below, pointing at around +120º (III). Negative P wave in aVL and I, positive in III. Reverse progression of r wave in precordial leads V_2 to V_5 (decreasing).

Conclusion: true dextrocardia.

ECG/VCG correlation of typical true dextrocardia

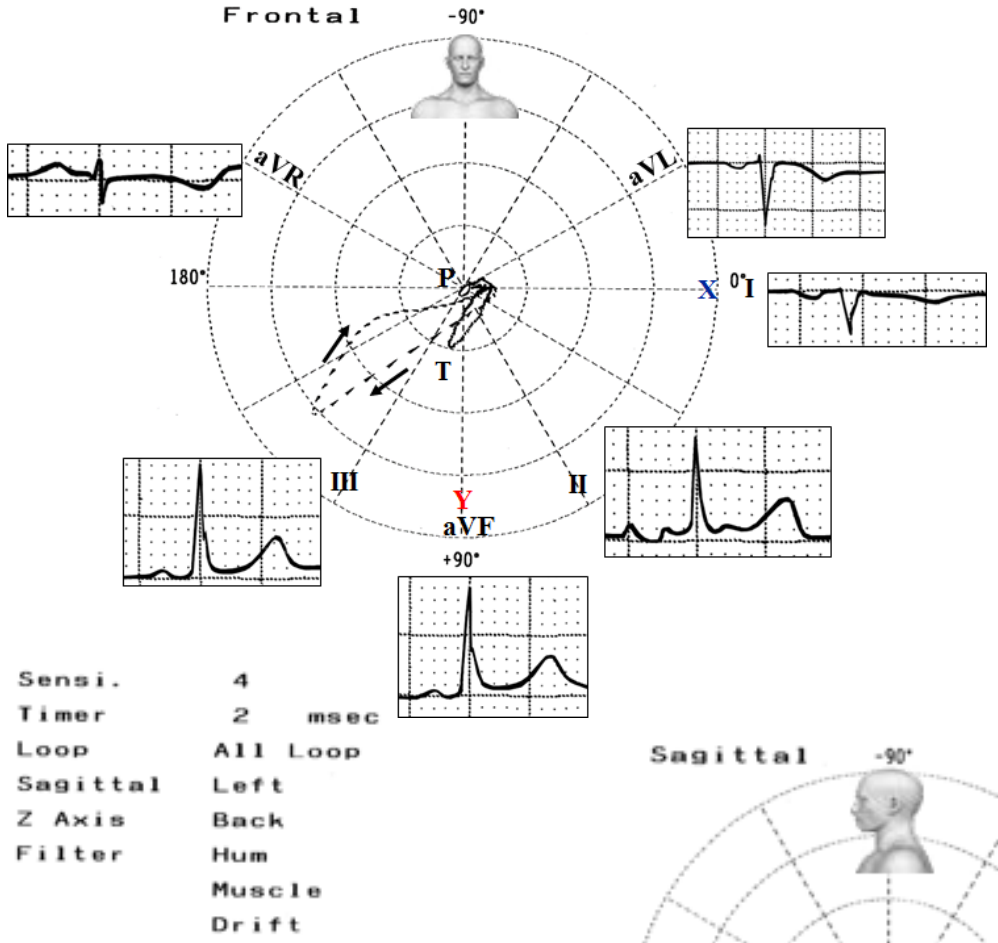

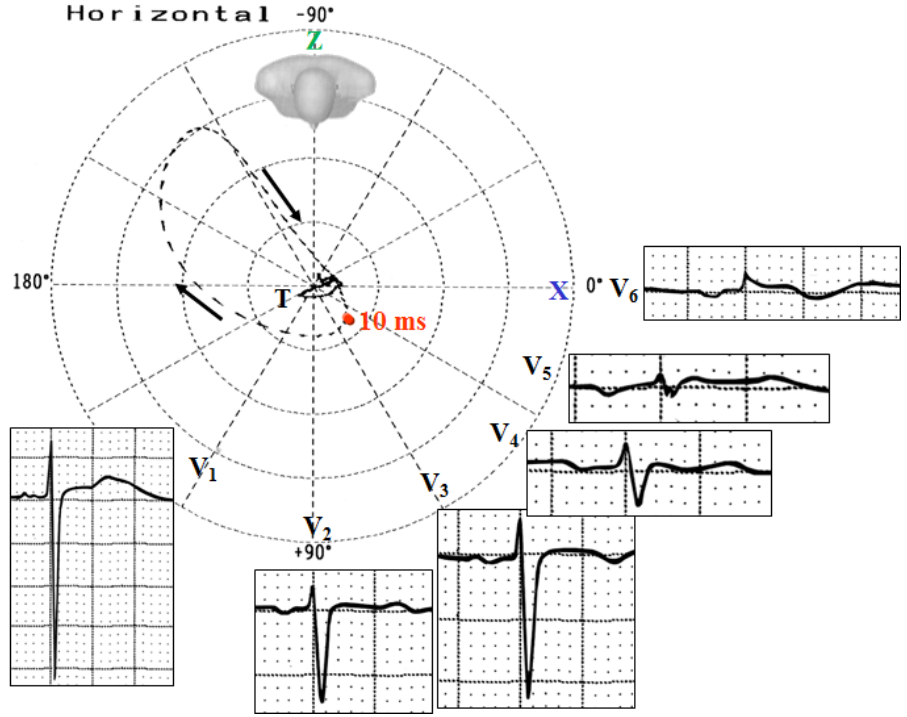

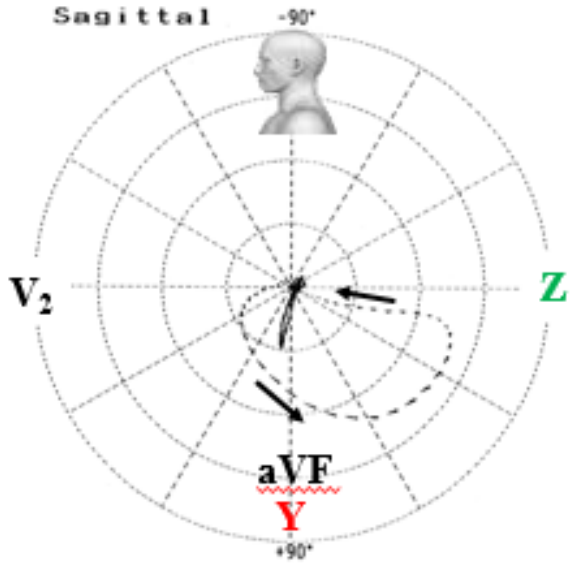

FP - SÂP vector heading from left to right, from up to down, pointing at around +120º (III). This fact will originate negative P waves in aVL and I, positive in III, and aVF and variable in II and aVR.

HP - The following stands out: initial 10 ms vector heading forward and to the left; QRS loop of clockwise rotation and predominantly located in the right posterior quadrant; reversed progression of the R wave in the precordial leads V_1 to V_6 (decreasing); maximal vector located in the right posterior quadrant; negative P wave in V_5-V_6; negative T wave in V_5-V_6.

Right-axis deviation (RAD) is defined as QRS axis between + 90° to ± 180° in adults. Causes of RAD include:

1. **Vertically orientated heart, tall, thin patient, ectomorph biotype (**an individual having a type of body build in which ectodermal tissue predominate: there is relatively slight development ofboth the visceral and body structures, the body being linear and delicate.**) or slender subjects** (*Slender Man* is a fictional *creepypasta* character depicted as an unnaturally tall, thin, spectral man with a featureless white face and a black suit and tie, sometimes with long black tentacles and sometimes without. The history and mythology behind the *Slender Man* character has branched off in various directions since its internet conception and his intentions are always left mysteriously vague, but the *Slender Man* stories most frequently involve the stalking, kidnapping, brainwashing, or murder of children.);
2. **Normal pediatric ECG:** As normal variation in newborn babies and infants the QRS axis is usually located in the right inferior quadrant and averigües ≈ +125º, but it can reach up to ±180º.(**Kim 2017**)
3. **Right ventricular hypertrophy /enlargement types A and B Vectorcardiographic** (**Nikus 2018**)
4. **Acute right ventricular strain, e.g. acute pulmonary embolism**
5. **Chronic Obstructive Pulmonary Disease (COPD)**
6. **Isolate Left Posterior Fascicular Block (diagnosis of exclusion):** Frontal plane axis between +90° and ±180° in adults. Owing to the more rightward axis in children up to 16 years of age, this criterion should only be applied to them when a distinct rightward change in axis is documented, rS pattern in leads I and aVL, qR pattern in leads III and aVF, RIII>II, ventricular activation time or R-wave peak time in aVF ≥ 45ms, QRS duration < 120 ms when isolate (very rare).
7. **Hereditary familial right axis deviation** with pseudo LPFB and incomplete right bundle branch block (**Lorber 1988.**)

7. **Right End Conduction Delay** (**RECD**) by the inferior fascicle (or contingent) of the right bundle branch or RECD type II of our classification (**Pérez-Riera 2018**). Other Synonymous: **Zonal, fascicular, parietal, peripheral, distal or Purkinje right ventricular blocks**

Concept: Electrovectorcardiographic changes, secondary to physiological delay or to true dromotropic disturbances in the territory of one of the three fascicles(or best contingents) of the right bundle branch, in isolation in the Right Ventricular Free Wall(RVFW). To speak about blocking it is necessary the presence of dromotropic disorder or slowing of ventricular activation process because in its absence can not call it so properly. These "blocks" cause localized or regional delay on basal portion of the RVFW. Zonal right ventricular blocks correspond to block of the superoanterior division of the right bundle on RVFW (on RVOT) or inferoposterior zone (on RVIT) of the RVFW.

Others denominations: **Parietal focal blocks (Masini 1952; Alzamora-Castro 1953; Rossi 1954; Noseda 1963); right focal blocks; peripheral blocks of the right bundle branch; right peripheral fascicular blocks (Pastore 1983); right peripheral blocks; distal right bundle blocks; divisional blocks of the right bundle branch; fascicular right block of the His bundle; delayed activation on the free wall of the right ventricle.** Electrocardiographically they are characterized by QRS duration is < 120ms, frequent absence of evident final broad r' in V_1 (**Uhley 1961**). Blocks of the superoanterior division of the right bundle branch on RVFW produce prolongation of ventricular activation time (VAT) or R-wave peak time on aVR, V_{3R} and eventually in V_1 (VAT ≥50 ms, maximum normal = 40 ms). Additionally, frequently concomitant SI-SII-SIII pattern indistinguishable from the positional SI-SII-SII produced by RVH(**Bayes de Luna 1987**), QRS axis on superior quadrants (above and between ± ±180º and 0º). Concomitantly, is registered slurred of S waves in leads to "face" the opposing regions (**de Micheli 2009**). This is the block resgistered in the Brugada syndrome (**Pérez-Riera 2012**) and canceled forms of ARVC(**Corrado 1996**). Experimentally, it has been demonstrated that these blocks result from a peripheral delay of the stimulus localized in a certain right ventricular zone on RVFW**.** (**Bayes de Luna 1982**).

Distribution of the three fascicles of the right bundle branch of the His bundle in the RVFW (Lev 1964-1968; Mahaim 1931; Lenegre 1958)

Distribution of three hypothetical divisions (or better contingents) of the right bundle branch in the right free wall ventricle.

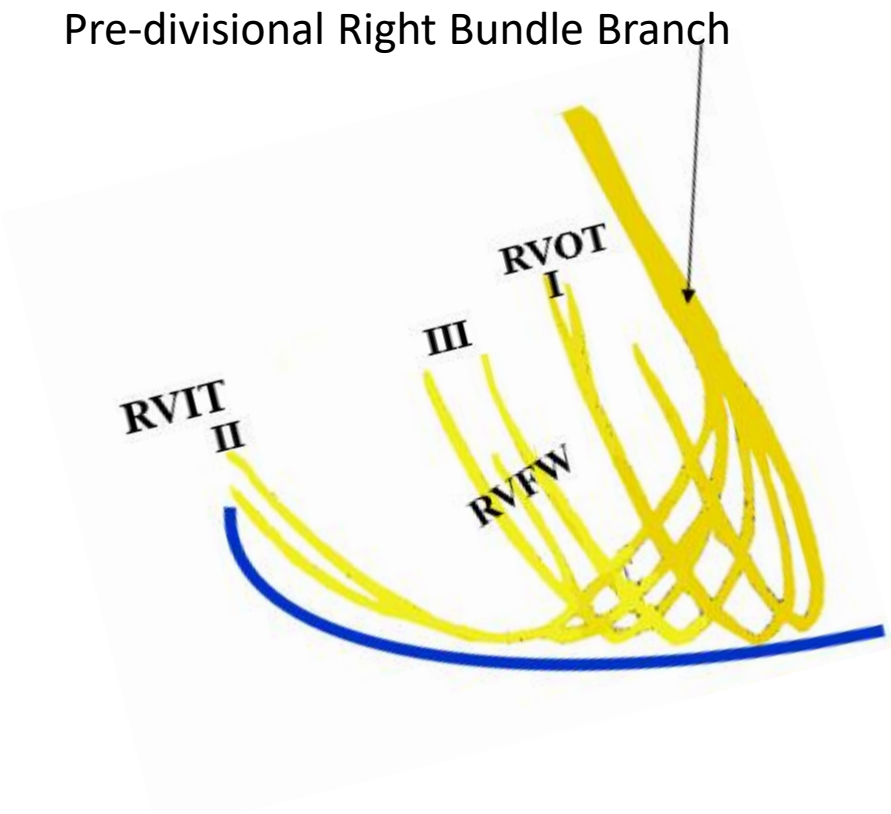

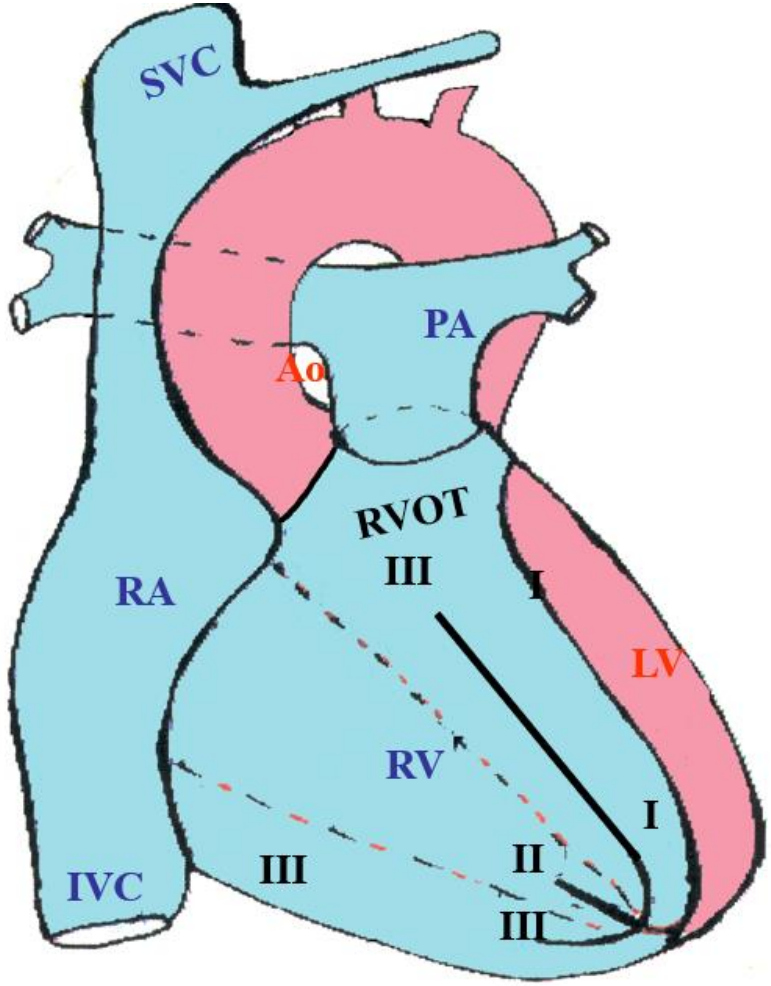

I - Territory of superior or subpulmonary fascicle….. RVOT
II – Territory of inferior or posteroinferior fascicle….. Right Ventricular Inflow Tract **RVIT**
III – Territory of middle fascicle
RVFW: Right Ventricular Free Wall. Divisional Right Bundle Branch
RVOT: Right Ventricular Outflow Tract: Located between supraventricular crest and pulmonary valve; comprised of the conus arteriosus (infundibulum), ventricular septum and right ventricular free wall.

Frontal Plane: Location of End Conduction Delay (RECD) in the 3 types

Type I or right superior subdivision block (**de Micheli 1987**)

- Type IA: QRS loop predominantly located in the left superior quadrant, (SÂQRS with extreme deviation to the left), counterclockwise rotation and RECD located in the right superior quadrant. Very similar to LAFB;
- Type IB: QRS loop pointed, clockwise or in eight, with the initial portion located in the left inferior quadrant and RECD located in the right superior quadrant. SÂQRS difficult to determine or shifted to the right;
- Type IC: QRS loop of clockwise rotation with SÂQRS with no deviation or with a mild shift to the right. In the three types with RECD located in the right superior quadrant.

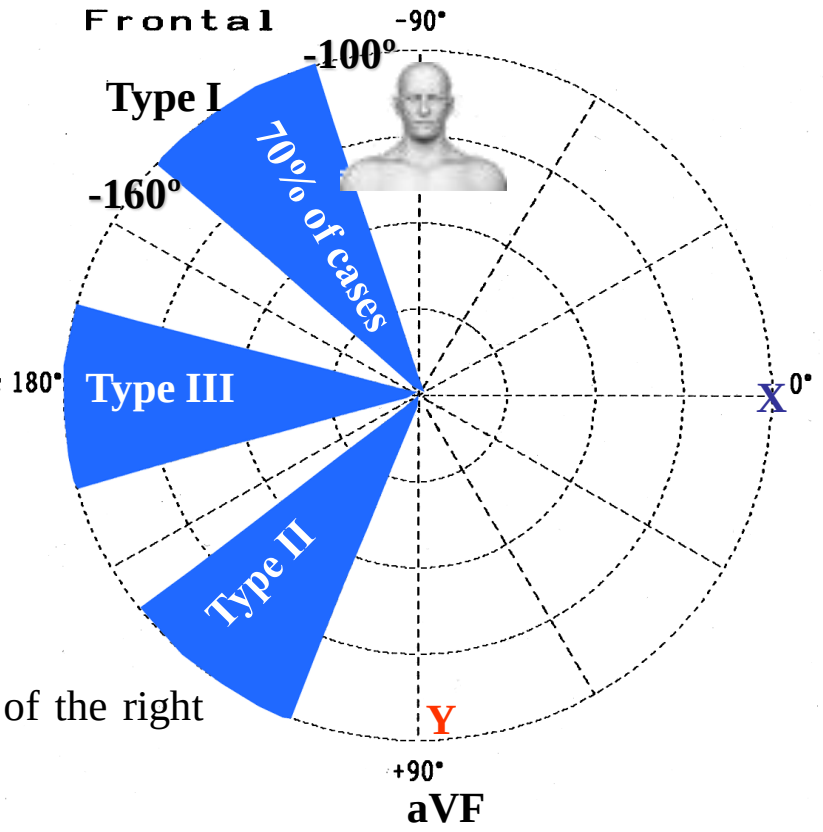

Type III: **RECD** located on the right portion of the 0±180° line, corresponding to the territory of distribution of the middle fascicle of the right branch;

Type II: **RECD** located in the right inferior quadrant, in the territory of the inferior fascicle of the right branch.

Classification of **RECD,** taking into account the location of the end delay of the QRS loop in the frontal plane in Type I, II and III. New proposal of VCG classification.

VCG Type I RECD variants according to QRS rotation on FP

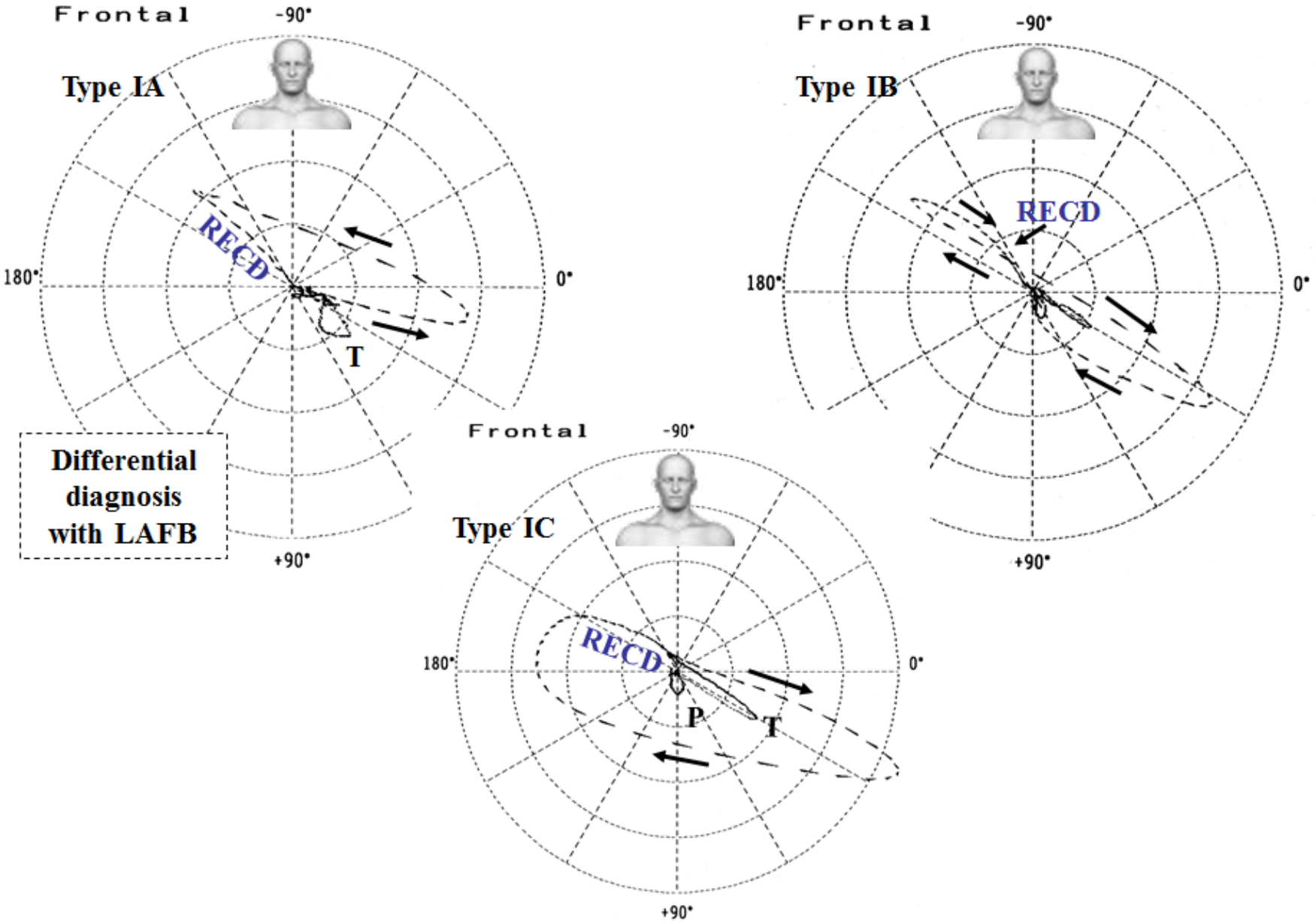

Vectorcardiographic loop in the frontal plane of the three subtypes of Type I. It is clear that only type IA may be confused with LAFB.

Name: CJO **Sex:** male. **Age:** 22 yo **Race:** White
Weight: 70 Kg **Height:** 1.71 m **Biotype:** Athletic **Date:** 15/05/2001

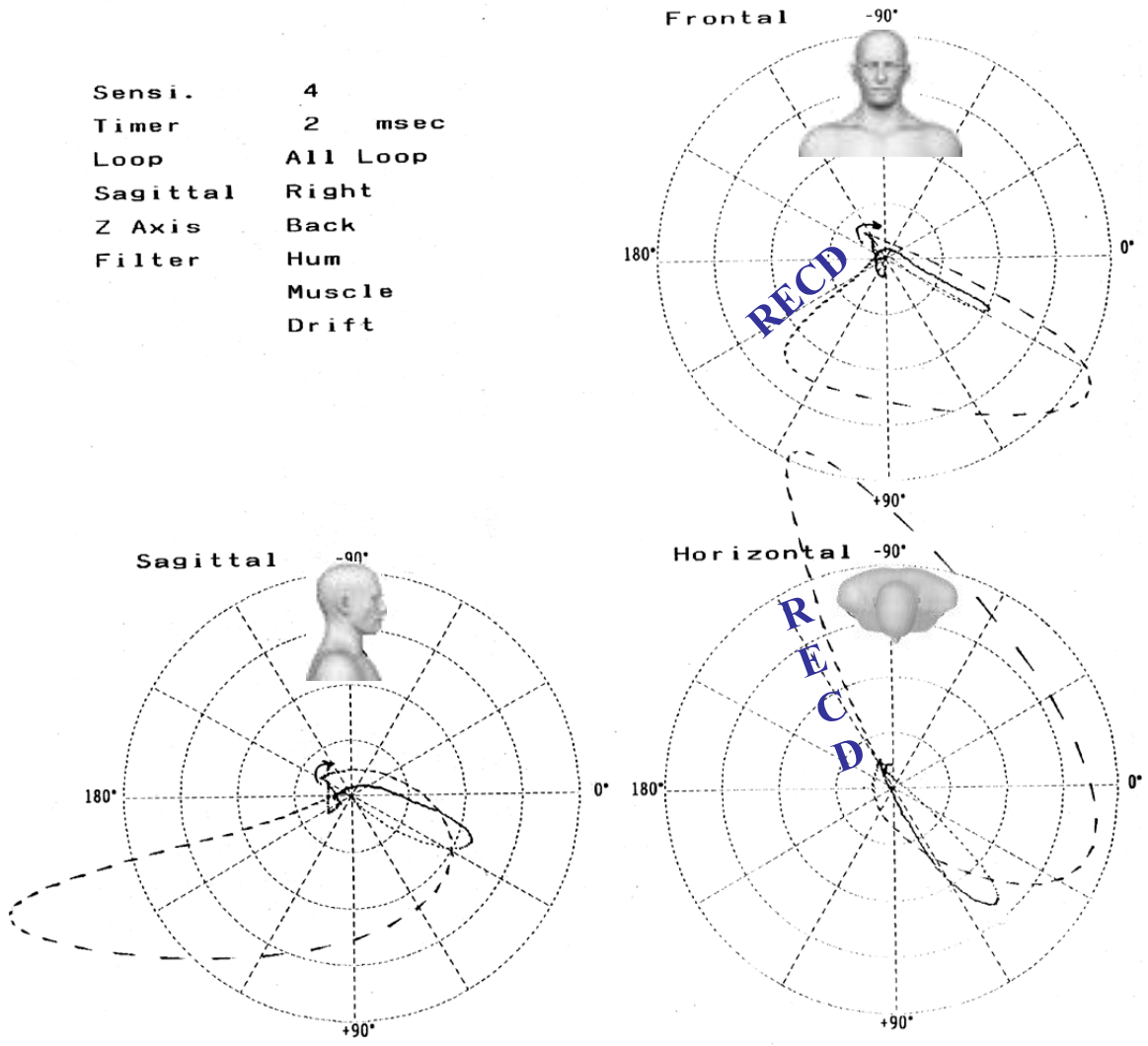

VCG of RECD type II Right axis deviation Differential diagnosis with LPFB.

ECG/VCG correlation on Frontal Plane

Name: CJO; **Sex:** male; **Age:** 22 yo; **Race:** White; **Weight:** 70 Kg; **Height:** 1.71 m; **Biotype:** Athletic; **Date:** 15/05/2001

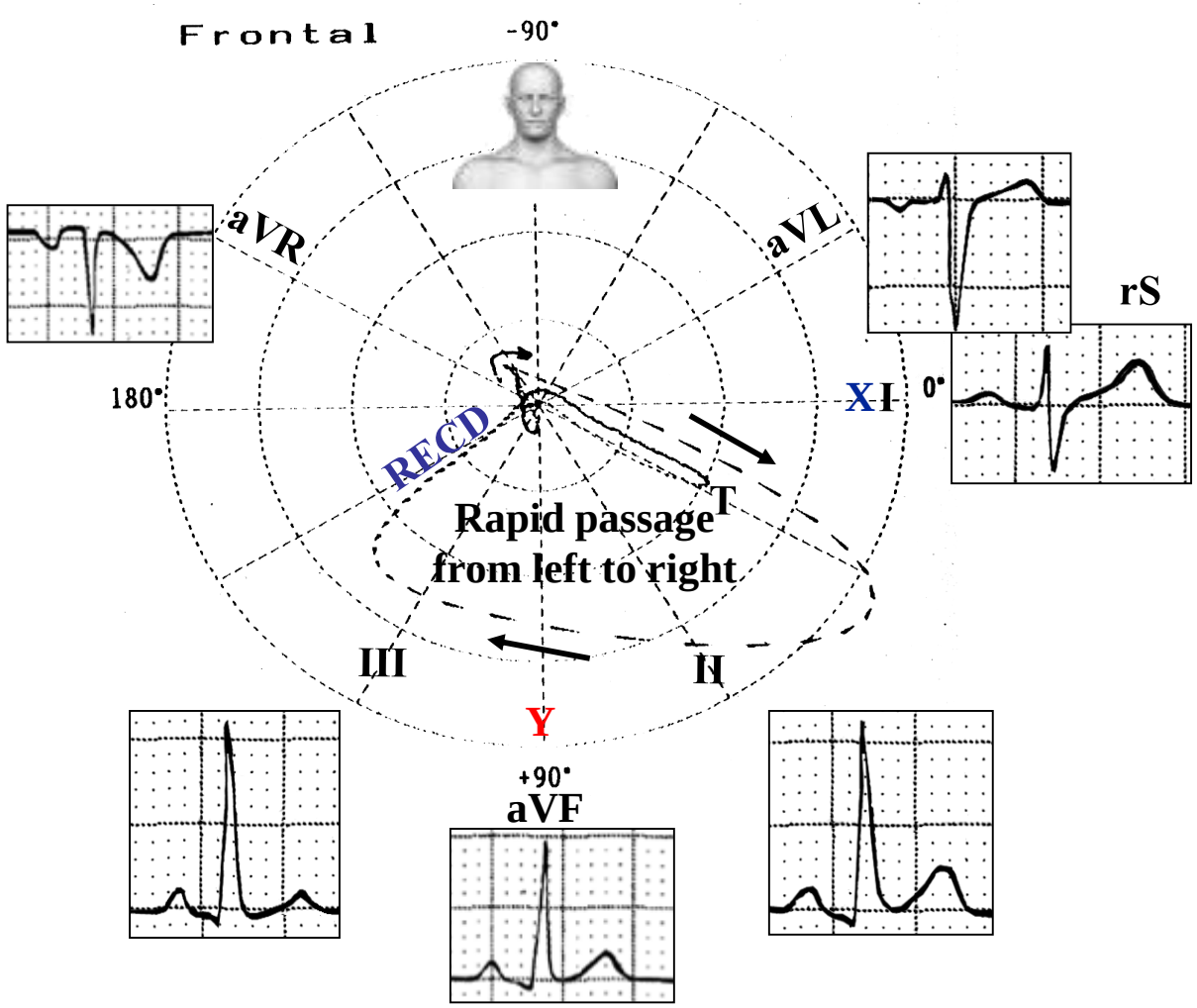

RECD type II: RECD located in the right inferior quadrant in the territory of the inferior fascicle of the right bundle branch. SÂQRS: +95º. SI-RII-RIII pattern (RIII < 15 mm). I and aVL: rS. II and III: qR. The descending ramp of R wave is slightly slow. It may present differential diagnosis with LPFB.

ECG/VCG correlation on Horizontal Plane

Name: CJO; **Sex:** male; **Age:** 22 yo; **Race:** White; **Weight:** 70 Kg; **Height:** 1.71 m; **Biotype:** Athletic;**Date:** 15/05/2001

QRS loop with initial portions to the front, counterclockwise rotation, important posterior dislocation, rapid passage from left to right and **RECD** located to the back and the left.

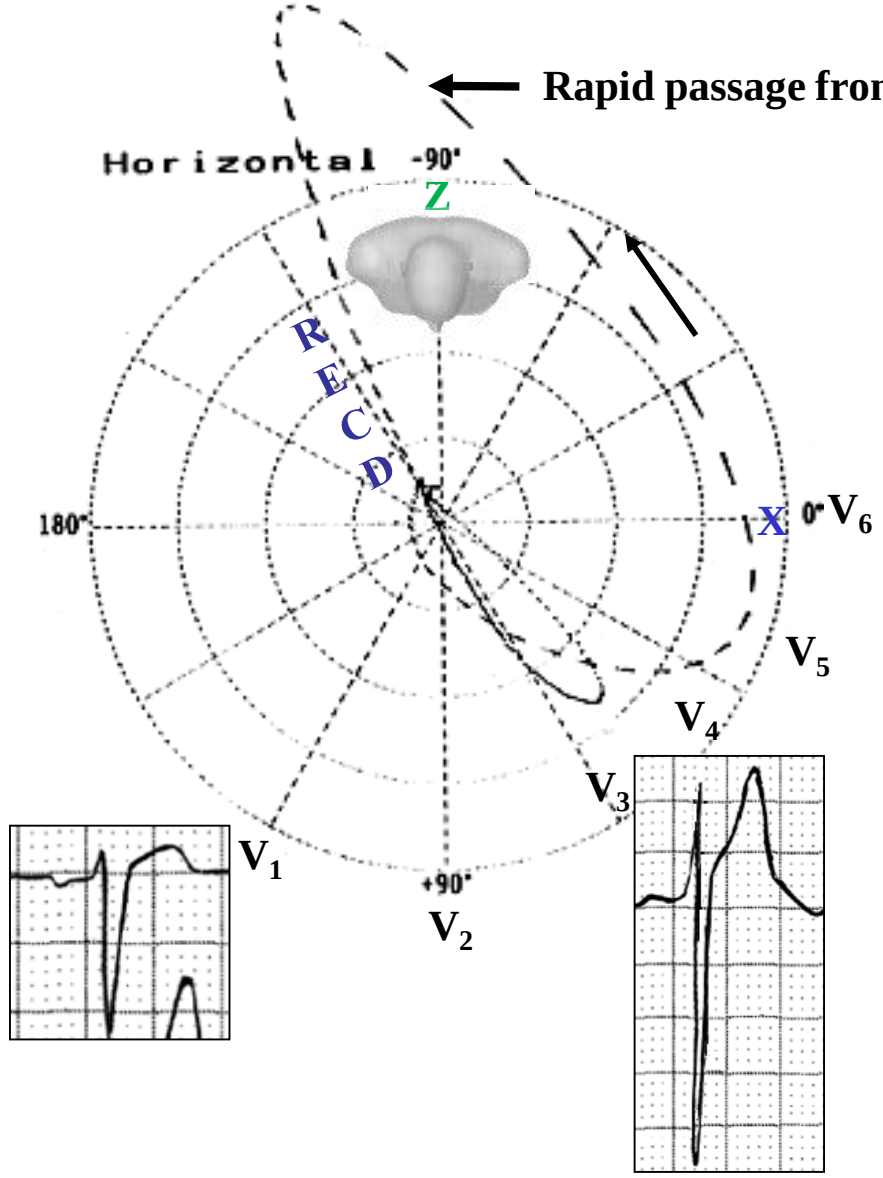

Differential diagnosis between RECD type II and Left Posterior Fascicular Block (LPFB)

	RECD type II or Right Posterior Subdivision Block	LPFB
PR interval	Normal.	Frequent prolongation.
Association with inferior infarction	No.	Frequent.
Voltage of RII and RIII	≤ 10 mm.	≥ 15 mm.
RII/RIII voltage ratio	RII >RIII.	RIII > RII.
Notch in the descending ramp of R wave of inferior leads	Absent.	Constant middle-final notch.
Ventricular activation time in aVF, V5 and V6	Normal.	Increased: up to 30 ms.
Ventricular activation time in aVL	Normal.	Decreased: up to 15 ms.
QRS loop in the FP	Clockwise rotation and with characteristic rapid passage from left to right between 30 and 50 ms. RECD on inferior right quadrant.	Clockwise, aspect of “fat” loop and maximal vector close to + 120°.

RECD type II or Right Posterior Subdivision Block

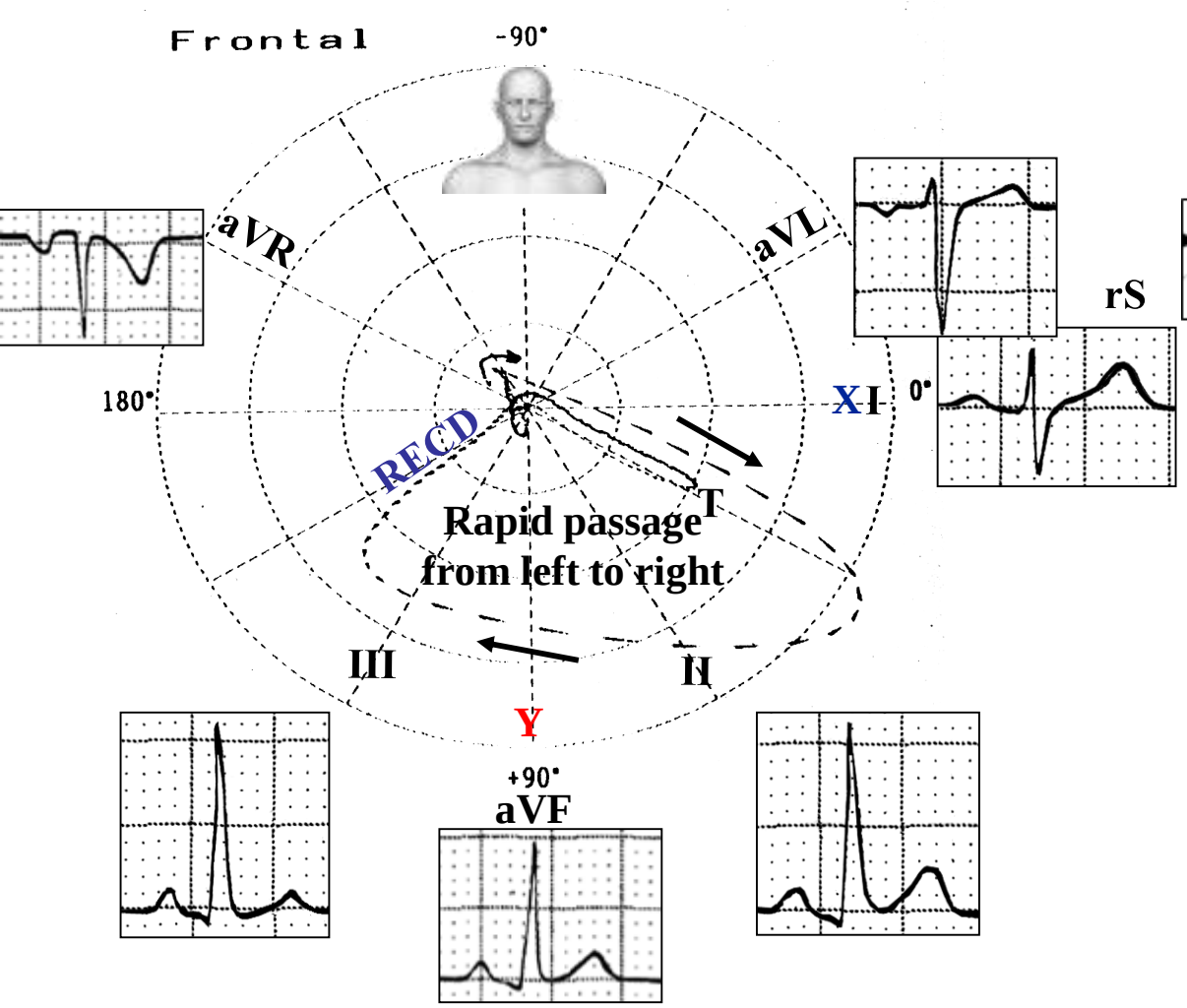

Truly LPFB

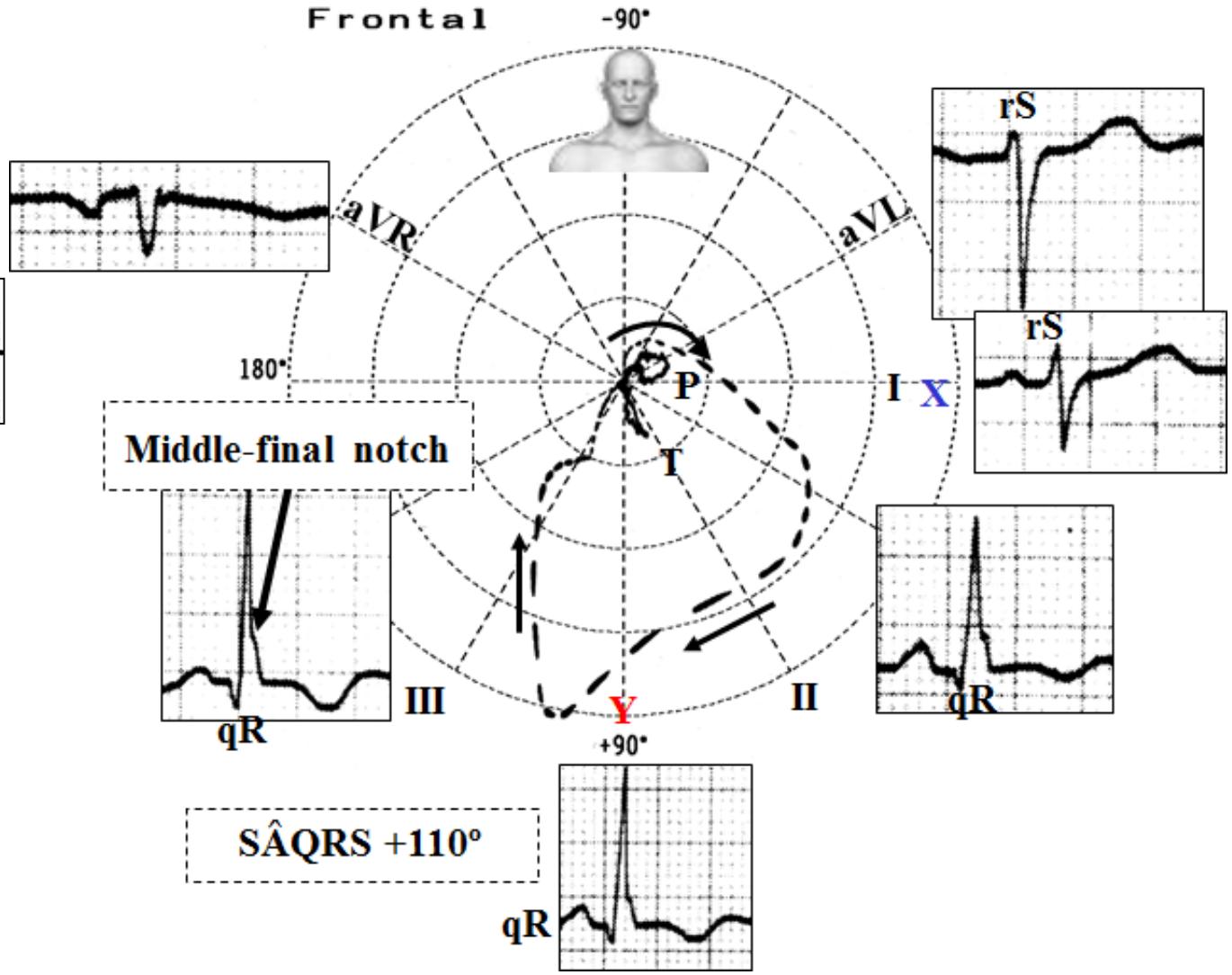

Right end conduction delay (RECD) by the inferior fascicle of the RBB or RECD type II of our classification (**Pérez-Riera 2005**): characterized by presenting ECD located in the right inferior quadrant in the territory of the inferior fascicle of the right branch. It corresponds to the territory of the right inferior fascicle. The differential diagnosis occurs with LPFB. Many of the cases described in literature as LPFB are, the way we see it, RECD type II, and since their ECG/VCG differences are very subtle, the diagnosis must always be clinical-ECG-VCG.

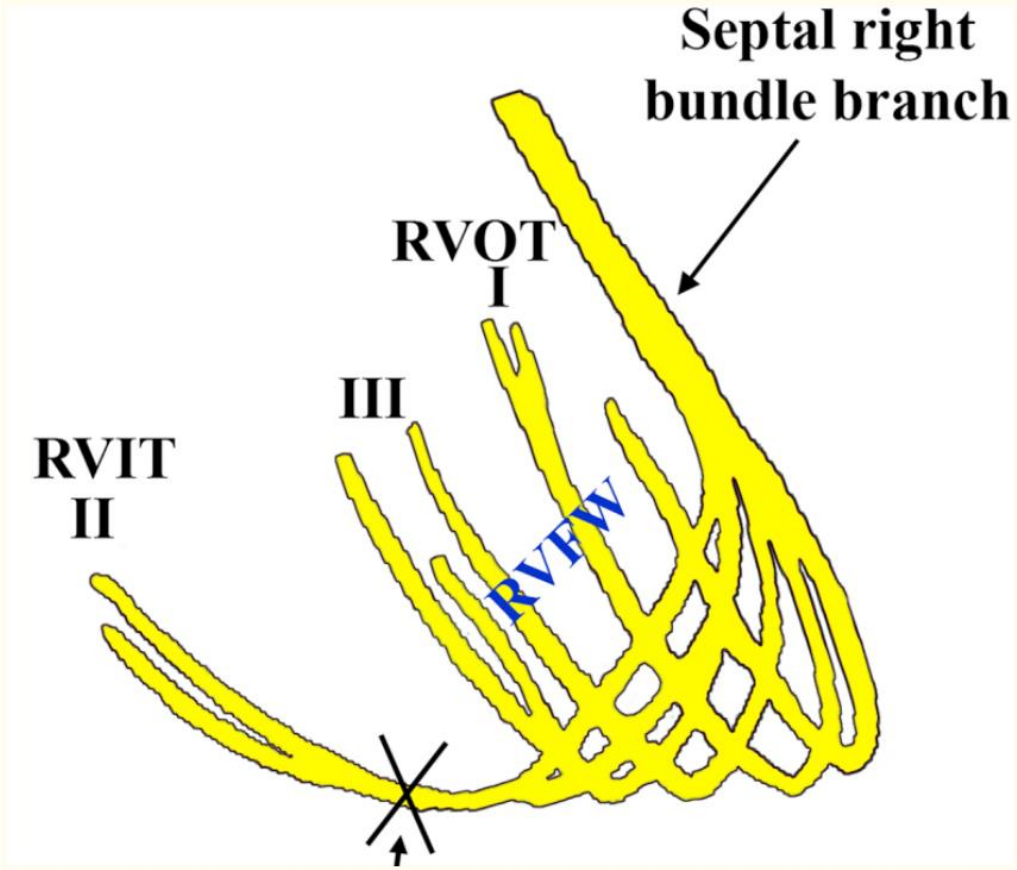

Outline of the inferior divisional block in RVIT (RECD type II) (**Lev M. 1964.**).(**Lev M. 1968**) (**Mahaim 1931.**) RVIT: right ventricular inflow tract; RVOT: right ventricular outflow tract; RVFW: right ventricular free wall.

RECD are ECG/VCG changes, secondary to physiological delay or to true dromotropic disorders in the territory of one of the hypothetical three fascicles or actually, fiber contingents of the RBB on the free wall of the RV, in isolation in the right ventricular free wall. In case of block, there should be a dromotropic disorder or slowing of the ventricular activation process. These blocks cause localized or regional delay in the basal portion of the RV free wall. Zonal right ventricular blocks correspond to block of the superoanterior division of the right bundle on RV free wall (on RVOT) or inferoposterior zone (on RVIT) of the RVFW.

Clinical significance of Right End Conduction Delay (RECD)

In 90% of cases they represent normal variants. The clinical significance and interest lie in the fact that:

1. *They may be confused with LAFB and LPFB (**Pérez-Riera 2005**);*
2. *They may be confused with electrically inactive areas in the anterior and the inferior walls (**Pastore 1985**.);*
3. *They may represent the ECG/VCG pattern of the Brugada syndrome (**Perez-Riera 2012**).*
4. *They may represent the ECG/VCG pattern of the Arthritogenic Right Ventricular Cardiomyopathy/dysplasia(**Nava**)* In 1988, researchers from Padua (Italy) showed vectorcardiographic tracings characterized by what is known today as RECD, by the superior fascicle of the right branch, in a series of 6 patients, 5 of which had ARVC/D as it was shown, and one of them was attributed to IVF (Nava 1998). Tracings of this kind were interpreted as early repolarization (Nava 1988)

36-year-old patient, episode of VF

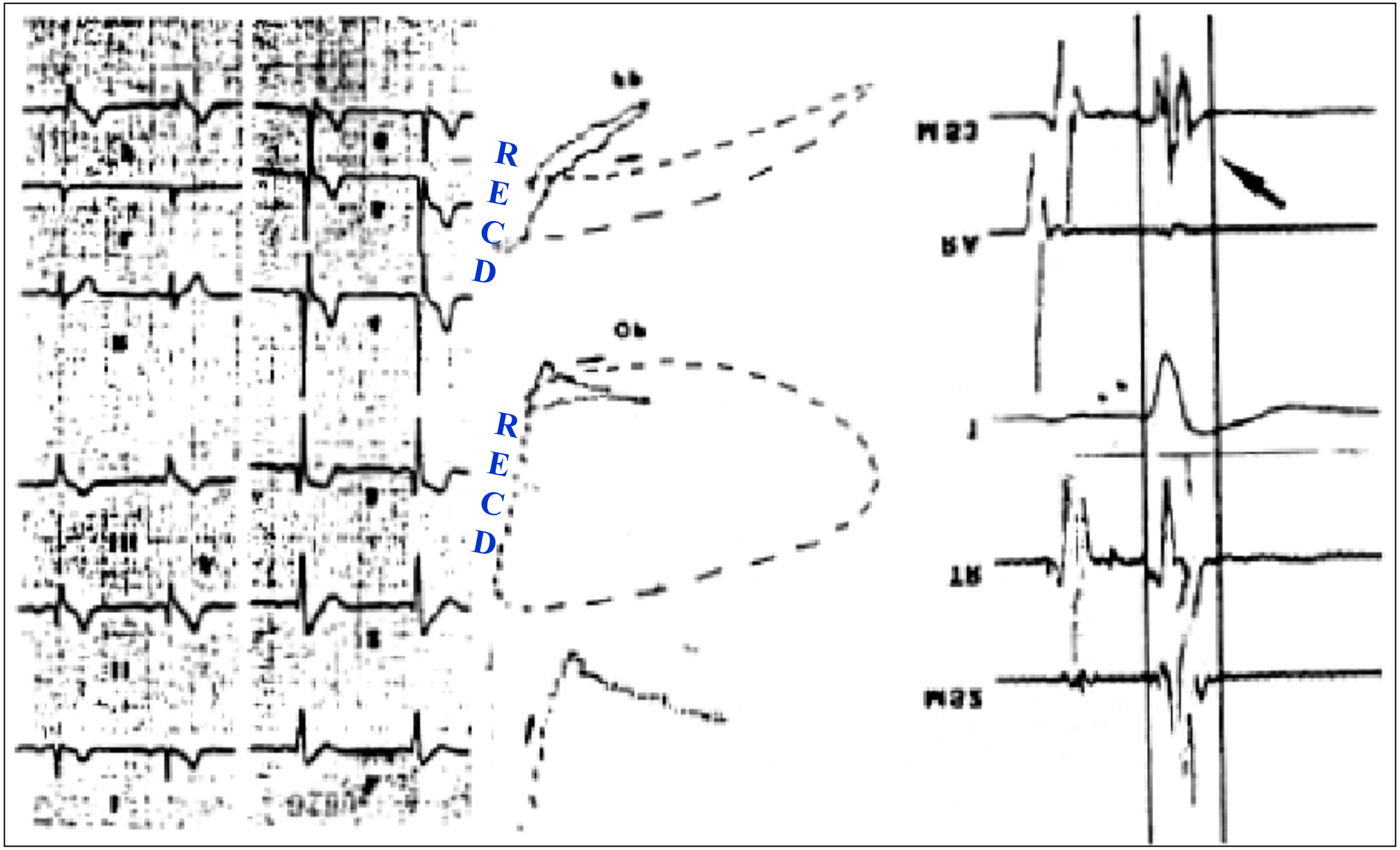

The authors interpreted this tracing as early repolarization pattern. Today we know that this is the typical type 1 ECG Brugada pattern, which from the vectorcardiographic point of view is diagnosed as **RECD** by one of the RB fascicles of the RBB (Nava 1988).

ECG/VCG correlation in the frontal plane, Dr. Nava's patient

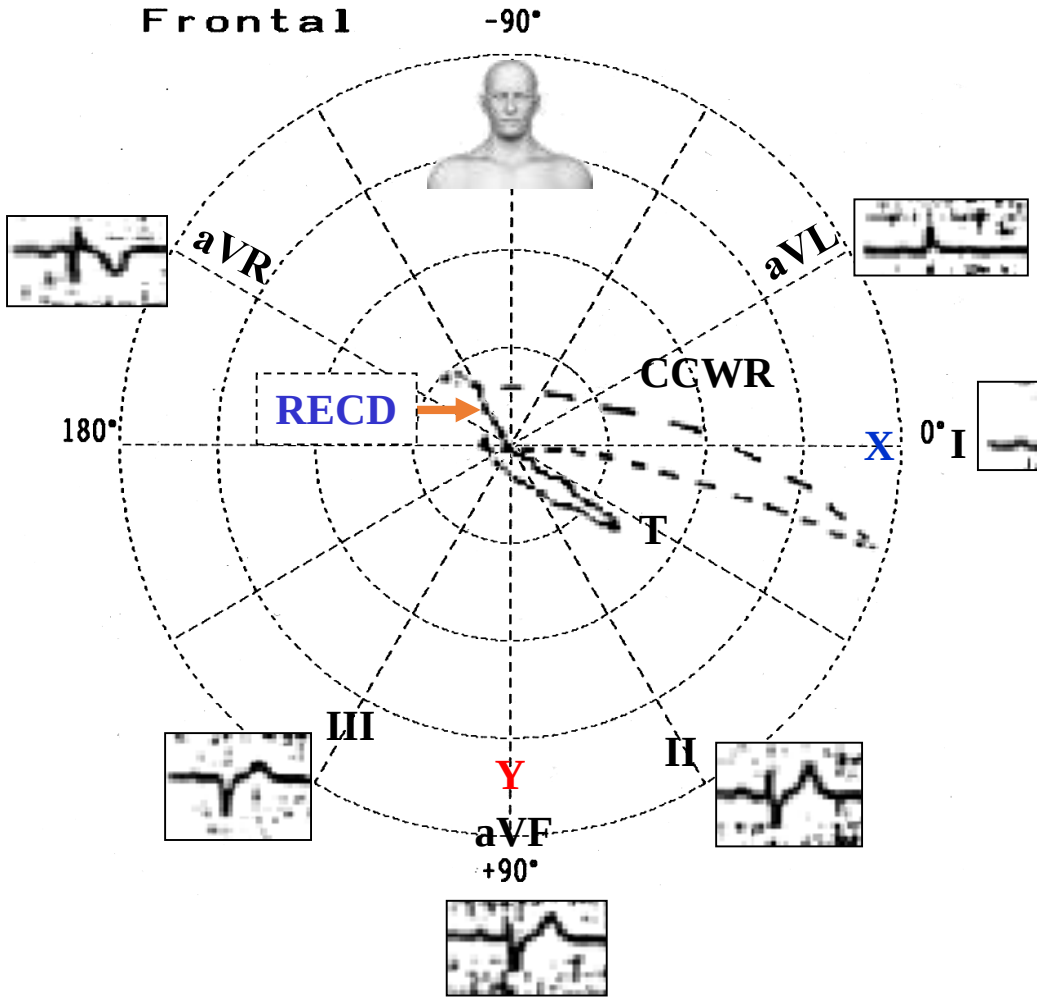

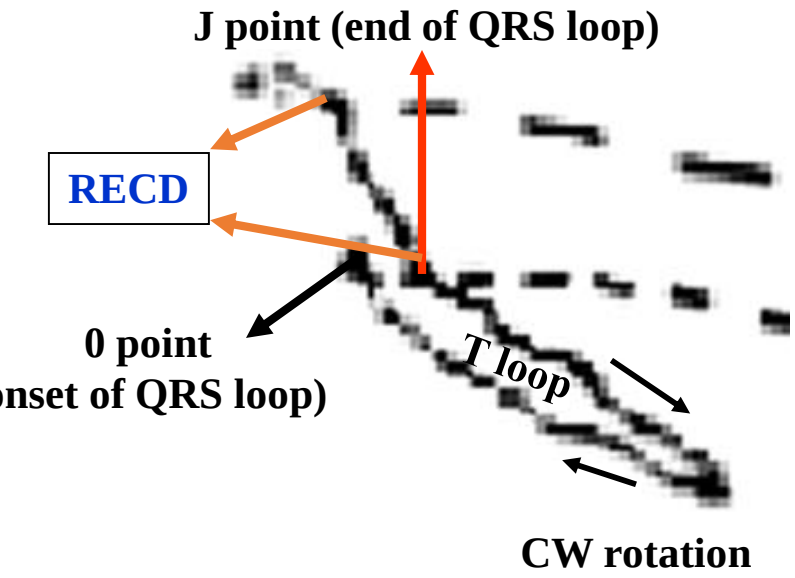

SÂQRS with extreme shift in left superior quadrant between -30° and -90°. Initial 10 to 20 ms vector heading below and to the left, rapid passage from left to right between 50 to 60 ms. The 0 point (onset of QRS loop) does not match J point (end of QRS loop). Both points move away in a proportional way to the degree of ST segment shift.

Conclusion: RECD on right superior quadrant by the superior fascicle of the right branch, located in the RVOT.

ECG/VCG correlation in the horizontal plane, Dr. Nava's patient

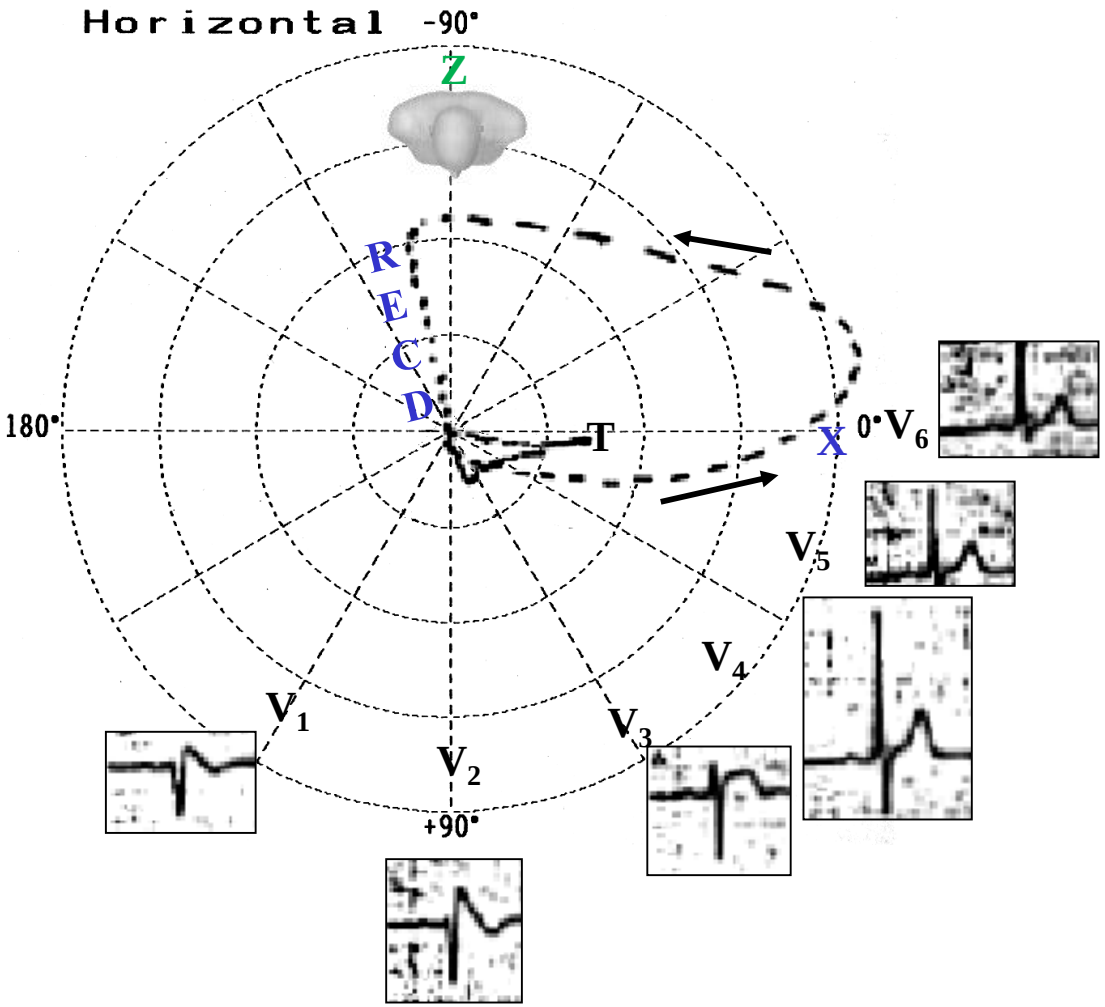

Initial 10 to 20 ms vector heading forward and leftward (typical right bundle branch block), CCW rotation and RECD located in the right posterior quadrant.

Conclusion: RECD with typical type 1 ECG Brugada pattern in the right precordial leads. It is a classical Brugada phenocopy.

Three electrocardiographic patterns that support the hypothesis of depolarization mechanism in the Brugada syndrome

Point of view

Which is the clinical significance of concomitant prominent R-wave sign in aVR lead, wide and/or large S-wave in lead I and increase in the duration of QRS complexes and QT/ QTc intervals only in the right precordial leads in the BrS? Answer Prominent R-wave sign in lead aVR (**Babai Bigi et al., 2007**), wide and/or large S-wave in lead I (**Caló 2016**) represent right end(or terminal) conduction delay (**RECD**) on RVOT whose depolarization points to the aVR lead located on right superior quadrant/ or right upper quadrant. (yellow quadrant in the figure below). In these cases, the frontal plane can show extreme right axis deviation (QRS axis between -90° and ±180°, also called Northwest axis, “no man’s land” (i.e., "N-M-L".) or right shoulder axis (RVOT area). Consequently, QRS complexes are predominantly negatives in lead I and aVF.

Right distal or superior peripheral block of the right bundle branch observed in BrS and concealed forms of ARVC/D.

Figure 1

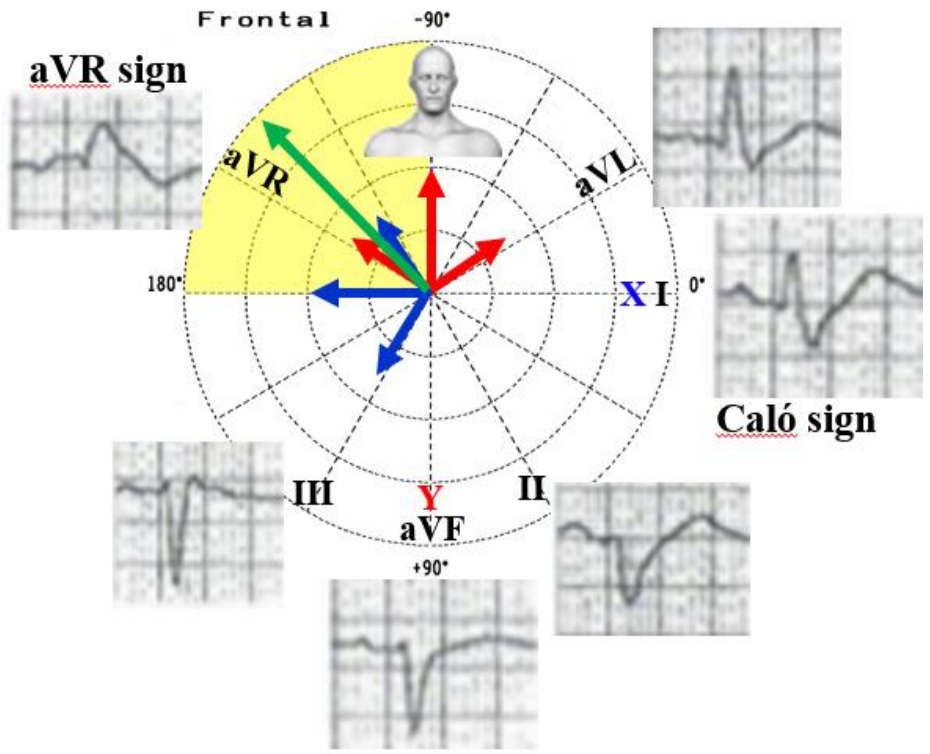

This frontal plane belongs to a symptomatic BrS patient with spontaneous Brugada type 1 ECG pattern. We verified that both signs are present: the “aVR sign” (prominent final R wave on aVR lead; R wave ≥3 mm or R/q ≥0.75) and wide and/or large S-wave in lead I (“Caló sign” 2016). Both signals, reflect terminal or right end conduction delay (**RECD**) on the right ventricular outflow tract (RVOT) and subsequently more electrical heterogeneity in the ventricular wall thickness.

Extreme axis deviation, Northwest axis, "no man's land" or right shoulder axis (RVOT area) Negative QRS complexes in lead I and negative QRS complexes in lead aVF.

Possible causes:

- Ventricular tachycardia,
- Accelerated Idioventricular Rhythm
- Ventricular ectopy
- Hyperkalaemia
- Severe right ventricular hypertrophy
- Right distal superior peripheral block: eventually observed in BrS.

The aVR sign

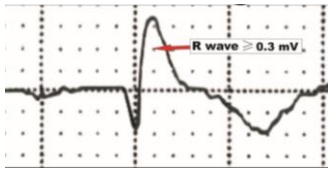

High right precordial leads V_{1H}, V_{2H} and V_{3H} and unipolar aVR face the RVOT (A)

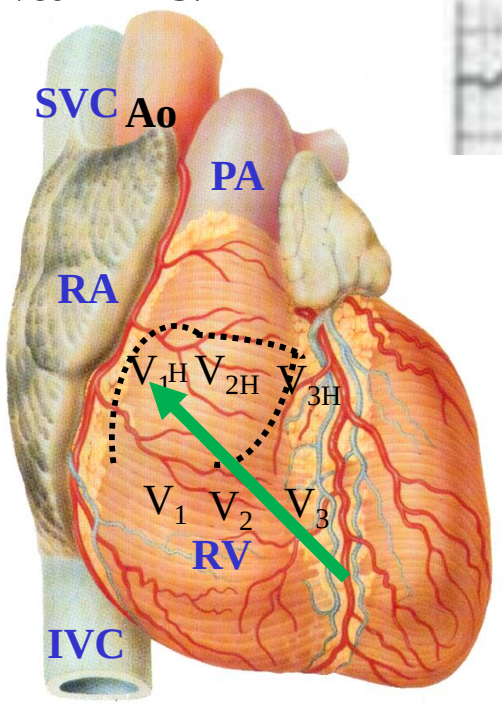

aVR sign

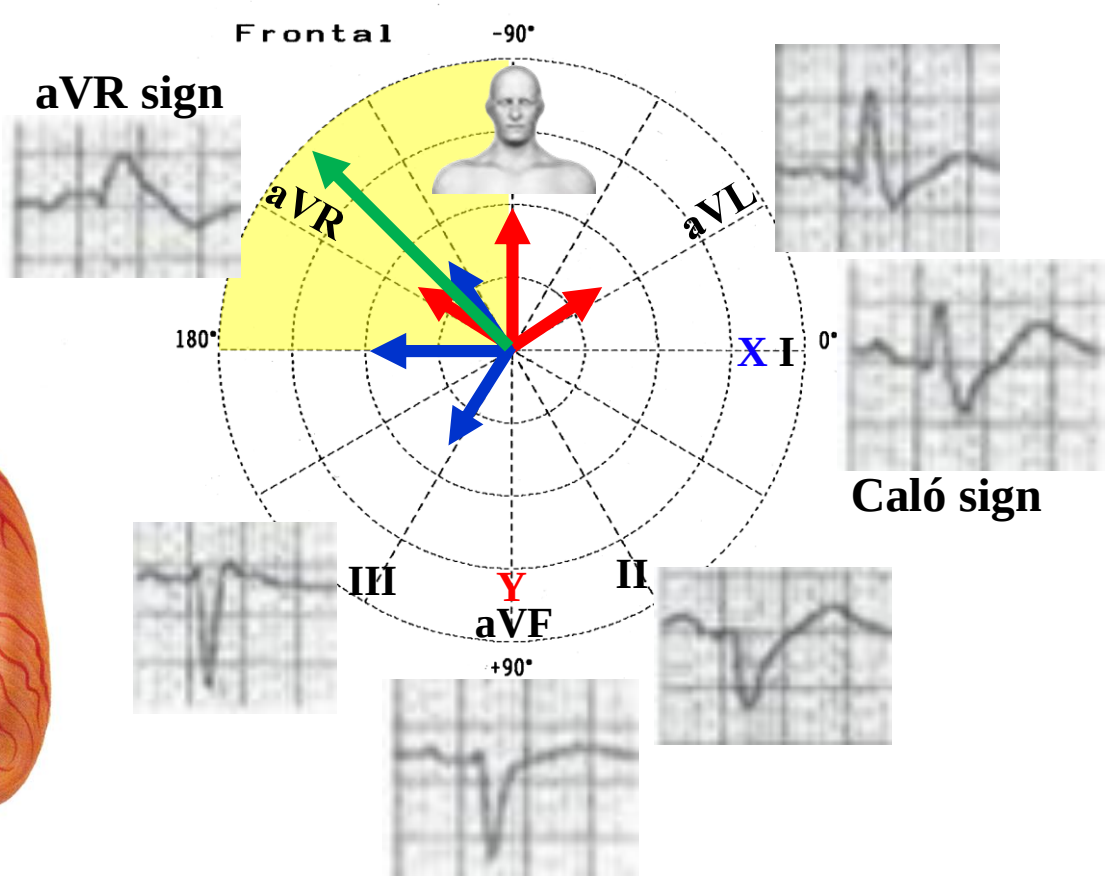

Caló sign

Significant S wave in lead I (Calo et al., 2016). The presence of a wide and/or large S-wave in lead I is a powerful predictor of life-threatening ventricular arrhythmias in patients with BrS and no history of cardiac arrest at presentation. However, the prognostic value of a significant S-wave in lead I should be confirmed by larger studies and by an independent confirmation cohort of healthy subjects.

The aVR sign: Presence of prominent final R wave on aVR lead; R wave ≥3 mm or R/q ≥0.75. The R-wave sign, reflect terminal o right end conduction delay (RECD) in the in the RVOT and or RV free wall and subsequently more electrical heterogeneity, which in turn is responsible for a higher risk of arrhythmia.

Concomitant R-wave sign and significant S wave in lead I (Babai Bigi/Caló) Both are expression of RVOT dromotropic disturbance

BrS with QRS axis Extreme-axis right deviation-90° to ± 180° (Northwest axis "no man's land") or right shoulder axis

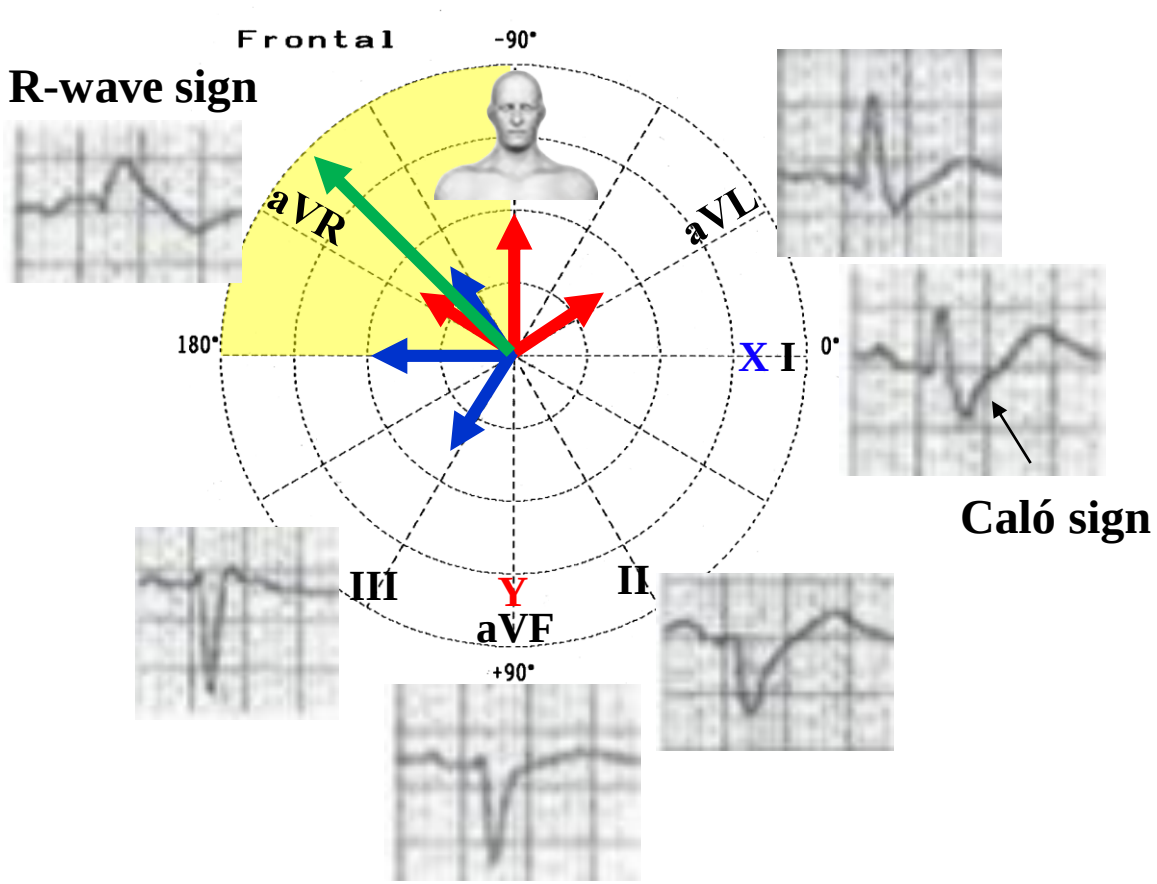

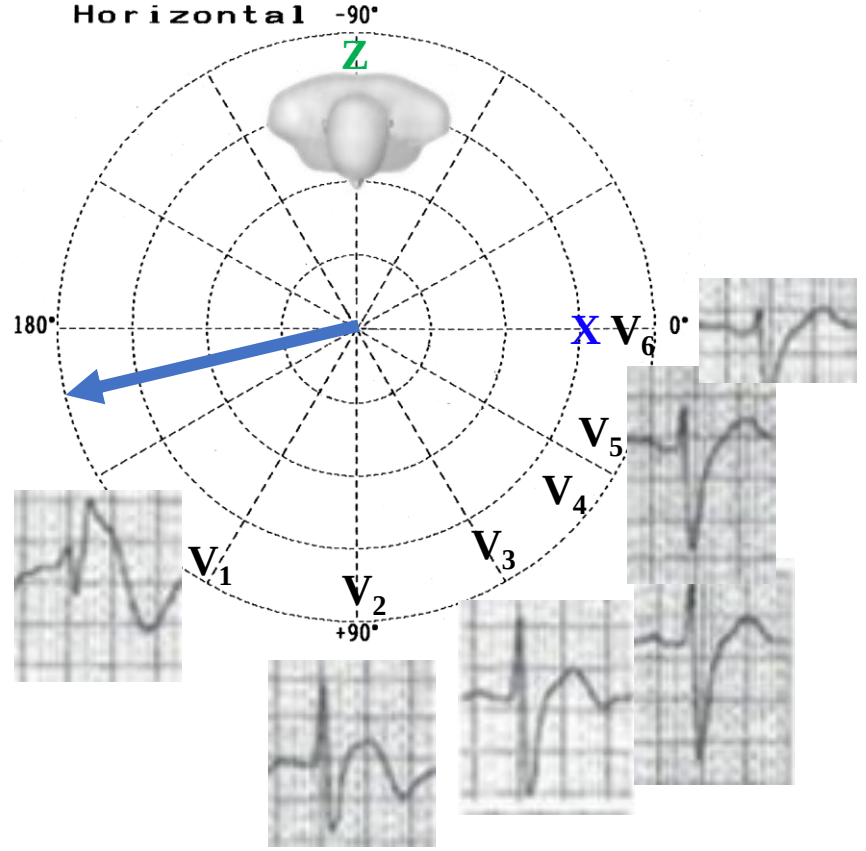

The aVR sign: Presence of prominent final R wave on aVR lead; R wave ≥3 mm or R/q ≥0.75 in lead aVR (aVR sign). The R-wave sign, reflect terminal o right end conduction delay (RECD) in the in the RVOT and or RV free wall and subsequently more electrical heterogeneity, which in turn is responsible for a higher risk of arrhythmia.

The Caló sign The presence of a wide and/or large S-wave in lead I is a powerful predictor of life-threatening ventricular arrhythmias in patients with BrS and no history of cardiac arrest at presentation. However, the prognostic value of a significant S-wave in lead I should be confirmed by larger studies and by an independent confirmation cohort of healthy subjects.

Other possible clinical causes of extreme QRS right axis deviation QRS axis on right upper quadrant described in the literature include:

1. **Ventricular tachycardia (VT):** Extreme right axis deviation predominantly QRS complexes positive in aVR and negative in I + aVF (QRS axis between -90° and ±180°: in the right upper quadrant.), “Northwest axis”, “no man’s land” (i.e., "N-M-L".) or “right shoulder axis” (on RVOT area). An axis in "N-M-L" implies (but is not proof of) an apical origin to the rhythm and should make one think of and exclude the possibility of VT. As a general rule, until it is proven otherwise, assume any wide QRS complex tachycardia is VT. Even though this one clue carries significant weight in supporting the interpretation of VT, that conclusion cannot be made based solely on this single criterion. This axis is just one of a long list of criteria and should be used in conjunction with all of them as they carry a lot of strength when used collectively.
2. Fascicular VT originating from the posterior papillary muscle (PPM-FVT) This variant exhibited right bundle branch block and extreme right axis or horizontal axis deviation. PM-FVT is a distinct entity that is characterized by distinctive ECG characteristics and less sensitivity to verapamil administration compared with common type FVT. Ablation targeting the mid-diastolic Purkinje potentials around the PMs during tachycardia can be effective in suppressing this arrhythmia. (**Komatsu Y2017**)
3. **Accelerated Idioventricular Rhythm: similar mechanism to the previous item**
4. **Ventricular ectopy: similar mechanism to the previous item. Ventricular ectopy.**
5. **Hyperkaliemia**
6. **Extreme Severe right ventricular hypertrophy**
7. **Acute myocardial infarction with new onset extreme right axis deviation and right bundle branch block (RBBB).** This ECG observation represent a hazardous signal of poor prognosis because is indicative of a severe obstruction of a major coronary artery. This electrocardiographic marker can identify coronary artery occlusion where ST-segments are hard to evaluate, and hence, patients may benefit

7. most from early and complete revascularization strategies such as primary angioplasty. (**Wang 2018**.)

8. Double outlet right ventricle associated with persistent common atrioventricular canal and pulmonary stenosis. (**Antonelli 1986**.)

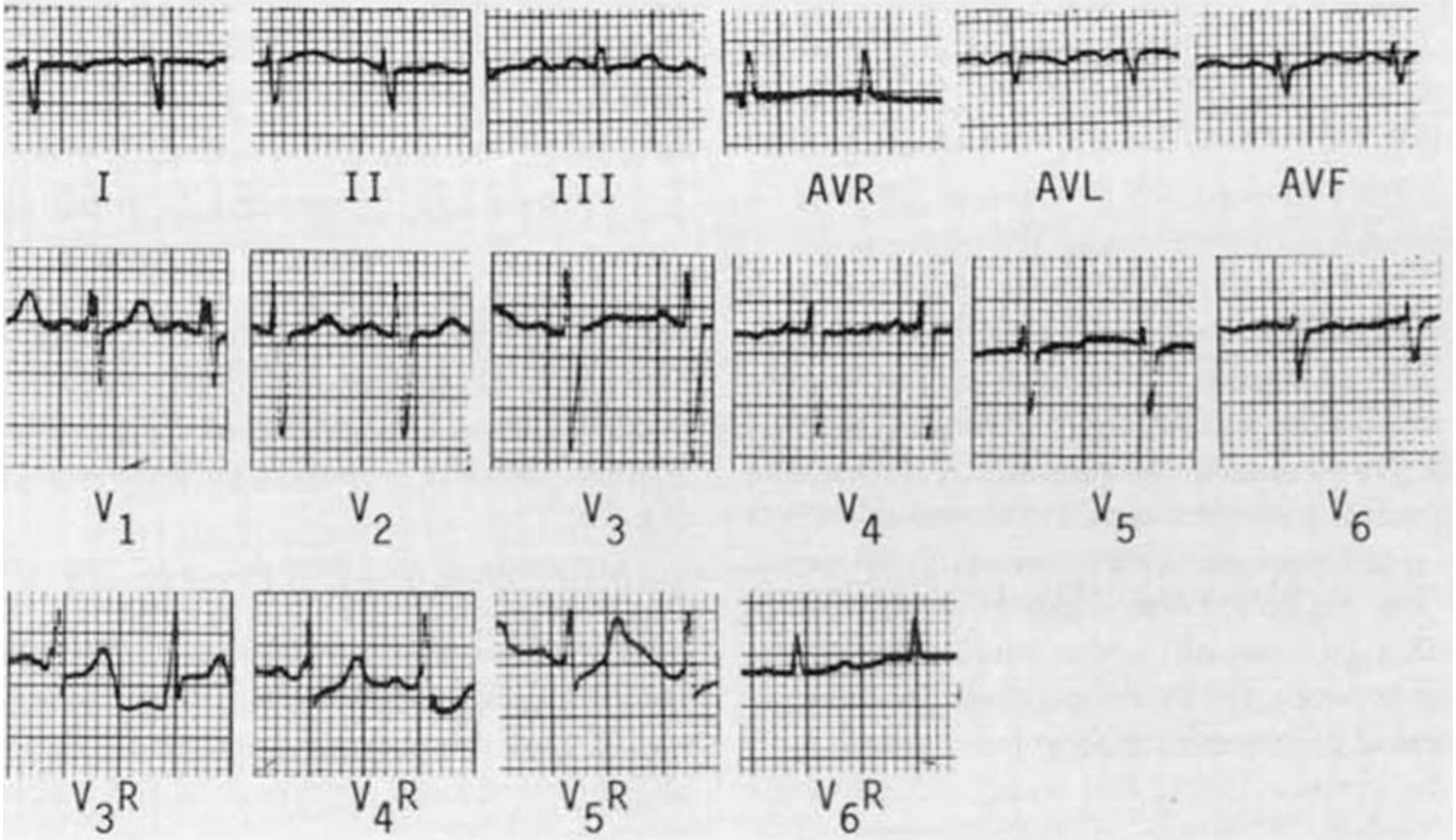

Sinus rhythm, heart rate of 140 beats/min, PR interval = 120ms. QRS duration 60 ms, QRS electric axis in the frontal plane (AQRS) on upper right quadrant (- 170°), positive T waves in V1-V2 leads and deep S waves across all the precordial leads.

Increase in the duration of QRS complexes only in the right precordial leads (from V1 to V3), being normal in the left leads (V4 to V6) in the absence of right bundle branch block: Parietal block

Pitzalis et al identified the selective prolongation of QT interval duration in the right precordial leads (V_1 to V_3) in comparison to the left ones (V4 to V6). In other words, lengthening of QT intervals in the right precordial leads. QRSD of $^{V1+V2+V3}/_{V4+V5+V6} \geq 1.2$. This feature is considered typical of ARVC/D, but it was also observed in BrS (**Pitzalis 2003**). As the QT interval is made up by ventricular depolarization (QRS) plus ventricular repolarization (ST/T) we think that this selective prolongation represents a certain degree of parietal block in the RVOT, as the one observed in ARVC/D. If the QT interval is prolonged only from V_1 to V_3, being normal or lesser from V_4 to V_6, it is clear that this increase may be due to prolongation of ventricular depolarization (QRS complex) and/or by ST/T prolongation (repolarization). If we admit that in BrS there is some degree of bundle branch block, clearly the QT interval prolongation is due partly to this. The QTc interval constitutes the classical measurement for ventricular repolarization; however, this parameter includes ventricular depolarization (QRS), and therefore represents the so-called electric systole, which includes depolarization (QRS) and ventricular repolarization (ST/T = JT interval).

The figure shows that the QRS duration complexes and QT intervals of the right precordial leads (V_1-V_2-V_3) is greater than in the left precordial leads (V_4-V_5-V_6) and that QT ratio $^{V1+V2+V3}/_{V4+V5+V6}$ is ≥1.2 such as ARVC/D.

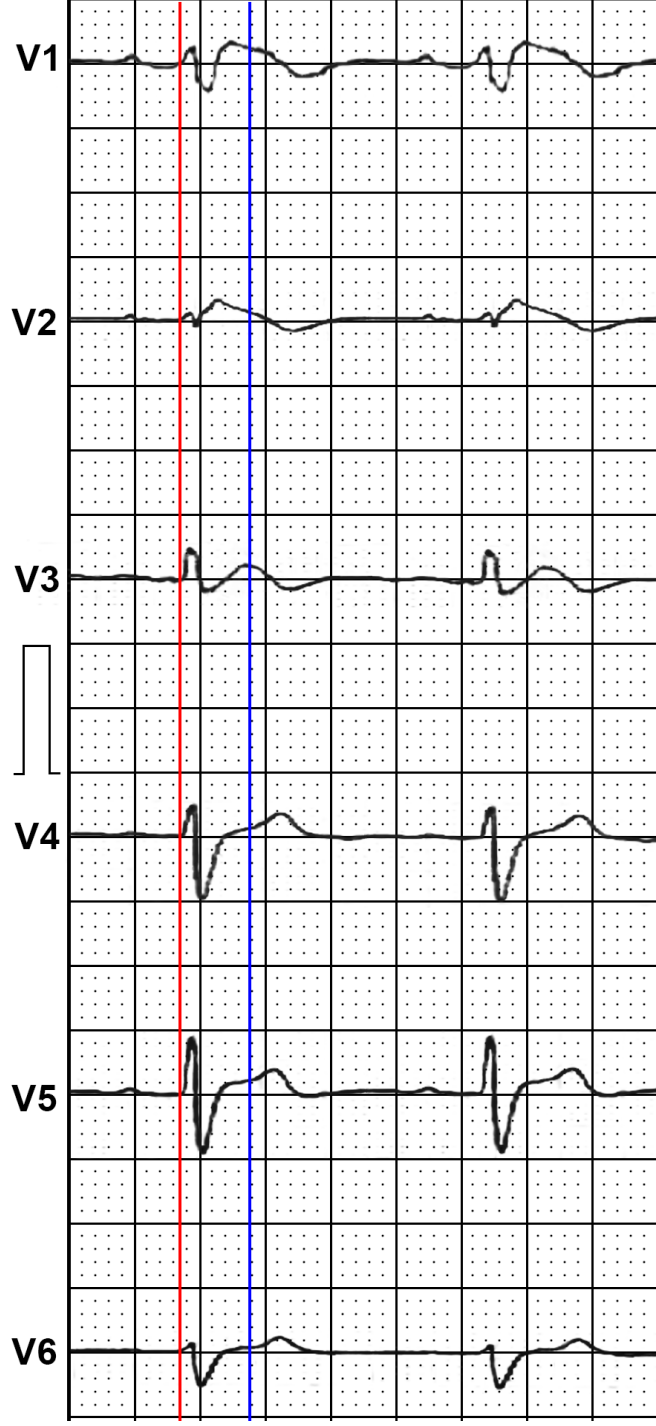

Pectus carinatum or Pigeon chest

Pectus carinatum is the second most common chest wall deformity observed in children. Whereas the more common pectus excavatum deformity has received a great deal of recent attention in the literature due to the associated cardiac and pulmonary dysfunction and alternative surgical options, recent evidence affirms the long held belief that pectus carinatum can lead to significant psychological distress and thus warrants an equally aggressive management approach. Numerous studies have demonstrated the efficacy of both operative repair and nonoperative bracing for correction of pectus carinatum. The authors' current approach to evaluation and management of children with pectus carinatum will be reviewed. It is an uncommon birth defect in which a child's breastbone protrudes outward abnormally, Sometimes the deformity isn't noticeable until after the adolescent growth spurt.

For most children and teens, the main issue with pectus carinatum is the way it looks. However, some will also have problems with shortness of breath, especially during exercise.

Definition

Pectus carinatum is a term used to characterize a range of chest wall deformities defined by anterior protrusion of the sternum and adjacent costal cartilages, and is in distinction to the more common pectus excavatum, which describes chest wall depression deformities. Pectus carinatum deformities can be subclassified into two distinct entities depending on the component of the sternum involved. The chondrogladiolar variant describes protrusion of the gladiolus, or body of the sternum. This deformity has also been referred to as 'keel chest'. The chondromanubrial variant describes protrusion of the manubrium, or superior component of the sternum, and has been termed the 'pouter pigeon breast', 'Currarino–Silverman syndrome', 'horseshoe chest', and 'horns of steer'. This deformity can present as either an isolated manubrial protrusion or 'mixed' defect with manubrial protrusion and gladiolar depression.

Pectus carinatum refers to a chest wall abnormality in which the breastbone is pushed outward. It generally presents during childhood and worsens through adolescence. If the condition occurs in isolation, it is often not associated with any additional signs or symptoms. Rarely, affected people report shortness of breath during exercise, frequent respiratory infections, and/or asthma. The underlying cause of isolated pectus carinatum is unknown. Pectus carinatum can also be associated with a variety of genetic disorders and syndromes.

Epidemiology

Pectus carinatum is a relatively common chest wall deformity occurring with a male to female ratio of approximately 4 : 1. Two groups have investigated the overall prevalence of both pectus deformities in children. Westphal et al., in a cohort of 1332 children aged 11–14 years of age

1. **Marfan syndrome** is a disorder of the connective tissue. Connective tissue provides strength and flexibility to structures throughout the body such as bones, ligaments, muscles, walls of blood vessels, and heart valves. Marfan syndrome affects most organs and tissues, especially the skeleton, lungs, eyes, heart, and the large blood vessel that distributes blood from the heart to the rest of the body (the aorta). It is caused by mutations in the FBN1 gene, which provides instructions for making a protein called fibrillin-1. Marfan syndrome is inherited in an autosomal dominant pattern. At least 25% of cases are due to a new (*de novo*) mutation. Marfan patients show a higher frequency of LAE and LVH on 12-lead ECGs compared with controls, these findings are not supported by echocardiography. Serial 12-lead ECGs in routine follow-up of asymptomatic pediatric Marfan patients may be more appropriate for a subgroup of Marfan patients only, specifically those with prolonged QTc interval at their baseline visit.(**Arunamata 2018**)
2. **Noonan syndrome:** is a disorder that involves unusual facial characteristics, short stature, heart defects present at birth, bleeding problems, developmental delays, and malformations of the bones of the rib cage. Noonan syndrome is caused by changes in one of several autosomal dominant genes. A person who has Noonan syndrome may have inherited an altered (mutated) gene from one of his or her parents, or the gene change may be a new change due to an error carried by the egg or sperm or occurring at conception. Alterations in four genes - *PTPN11*, *SOS1*, *RAF1* and *KRAS* - have been identified to date. Approximately 50 percent of individuals with Noonan syndrome have mutations in the *PTPN11* gene. Twenty percent of those with Noonan Syndrome have mutations in the *SOS1*. Mutations in the *RAF1* gene account for between 10 and 15 percent of Noonan syndrome cases. About 5 percent of people with Noonan syndrome have mutations in the *KRAS* gene and usually have a more severe or atypical form of the disorder. The cause of Noonan syndrome in the remaining 10 to 15 percent of people with this disorder is not yet known. . Noonan syndrome is present in about 1 in 1,000 to 1 in 2,500 people. Symptoms of Noonan syndrome may include a characteristic facial appearance, short stature. congenital heart disease, abroad or webbed neck, minor eye problems such as strabismus in up to 95% of individuals, bleeding problems such as a history of abnormal bleeding or bruising., an unusual chest shape with widely-spaced and low set nipples, developmental delay of varying degrees, but usually mild, in males, undescended testes (cryptorchidism).
3. **Morquio A syndrome** is an autosomal recessive disorder, one of 50 lysosomal storage diseases (LSDs), and is caused by the deficiency of N-acetylgalactosamine-6-sulfate sulfatase (GALNS). Deficiency of this enzyme causes specific glycosaminoglycan (GAG) accumulation: keratan sulfate (KS) and chondroitin-6-sulfate (C6S). The majority of KS is produced in the cartilage, therefore, the undegraded substrates accumulate mainly in cartilage and in its extracelluar matrix (ECM), causing direct leads to direct impact on cartilage and bone development

3. and leading to the resultant systemic skeletal spondyloepiphyseal dysplasia. Chondrogenesis, the earliest phase of skeletal formation that leads to cartilage and bone formation is controlled by cellular interactions with the ECM, growth and differentiation factors and other molecules that affect signaling pathways and transcription factors in a temporal-spatial manner. In Morquio A patients, in early childhood or even at birth, the cartilage is disrupted presumably as a result of abnormal chondrogenesis and/or endochondral ossification. The unique clinical features are characterized by a marked short stature, odontoid hypoplasia, protrusion of the chest, kyphoscoliosis, platyspondyly, coxa valga, abnormal gait, and laxity of joints. Morquio A syndrome (Mucopolysaccharidosis type IVA, MPA IVA) is an autosomal recessive lysosomal storage disorder (LSD) caused by deficiency of N-acetylgalactosamine-6-sulfate sulfatase (GALNS). This enzyme deficiency leads to progressive accumulation of excessive glycosaminoglycans (GAGs), keratan sulfate (KS) and chondroitin-6-sulfate (C6S) primarily in the lysosomes of bone, cartilage, and ligaments and in the extracellular matrix (ECM) of these tissues,(**Neufeld 2001**.), since KS is produced mainly in cartilage tissue. The excessive storage of GAGs causes systemic skeletal spondyloepiphyseal dysplasia seen as striking short trunk stature, cervical spinal cord compression, pectus carinatum, kyphoscoliosis, knock-knee, hypermobile joints, and an abnormal gait with an increased tendency to fall.(**Montaño 2007**) Many patients become wheelchair-dependent in their second decade and undergo multiple surgeries to alleviate serious medical complications. The respiratory failure from obstructive and restrictive lung and spinal cord injury results in significant mortality. Patients often do not survive beyond their twenties.

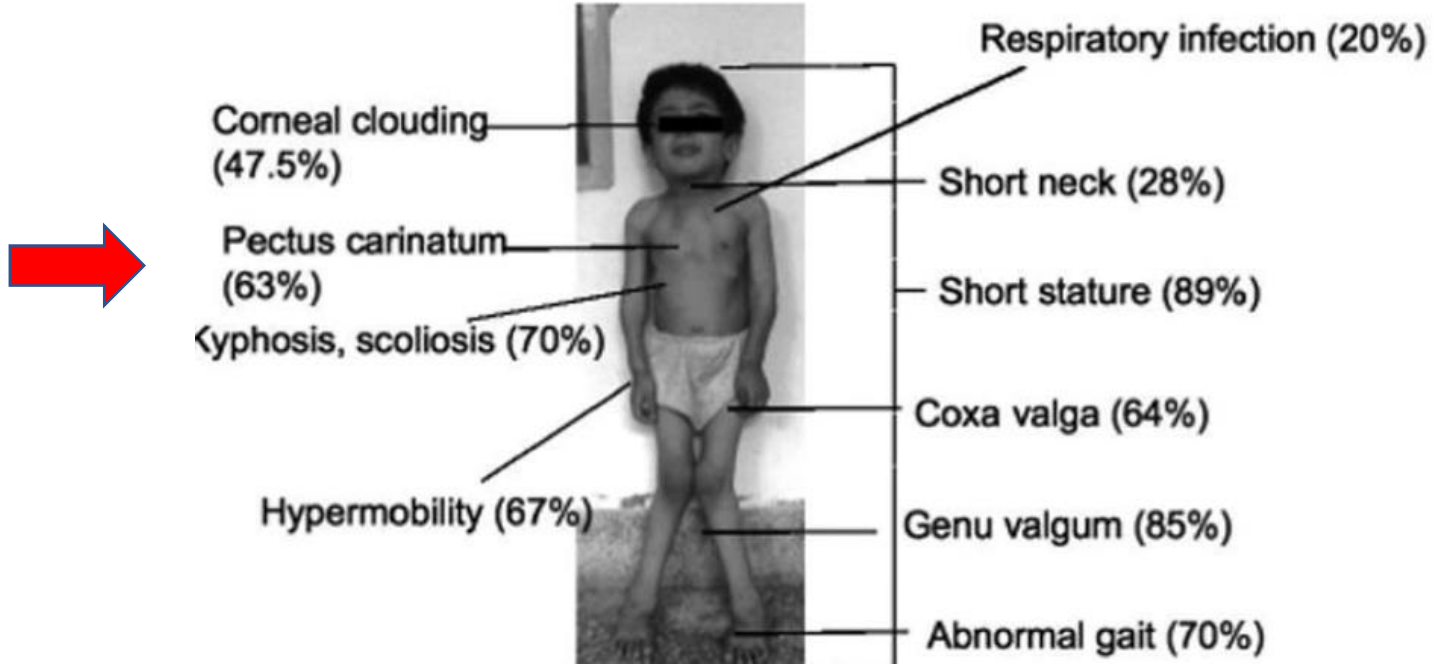

4. **Homocystinuria:** Homocystinuria is an inherited disorder with autosomal receive pattern of inheritance in which the body is unable to process certain building blocks of proteins (amino acids) properly. There are multiple forms of homocystinuria, which are distinguished by their signs and symptoms and genetic cause. The most common form of homocystinuria is characterized by nearsightedness (myopia), dislocation of the lens at the front of the eye, an increased risk of abnormal blood clotting, and brittle bones that are prone to fracture (osteoporosis) or other skeletal abnormalities. Some affected individuals also have developmental delay and learning problems. Less common forms of homocystinuria can cause intellectual disability, failure to grow and gain weight at the expected rate (failure to thrive), seizures, problems with movement, and a blood disorder called megaloblastic anemia. Megaloblastic anemia occurs when a person has a low number of red blood cells (anemia), and the remaining red blood cells are larger than normal (megaloblastic). The signs and symptoms of homocystinuria typically develop within the first year of life, although some mildly affected people may not develop features until later in childhood or adulthood. The most common form of homocystinuria affects at least 1 in 200,000 to 335,000 people worldwide. The disorder appears to be more common in some countries, such as Ireland (1 in 65,000), Germany (1 in 17,800), Norway (1 in 6,400), and Qatar (1 in 1,800). The rarer forms of homocystinuria each have a small number of cases reported in the scientific literature. Mutations in the *CBS*, *MTHFR*, *MTR*, *MTRR*, and *MMADHC* genes cause homocystinuria. Mutations in the *CBS* gene cause the most common form of homocystinuria. The *CBS* gene provides instructions for producing an enzyme called cystathionine beta-synthase. This enzyme acts in a chemical pathway and is responsible for converting the amino acid homocysteine to a molecule called cystathionine. As a result of this pathway, other amino acids, including methionine, are produced. Mutations in the *CBS* gene disrupt the function of cystathionine beta-synthase, preventing homocysteine from being used properly. As a result, this amino acid and toxic byproducts substances build up in the blood. Some of the excess homocysteine is excreted in urine. Rarely, homocystinuria can be caused by mutations in several other genes. The enzymes made by the *MTHFR*, *MTR*, *MTRR*, and *MMADHC* genes play roles in converting homocysteine to methionine. Mutations in any of these genes prevent the enzymes from functioning properly, which leads to a buildup of homocysteine in the body. Researchers have not determined how excess homocysteine and related compounds lead to the signs and symptoms of homocystinuria.
5. **Osteogenesis imperfecta** also known as brittle bone disease, is a heritable disorder of the extracellular matrix. This disorder manifests mainly as bone fragility, although other organs can be involved. Abnormalities of the teeth, known as dentinogenesis imperfecta, and soft tissues, such as discoloration of the sclera and joint hyperlaxity are often observed. It is caused by Mutations in the two genes coding for collagen type I, COL1A1 and COL1A2, are the most common cause of osteogenesis imperfecta. In the past 10 years, defects in at least 17 other genes have been identified as responsible for osteogenesis imperfecta phenotypes, with either dominant or recessive transmission. Intravenous bisphosphonate infusions are the most widely used medical treatment. This has a marked effect on vertebra in growing children

5. and can lead to vertebral reshaping after compression fractures. However, bisphosphonates are less effective for preventing long-bone fractures. At the moment, new therapies are under investigation. Osteogenesis imperfecta affects approximately 1 in 10 000 to 20 000 births (**Lim 2017**). It is a genetically heterogeneous skeletal dysplasia with higher mortality than general population. In a recent cohort, people with osteogenesis imperfecta had higher risk of death from respiratory and gastrointestinal diseases and trauma (**Folkestad 2016**). In addition to the low-bone mass achieved, patients with osteogenesis imperfecta experience age-associated bone loss, increasing even more the risk of fractures . Women undergo perimenopause loss and the rate of fractures in postmenopausal women with osteogenesis imperfecta is twice as high as that of osteogenesis imperfecta in premenopausal women (**Folkestad 2017**). The predominant cause of osteogenesis imperfecta are mutations in the two genes that encode type I collagen. The protein is a heterotrimer, containing two a1(I) and one a2(I) chains . It is synthesized as a procollagen molecule, and undergoes multiple posttranslational modifications. Flanking propeptides are removed by specific proteases, then, the molecule spontaneously assembles.
6. **Coffin-Lowery syndrome:** is a condition that affects many parts of the body. The signs and symptoms are usually more severe in males than in females, although the features of this disorder range from very mild to severe in affected women. Males with Coffin-Lowry syndrome typically have severe to profound intellectual disability and delayed development. Affected women may be cognitively normal, or they may have intellectual disability ranging from mild to profound. Beginning in childhood or adolescence, some people with this condition experience brief episodes of collapse when excited or startled by a loud noise. These attacks are called stimulus-induced drop episodes (SIDEs). Most affected males and some affected females have distinctive facial features including a prominent forehead, widely spaced and downward-slanting eyes, a short nose with a wide tip, and a wide mouth with full lips. These features become more pronounced with age. Soft hands with short, tapered fingers are also characteristic of Coffin-Lowry syndrome. Additional features of this condition include short stature, an unusually small head (microcephaly), progressive abnormal curvature of the spine (kyphoscoliosis), and other skeletal abnormalities. The incidence of this condition is uncertain, but researchers estimate that the disorder affects 1 in 40,000 to 50,000 people. Mutations in the *RPS6KA3* gene cause Coffin-Lowry syndrome. This gene provides instructions for making a protein that is involved in signaling within cells. Researchers believe that this protein helps control the activity of other genes and plays an important role in the brain. The protein is involved in cell signaling pathways that are required for learning, the formation of long-term memories, and the survival of nerve cells. Gene mutations result in the production of little or no RPS6KA3 protein, but it is unclear how a lack of this protein causes the signs and symptoms of Coffin-Lowry syndrome. Some people with the features of Coffin-Lowry syndrome do not have identified mutations in the *RPS6KA3* gene. In these cases, the cause of the condition is unknown. This condition is inherited in an X-linked dominant pattern. A condition is considered X-linked if the mutated gene that causes the disorder is located on the X chromosome, one of thetwo sexchromosomes. The inheritance is

6. dominant if one copy of the altered gene in each cell is sufficient to cause the condition. In most cases, males (who have one X chromosome in each cell) experience more severe signs and symptoms of the disorder than females (who have two X chromosomes in each cell). A characteristic of X-linked inheritance is that fathers cannot pass X-linked traits to their sons.Between 70% and 80% of people with Coffin-Lowry syndrome have no history of the condition in their families. These cases are caused by new mutations in the *RPS6KA3* gene. The remaining 20 percent to 30 percent of affected individuals have other family members with Coffin-Lowry syndrome.
7. **Cardio faciocutaneous syndrome:** ardiofaciocutaneous syndrome is a disorder that affects many parts of the body, particularly the heart (cardio-), facial features (facio-), and the skin and hair (cutaneous). People with this condition also have delayed development and intellectual disability, usually ranging from moderate to severe. Heart defects occur in most people with cardiofaciocutaneous syndrome. The heart problems most commonly associated with this condition include malformations of one of the heart valves that impairs blood flow from the heart to the lungs (pulmonic stenosis), a hole between the two upper chambers of the heart (atrial septal defect), and a form of heart disease that enlarges and weakens the heart muscle (hypertrophic cardiomyopathy). Cardiofaciocutaneous syndrome is also characterized by distinctive facial features. These include a high forehead that narrows at the temples, a short nose, widely spaced eyes (ocularhypertelorism), outside corners of the eyes that point downward (down-slanting palpebralfissures), droopy eyelids (ptosis), a small chin, and low-set ears. Overall, the face is broad and long, and the facial features are sometimes described as "coarse“ Skin abnormalities occur in almost everyone with cardiofaciocutaneous syndrome. Many affected people have dry, rough skin; dark-colored moles (nevi); wrinkled palms and soles; and a skin condition called keratosis pilaris, which causes small bumps to form on the arms, legs, and face. People with cardiofaciocutaneous syndrome also tend to have thin, dry, curly hair and sparse or absent eyelashes and eyebrows.Infants with cardiofaciocutaneous syndrome typically have weak muscle tone (hypotonia), feeding difficulties, and a failure to grow and gain weight at the normal rate (failure to thrive). Additional features of this disorder in children and adults can include an unusually large head (macrocephaly), short stature, problems with vision, and seizures. The signs and symptoms of cardiofaciocutaneous syndrome overlap significantly with those of two other genetic conditions, Costello syndrome and Noonan syndrome. The three conditions are distinguished by their genetic cause and specific patterns of signs and symptoms; however, it can be difficult to tell these conditions apart, particularly in infancy. Unlike Costello syndrome, which significantly increases a person's cancer risk, cancer does not appear to be a major feature of cardiofaciocutaneous syndrome. Cardiofaciocutaneous syndrome is a very rare condition whose incidence is unknown. Researchers estimate that 200 to 300 people worldwide have this condition. Cardiofaciocutaneous syndrome can be caused by mutations in several genes. Mutations in the *BRAF* gene are most common, accounting for 75 to 80 percent of all cases. Another 10 to 15 percent of cases result from mutations in one of two similar genes, *MAP2K1* and *MAP2K2*. Fewer than 5 percent of cases are caused by mutations in the *KRAS* gene.The *BRAF*, *MAP2K1*, *MAP2K2*,

7. and *KRAS* genes provide instructions for making proteins that work together to transmit chemical signals from outside the cell to the cell's nucleus. This chemical signaling pathway, known as the RAS/MAPK pathway, is essential for normal development before birth. It helps control the growth and division (proliferation) of cells, the process by which cells mature to carry out specific functions (differentiation), cell movement, and the self-destruction of cells (apoptosis). Mutations in any of these genes can result in the characteristic features of cardiofaciocutaneous syndrome. The protein made from the mutated gene is overactive, which alters tightly regulated chemical signaling during development. The altered signaling interferes with the development of many organs and tissues, leading to the signs and symptoms of cardiofaciocutaneous syndrome. Some people with the signs and symptoms of cardiofaciocutaneous syndrome do not have an identified mutation in the *BRAF*, *MAP2K1*, *MAP2K2*, or *KRAS* gene. In these cases, affected individuals may actually have Costello syndrome or Noonan syndrome, which are also caused by mutations in genes involved in RAS/MAPK signaling. The proteins produced from these genes are all part of the same chemical signaling pathway, which helps explain why mutations in different genes can cause conditions with such similar signs and symptoms. The group of related conditions that includes cardiofaciocutaneous syndrome, Costello syndrome, and Noonan syndrome is often called the RASopathies.
8. Certain chromosome abnormalities.

In these cases, the condition has an underlying genetic cause and is associated with additional features that are characteristic of the genetic disease. Pectus carinatum is primarily a cosmetic concern and treatment, therefore, depends on the severity of the condition and the interests of the affected person and their family. In those who choose to pursue treatment, bracing and/or surgery may be an option.

SymptomsThe main symptom of pectus carinatum is a breastbone that sticks out. Sometimes the deformity isn't noticeable until after the adolescent growth spurt. Some people will also have shortness of breath, especially during exercise. Recent evidence confirms that children with pectus carinatum have a disturbed body image and a reduced quality of life.

Diagnosis

Usually can diagnose pectus carinatum by examining the chest. Imaging tests like CT scans can help determine the severity of the disorder.A pectus carinatum prevalence of 0.675% and pectus excavatum prevalence of 1.275%. Coskun et al., in their cohort of 1342 children aged 7–14 years of age, reported a similar pectus carinatum prevalence of 0.6% but reported a pectus excavatum prevalence of 2.6%. The chondro gladiolar variant is by far the most common, found in 92.3 to 95% of children with pectus carinatum deformity.

References

1. Alzamora-Castro V, Abugattas R, Rubio C, Bouroncle J, Zapata C, Santa-Marie E, Battilana G, Binder T, Subiria R, Paredes D. Parietal focal block; an experimental and electrocardiographic study. Circulation. 1953 Jan;7(1):108-15.
2. Antonelli D, Mazor G, Avni G.Double outlet right ventricle associated with persistent common atrioventricular canal and pulmonary stenosis. Cardiology. 1986;73(3):160-3
3. Arunamata AA, Nguyen CT, Ceresnak SR, Dubin AM, Olson IL, Murphy DJ1, Selamet Tierney ES1.Utility of serial 12-lead electrocardiograms in children with Marfan syndrome.Cardiol Young. 2018 Aug;28(8):1009-1013. doi: 10.1017/S1047951118000707
4. Babai Bigi, M. A., Aslani, A., & Shahrzad, S. (2007). aVR sign as a risk factor for life-threatening arrhythmic events in patients with Brugada syndrome. *Heart Rhythm, 4*(8), 1009-1012. doi: 10.1016/j.hrthm.2007.04.017
5. Basagoitia AM, Iturralde P, Galván O, Rosado J, Vázquez C, Colín L, Romero L, González Hermosillo J. [Disorders of the rhythm and conduction in patients operated on for a total correction of tetralogy of Fallot]. Arch Inst Cardiol Mex. 1991 Jan-Feb;61(1):27-32.
6. Bastaroli JC, Mordeglia FJ, Gandulla LM. [Well-marked deviation of the axis to the left and myocardial disease. Renewal of an old concept]. Medicina (B Aires). 1968 May-Jun;28(3):144-58.
7. BRANDENBURG RO, DUSHANE JW. Clinical features of persistent common atrioventricular canal. Proc Staff Meet Mayo Clin. 1956 Sep 19;31(19):509-13.
8. Bayés de Luna A , Cosin J, Carrió J, Chorao de Aguiar AJ, Ribeiro C, Creixells C, Martin G, Gimeno V, Ramirez A, Casan P, Artigas A, Gras J, Subirana MT, Cabadés A, Guimaraes H. Right Ventricular peripheric blocks: Diagnostic Problem. In Masoni A, Alboni P, eds. Cardiac Electrophysiology Today. Academic Press, London; New York, 1982, 401.
9. Bayés de Luna A, Carrió I, Subirana MT, Torner P, Cosín J, Sagués F, Guindo J. Electrophysiological mechanisms of the SI SII SIII electrocardiographic morphology.J Electrocardiol. 1987 Jan;20(1):38-44.
10. Brenyo A, Rao M, Barsheshet A, Cannom D, Quesada A, McNitt S, Huang DT, Moss AJ, Zareba W.QRS axis and the benefit of cardiac resynchronization therapy in patients with mildly symptomatic heart failure enrolled in MADIT-CRT.J Cardiovasc Electrophysiol. 2013 Apr;24(4):442-8. doi: 10.1111/jce.12057.
11. Calcaterra G, Puglisi R.Left axis deviation in healthy infants and children.Int J Cardiol. 1989 Aug;24(2):236-8.
12. Calo, L., Giustetto, C., Martino, A., Sciarra, L., Cerrato, N., Marziali, M., . . . Gaita, F. (2016). A New Electrocardiographic Marker of Sudden Death in Brugada Syndrome: The S-Wave in Lead I. *J Am Coll Cardiol*, *67*(12), 1427-1440. doi: 10.1016/j.jacc.2016.01.024

13. Calò L.Patients with left bundle branch block and left axis deviation show a specific left ventricular asynchrony pattern: Implications for left ventricular lead placement during CRT implantation.J Electrocardiol. 2018 Mar - Apr;51(2):175-181. doi: 10.1016/j.jelectrocard.2017.10.0
14. Canudas-Romo V, et al. Mortality and causes of death in patients with osteogenesis imperfecta: a register-based nationwide cohort study. J Bone Miner Res 2016; 31:2159–2166.
15. Caro M, Conde D, Pérez-Riera AR, de Almeida AP, Baranchuk A.The electrocardiogram in Down syndrome. Cardiol Young. 2015 Jan;25(1):8-14. doi: 10.1017/S1047951114000420.
16. Childers R, Lupovich S, Sochanski M, Konarzewska H.Left bundle branch block and right axis deviation: a report of 36 casesJ Electrocardiol. 2000;33 Suppl:93-102.
17. Chou FS, Johnson AJ, Ghimire LV.The Significance of Left Axis Deviation in the Pediatric Population: A Meta-Analysis.Pediatr Cardiol. 2019 Mar 16. doi: 10.1007/s00246-019-02086-3.
18. Conover, Mary Boudreau (2003-01-01). *Understanding Electrocardiography*. Elsevier Health Sciences. ISBN 978-0323019057
19. Daliento L, Corrado D, Buja G, John N, Nava A, Thiene G. Rhythm and conduction disturbances in isolated, congenitally corrected transposition of the great arteries. Am J Cardiol. 1986 Aug 1;58(3):314-8.
20. Davachi F, Moller JH. The electrocardiogram and vectorcardiogram in single ventricle. Anatomic correlations. Am J Cardiol. 1969 Jan;23(1):19-31.
21. de Micheli A, Medrano GA, Iturralde-Torres P. [Uncomplicated and complicated myocardial peripheral blocks]. Arch Cardiol Mex. 2009 Dec;79 Suppl 2:3-12.
22. Ewy GA, Karliner J, Bedynek JL Jr. Electrocardiographic QRS axis shift as a manifestation of hyperkalemia.JAMA. 1971 ;215(3):429-32.
23. Feldt RH, DuShane JW, Titus JL. The atrioventricular conduction system in persistent common atrioventricular canal defect: correlations with electrocardiogram. Circulation. 1970 Sep;42(3):437-44.
24. Folkestad L, Hald JD, Ersboll AK, et al. Fracture rates and fracture sites in patients with osteogenesis imperfecta: a nationwide register-based cohort study. J Bone Miner Res 2017; 32:125–134.
25. Froelicher V1, Ashley E1, Perez MV1Large Q and S waves in lead III on the electrocardiogram distinguish patients with hypertrophic cardiomyopathy from athletes.Heart. 2018 Nov;104(22):1871-1877. doi: 10.1136/heartjnl-2017-312647

26. Galloway CD, Valys AV, Shreibati JB, Treiman DL, Petterson FL, Gundotra VP, Albert DE, Attia ZI, Carter RE, Asirvatham SJ, Ackerman MJ, Noseworthy PA, Dillon JJ, Friedman PA.Development and Validation of a Deep-Learning Model to Screen for Hyperkalemia From the Electrocardiogram.JAMA Cardiol. 2019 Apr 3. doi: 10.1001/jamacardio.2019.0640Folkestad L, Hald JD, Gheshlaghi F, Mehrizi MK, Yaraghi A, Sabzghabaee AM, Soltaninejad F, Eizadi-Mood N. ST-T segment changes in patients with tricyclic antidepressant poisoning.J Res Pharm Pract. 2013 Jul;2(3):110-3. doi: 10.4103/2279-042X.122381
27. Gup AM, Franklin RB, Hill JE Jr. The vectorcardiogram in children with left axis deviation and no apparent heart disease. Am Heart J1965 May; 69:619–23.
28. Hakacova N, Wagner GS, Idriss SF, Electroanatomic relationships in patients with primum atrioventricular septal defect.JACC Cardiovasc Imaging. 2009 Dec;2(12):1357-65. doi: 10.1016/j.jcmg.2009.08.009
29. Kanawati J, Sy RW. Contemporary Review of Left Bundle Branch Block in the Failing Heart - Pathogenesis, Prognosis, and Therapy. Heart Lung Circ. 2018 Mar;27(3):291-300.
30. Katz LN, Wachtel H. The diphasic QRS type of electrocardiogram in congenital heat disease. Am Heart J 1937;13:202.
31. Kim YG1, Shin D1, Park MY2, Lee S1, Jeon MS1,3, Yoon D1, Park RW1,3.ECG-ViEW II, a freely accessible electrocardiogram database.PLoS One. 2017 Apr 24;12(4):e0176222. doi: 10.1371/journal.pone.0176222
32. Komatsu Y, Nogami A, Kurosaki K, Morishima I, Masuda K, Ozawa T, Kaneshiro T, Hanaki Y, Shinoda Y, Talib AK, Kowase S, Sekiguchi Y, Aonuma K.Fascicular Ventricular Tachycardia Originating From Papillary Muscles: Purkinje Network Involvement in the Reentrant Circuit.Circ Arrhythm Electrophysiol. 2017 Mar;10(3). pii: e004549. doi: 10.1161/CIRCEP.116.004549
33. Krongrad E, Ritter DG, Weidman WH, DuShane JW. Hemodynamic and anatomic correlation of electrocardiogram in double-outlet right ventricle. Circulation. 1972 Nov;46(5):995-1004.
34. Khurana C, Mazzone P, Mandell B. New onset left bundle branch block with right axis deviation in a patient with Wegener's granulomatosis. J Electrocardiol. 2000 Apr;33(2):199-201.
35. Lenègre J.: Contribution a l'Etude des Blocs de Branche. Paris, JB Bailliere, 1958.
36. Lepeschkin E. Modern Electrocardiopgraphy: vol. 1. The P-Q-R-S-T-U complex (Williams & Wilkins, Baltimore, 1951).
37. Lev M. The normal anatomy of the conduction system in man and its pathology in atrioventricular block. Ann N Y Acad Sci. 1964 Jun 11;111:817-29.
38. Lev M. The conduction system. En: Gould S. Pathology of the heart and blood vessels. Springfield, III. Ed. Charles C Thomas, 1968, pág. 18
39. Lim J, Grafe I, Alexander S, et al. Genetic causes and mechanisms of osteogenesis imperfecta. Bone 2017; 102:40–49.

40. Lipoff JI. Anomalous origin of the left main coronary artery from the right sinus of Valsalva with coronary AV fistula of the conus artery. Chest. 1988 Jan;93(1):203-4.
41. Liu PY, Lin YP, Li YH, Su ZW, Han CL, Huang SC, Lin CS, Meng FC7, Wu HT8, Lin GM9.Electrocardiographic characteristics in young male patients with left primary spontaneous pneumothorax estimated by the collins equation.Indian Heart J. 2017 Nov - Dec;69(6):720-724. doi: 10.1016/j.ihj.2017.05.005
42. .Mahaim J. Masson & Cie; Paris: 1931. Les maladies organiques du faisceau de His-Tawara.
43. Massei V, Moroni E, Fabbrocini V. [Electrocardiographic aspects of pulmonary emphysema: right deviation of P axis under strain]. Arch Tisiol Mal Appar Respir. 1968 Jul;23(7):507-26.
44. Masini V, Testoni F, Farulla A. Focal blocks of the right intraventricular conduction: morphology,pathogenesis and clinical significance. Cardiologia. 1952; 21 (3):171-187.
45. McHenry PL, Phillips JF, Fisch C, Corya BR. Right precordial qrS pattern due to left anterior hemiblock. Am Heart J. 1971 Apr;81(4):498-502.
46. Medvedev ES, Slavina SE. Deviation of electric axis of the heart in pulmonary emphysema]. Klin Med (Mosk). 1951 Nov;29(11):62-8.
47. Mirowski M, Arevalo F, Medrano GA, Cisneros FA. Conduction disturbances in patent ductus arteriosus. A study of 20 cases before and after surgery with determination of the P-R index. Circulation. 1962 May;25:807-13.
48. Montaño AM, Tomatsu S, Gottesman GS, Smith M, Orii T. International Morquio A Registry: clinical manifestation and natural course of Morquio A disease. J Inherit Metab Dis. 2007;30:165–174
49. Nava A, Canciani B, Schiavinato ML, Martini B, Buja GF. La repolarisation precoce dans le precordiales droites: trouble de la conduction intraventriculaire droite? Correlations de l'electrocardiographie-vectorcardiographie avec l'electrophysiologie. *Mises Jour Cardiologiques.*1988;17:157–159.
50. Neufeld EF, Muenzer J. The mucopolysaccharidoses. In: Scriver CR, Beaudet AL, Sly WS, Valle D, Childs B, Kinzler KW, Vogelstein B, editors. The Metabolic and Molecular Bases of inherited Disease. 8th. McGraw-Hill; New York: 2001. pp. 3421–3452.
51. Nikolic G, Marriott HJ.Left bundle branch block with right axis deviation: a marker of congestive cardiomyopathy.J Electrocardiol. 1985 Oct;18(4):395-404.
52. Nikus K, Pérez-Riera AR, Konttila K, Barbosa-Barros R.Electrocardiographic recognition of right ventricular hypertrophy.J Electrocardiol. 2018 Jan - Feb;51(1):46-49. doi: 10.1016/j.jelectrocard.2017.09.004
53. Noseda V, Santi A, Aguggini G, et al. Experimental focal block in the sheep and the dog. An electrocardiographic and histological study. Cardiologia. 1963;42:243-55.

54. Ozdemir K1, Uluca Y, Daniş G, Tokac M, Altunkeser BB, Telli HH, Gök H.Importance of left anterior hemiblock development in inferior wall acute myocardial infarction.Angiology. 2001 Nov;52(11):743-7.
55. Qaddoura A, Digby GC, Kabali C, Kukla P, Zhan ZQ, Baranchuk AM. The value of electrocardiography in prognosticating clinical deterioration and mortality in acute pulmonary embolism: A systematic review and meta-analysis. Clin Cardiol. 2017 Oct;40(10):814-824.
56. Parharidis G1, Nouskas J, Efthimiadis G, Styliadis J, Gemitzis K, Hatzimiltiadis S, Karoulas T, Tsifodimos D.Complete left bundle branch block with left QRS axis deviation: defining its clinical importance.Acta Cardiol. 1997;52(3):295-30.
57. Pastore CA, Moffa PJ, Spiritus MO, et al. Fascicular blocks of the right branch. Standardization of vectorelectrocardiographic findings. Arq Bras Cardiol. 1983 Sep;41(3):161-6.
58. Pastore C.A., Moffa P.J., Tobias N.M. Segmental blocks of the right bundle-branch and electrically inactive areas. Differential electro-vectorcardiographic diagnosis. Arq Bras Cardiol. 1985;45:309–317.
59. Patanè S, Marte F, Di Bella G, Chiribiri A.Atrial fibrillation with intermittent right axis deviation in the presence of complete left bundle branch block.Int J Cardiol. 2008 Sep 16;129(1):e1-2.
60. Patanè S, Marte F, Dattilo G, et al. Acute myocardial infarction and left bundle branch block with changing axis deviation. Int J Cardiol. 2012;154(3):e47-9.
61. Pérez-Riera A.R., Ferreira C., Schapachnik E. Value of 12 lead electrocardiogram and derived methodologies in the diagnosis of Brugada disease. In: Antzelevitch C., Brugada P., Brugada J., Brugada R., editors. The Brugada syndrome: from bench to Bedside. Blackwell Futura; USA: 2005. pp. 87–100.
62. Peréz-Riera AR, Ferreira Filho C, de Abreu LC, Ferreira C, Yanowitz FG, Femenia F, Brugada P, Baranchuk A; International VCG Investigators Group. Do patients with electrocardiographic Brugada type 1 pattern have associated right bundle branch block? A comparative vectorcardiographic study. Europace. 2012 Jun;14(6):889-97.
63. Pérez-Riera AR, Barbosa-Barros R, Daminello-Raimundo R, de Abreu LC, Tonussi Mendes JE, Nikus K.Left posterior fascicular block, state-of-the-art review: A 2018 update.Indian Pacing Electrophysiol J. 2018 Nov - Dec;18(6):217-230. doi: 10.1016/j.ipej.2018.10.001
64. Perloff JK, Roberts NK, Cabeen WR. Left axis deviation: a reassessment. Circulation. 1979 Jul;60(1):12-21. Perrotta L, Kandala J, DI Biase L, Valleggi A, Michelotti F, Pieragnoli P, et al. Prognostic Impact of QRS Axis Deviation in Patients Treated With Cardiac Resynchronization Therapy.JCardiovascElectrophysiol. 2016 Mar;27(3):315-20. doi: 10.1111/jce.12887
65. Pietrzak R, Werner B. Electrocardiographic findings in children with different degrees of pulmonary regurgitation following surgical correction of tetralogy of Fallot. Kardiol Pol. 2012;70(1):38-43.

66. Pitzalis MV, Anaclerio M, Iacoviello M, Forleo C, Guida P, Troccoli R, Massari F, Mastropasqua F, Sorrentino S, Manghisi A, Rizzon P.QT-interval prolongation in right precordial leads: an additional electrocardiographic hallmark of Brugada syndrome. J Am Coll Cardiol. 2003 Nov 5;42(9):1632-7.
67. Rautenburg HW, Wagner R."Left anterior hemiblock" or "extreme left axis deviation" in the ECG of children. Monatsschr Kinderheilkd. 1983 Mar;131(3):150-6 Reddy SC, Zuberbuhler JR. Images in cardiovascular medicine. Himalayan P-waves in a patient with tricuspid atresia. Circulation. 2003 Jan 28;107(3):498.
68. Rosenbaum MB, Elizari MV, Lázzari JO. Los Hemibloqueos. Buenos Aires, Argentina: Paidós; 1968.
69. Rosenbaum MB, Elizari MV, Lázzari JO. The Hemiblocks. Oldsmar, Florida: Tampa Tracings; 197
70. Rossi P. Atypical electrocardiographic aspects of focal blocks of the right intraventricular conduction. Cuore Circ. 1954 Feb;38(1):16-22
71. Salazar J, Lej FA. Electrocardiographic changes following surgical repair of ostium primum defect. Acta Cardiol. 1978; 33(1): 55-61.
72. Sclarovsky S, Sagie A, Strasberg B, et al. Transient right axis deviation during acute anterior wall infarction or ischemia: Electrocardiographic and angiographic correlation. J Am Coll Cardiol. 1986;8:27–31.
73. Schwartz DB, Schamroth L.The effect of pregnancy on the frontal plane QRS axis.J Electrocardiol. 1979 Jul;12(3):279-81.
74. Sciarra L, Golia P, Palamà Z, Scarà A, De Ruvo E, Borrelli A, Martino AM, Minati M, Fagagnini A, Tota C, De Luca L, Grieco D, Delise P, Calò L.Patients with left bundle branch block and left axis deviation show a specific left ventricular asynchrony pattern: Implications for left ventricular lead placement during CRT implantation.J Electrocardiol. 2018 Mar - Apr;51(2):175-181. doi: 10.1016/j.jelectrocard.2017.10.006
75. Steurer G, Frey B, Gürsoy S, Tsakonas K, Celiker A, Andries E, Kuck K, Brugada P.Cardiac depolarization and repolarization in Wolff-Parkinson-White syndrome.Am Heart J. 1994 Nov;128(5):908-11.
76. Surawicz B, Childers R, Deal BJ, Gettes LS, Bailey JJ, Gorgels A, Hancock EW, Josephson M, Kligfield P, Kors JA, Macfarlane P, Mason JW, Mirvis DM, Okin P, Pahlm O, Rautaharju PM, van Herpen G, Wagner GS, Wellens H., American Heart Association Electrocardiography and Arrhythmias Committee, Council on Clinical Cardiology. American College of Cardiology Foundation. Heart Rhythm Society. AHA/ACCF/HRS recommendations for the standardization and interpretation of the electrocardiogram: part III: intraventricular conduction disturbances: a scientific statement from the American Heart Association Electrocardiography and Arrhythmias Committee, Council on Clinical Cardiology; the American College of Cardiology Foundation; and the Heart Rhythm Society. Endorsed by the International Society for Computerized Electrocardiology. J. Am. Coll. Cardiol. 2009 Mar 17;53(11):976-81.
77. Tutar HE1, Atalay S, Türkay S, Imamoglu A.QRS axis in isolated perimembranous ventricular septal defect and influences of morphological factors on QRS axis.J Electrocardiol. 2001 Jul;34(3):197-203.

78. Uhley HN, Rivkin L.ECG patterns following interruption of main and peripheral branches of the canine right bundle Am J Cardiol. 1961 Jun;7:810-6.
79. Wang Q, Pan S, Liu F, Yang D, Wang JK.Extreme Right Axis Deviation in Acute Myocardial Infarction: A Hazardous Signal of Poor Prognosis. Am J Case Rep. 2018 May 11; 19:553-556. doi: 10.12659/AJCR.908486

This is my beloved granddaughter named Lucia, beautiful as grandfather